THE EFFECT OF ARTIFICIAL REEF CONFIGURATION ON WAVE BREAKING INTENSITY RELATING TO RECREATIONAL SURFING CONDITIONS

by

CRAIG MICHAEL JOHNSON.

A thesis submitted in partial fulfillment
for the requirements of the degree of

MASTER OF SCIENCE

DEPARTMENT OF CIVIL ENGINEERING

UNIVERSITY OF STELLENBOSCH

Supervisor: D.E. Bosman

Submitted for Approval in

February 2009

Declaration

By submitting this thesis electronically, I declare that the entirety of the work contained therein is my own, original work, that I am the owner of the copyright thereof (unless to the extent explicitly otherwise stated) and that I have not previously in its entirety or in part submitted it for obtaining any qualification.

05 Feb 2009

Signature ***Date***

Abstract

Multi purpose reefs are a relatively new concept that incorporate functionalities of beach stabilization, breakwater/seawall protection, biological enhancement and recreational amenity. Economic benefits increase their attractiveness. There is, however, some degree of uncertainty in design guidelines as to the predictability of each of these aspects. With regards to recreational amenity enhancement, one such uncertainty exists in the ability to predict the reef configuration required to give a certain degree of surfability of a reef, and more specifically, to predict the shape of a plunging wave.

An extensive survey of the relevant literature has been conducted to provide a background on multi purpose reefs and the uncertainties in predicting the success of multi purpose reefs in achieving their design objectives. A study of wave breaking has been done, along with an analysis of existing breaker height and breaker depth formulae. The effects of bottom friction, refraction, shoaling, winds currents and varying water level on wave breaking has been addressed. Surfability aspects were reviewed including a definition of breaking intensity which is defined by the wave profile in terms of vortex shape parameters, and other surfability parameters that influence the surfability of a reef. Background on numerical modelling methods has been given, along with a description and some trial runs of a new and promising method, Smooth Particle Hydrodynamics. Numerical models were run using the open source SPHysics package in order to assess the applicability of the package in measuring vortex shape parameters. The SPHysics package is, however, still in a stage of development, and is not yet suitable for reef studies with very long domains and with high numbers of particles (required for sufficient resolution in the plunging vortex).

A theoretical examination was done on the relevant literature in order to gain an insight into the dynamics affecting the development of the plunging vortex shape. A case study of a natural surf reef was carried out in order to give qualitative estimation of the wave dynamics and reef structure required to give good quality surfing waves and high breaking intensity. The West-Cowell surfing reef factor was used as a tool in predicting wave focusing effects of a naturally occurring reef. Extensive two dimensional physical model laboratory studies were conducted in order to quantify the effects of the reef configuration and wave parameters on breaking intensity. Design guidelines were developed in order to assist in the prediction of breaking intensity for reefs constructed with surfing amenity enhancement as one of their design objectives.

The results show that large underwater topographic features can significantly affect the shape and size of incoming waves. Refraction, focusing and shoaling can transform ordinary waves into waves deemed suitable for surfing. The West-Cowell surfing reef factor gives reasonable results outside its applicable range. The 2D physical model laboratory tests show significant variations in vortex shape parameters due to interactions between broken and unbroken waves in a wave train and also to the reflections developed in the flume. Results show that the predicted trends agree with the observations. The results also show that the junction between the seaward reef slope and the horizontal crest may have an effect on the wave shape in the form of a secondary crest between the primary crests. Design guidelines based on the results are presented, and show that breaker height formulae for smooth planar slopes show good agreement with the values of breaker heights measured in the physical model tests, and that existing breaker depth formulae show average agreement. The design guidelines could assist with more effective design of artificial reefs for surfing purposes.

Opsomming

Meerdoelige riwwe is 'n betreklike nuwe konsep wat gebruik word vir strand stabilisering, breekwater/hawemuur beskerming, biologies verryking en ontspanningsvermaak. Ekonomiese voordele wat die riwwe inhou verhoog die aantreklikheid daarvan. Daar is wel 'n graad van onsekerheid in ontwerpsriglyne vir die voorspelbaarheid vir elk van hierdie funksionaliteite. 'n Voorbeeld van onsekerheid in ontwerp-riglyne vir ontspanningsgeriewe is die konfigurasie van die rif om 'n goeie golf vir branderplankry te verskaf, asook om die vorm van die brekende golf te bepaal.

'n Uitgebreide literatuurstudie oor veeldoelige riwwe en die onsekerhede in die ontwerp van 'n suksesvolle meerdoelige rif is gedoen. 'n Studie oor brekende golwe, die breker-hoogte en breker-diepte formules is ook gedoen. Die effekte van bodemwrywing, refraksie, vervlakking, winde, strome en wisselende watervlakke op brekende golwe is ook ondersoek. Aspekte van branderplankry-vermoë is hersien wat ook die definisie van golfbreking-intensiteit ingesluit het. Die golfbreking-intensiteit word deur die golf-profiel beskryf in terme van werwel-vorm parameters en ook ander parameters wat branderplankry-vermoë van 'n rif beinvloed. 'n Agtergrond oor numeriese modelerings metodes word ook gegee, saam met 'n beskrywing van 'n betreklike nuwe metode, genaamd die 'Smooth Particle Hydrodynamics' (SPH) metode. 'n Paar voorbeelde van die SPH metode word gewys. Die toepaslikheid van die numeriese model pakket, SPHysics, is ook ondersoek vir die bepaling van die werwel-vorm parameters. Dit blyk dat die SPHysics pakket, wat tans onder ontwikkeling is, nog nie werklik toepaslik is vir studies op groot riwwe nie. Die pakket kan nog nie die hoeveelheid partikels hanteer wat benodig word om die onderdompelende werwel met voldoende resolusie te beskryf nie.

'n Analise is gedoen met teoretiese formulasies soos beskryf in die toepaslike literatuur om 'n insig te kry in die dinamika wat die ontwikkeling van die onderdompelende werwel affekteer. 'n Gevalle studie van 'n natuurlike rif, vir branderplankry, is uitgevoer. Die doel van hierdie studie was om 'n kwalitatiewe skatting te maak van die golf-dinamika en rif-struktuur wat benodig word vir goeie kwaliteit golwe met 'n hoë brekings-intensiteit. Die sogenaamde West-Cowell golfry-rif faktor is gebruik om die fokus effek van golwe op 'n rif te voorspel. Uitgebreide twee-dimensionele (2D) fisiese model toetse is in 'n laboratorium gedoen om die effek van die rif-konfigurasie en golf-parameters op brekings-intensiteit te bepaal. Ontwerpriglyne is ontwikkel wat kan help met die bepaling van die brekings-intensiteit, as deel van die ontwerp van riwwe wat goeie branderplankry moet lewer.

Die resultate van die studie toon dat groot bodem-topografiese kenmerke die vorm en grootte van inkomende golwe beduidend kan affekteer. Effekte soos refraksie, fokus en vervlakking kan gewone golwe verander in golwe wat geskik sou wees vir brandplankry. Die West-Cowell golfry-rif faktor gee 'n redelike skatting van die fokus-effek van golfwe, selfs buite die gebied van toepassing. Die 2D fisiese model toetse toon beduidende variasies in die werwel-vorm parameters, as gevolg van die interaksies tussen brekende en nie-brekende golwe in 'n golftrein as ook die refleksies, wat ontwikkel in die 2D model kanaal. Die resultate toon wel die voorspelling ooreenstem met die waarnemings. Die resultate toon ook dat die golf-vorm geaffekteer kan word deur die aansluiting tussen die seekant-helling van die rif en die horisontale kruin. Dit blyk dat 'n sekondêre kruin tussen die primêre kruine ontwikkel. Die ontwerpriglyne word gegee wat gebasseer is die resultate van hierdie studie. Daar word aangetoon dat die breker-hoogte formules vir gladde plat hellings, goed oorenkom met die breker-hoogtes soos gemeet in die fisiese model toetse. Die bestaande breker-diepte formules toon swakker ooreenkoms. Die ontwerpriglyne kan gebruik word om meer effektiewe kunsmatige riwwe vir branderplankry te ontwerp.

Acknowledgments

Throughout the course of the preceding three years, my sincerest thanks are due to those who have significantly contributed to the successful completion of this thesis.

Firstly, the CSIR, without which I would have had neither the financial backing nor laboratory to conduct the investigations. I would to especially thank Mr. Dave Phelp and Mr. Kishan Tulsi respectively in this regard. Thanks to the laboratory staff, Mr. Rafick Jappie, Mr. Riaan Philander and Mr. Reagan Solomons for assistance with setup of the physical model studies. Further thanks to Dave and Kishan for granting me time at work and time off work to complete the investigations and this thesis. Ms Ursula von St Ange's friendly assistance was invaluable. Her endless knowledge of batch file writing and wave analysis programming saved endless hours of waiting for computer simulations and tireless wave analysis. Thanks are also due to Mr. Marius Rossouw, for his in depth expertise in wave theory. His sense of humour helped too. Dr. Wim van der Molen and Mr. Luther Terreblanche should not go unmentioned. Their experience and in-depth knowledge of programming with Fortran and MATLAB really opened my eye's to MATLAB's versatility.

I would like to thank the Hydrographer, South African Navy, for their permission to use the Hout Bay Naval Hydrographic charts in this thesis. Thanks are also due to Transnet-National Ports Authority for the use of the wave data from the Slangkop wave buoy.

At the University of Stellenbosch, thanks are due to Mr. Pierre Swiegers, for his assistance, and more importantly, dedication to the cause (both his and mine). Mr. James Joubert (of the Centre for Sustaninable and Renewable Energy Studies) should be thanked for his endless exuberation for the topic. Deeper thanks are due to my mentor and supervisor, Mr. Eddie Bosman, for his quick understanding of the challenges that were faced, and for his invaluable guidance along the best paths.

I would also like to thank my family for their undying support, and their understanding of my short lived priorities.

Most of all, the deepest thanks go my girlfriend, Alexia. Your unselfish acts of assuming endless household chores and your crazy sense of humour got me through the late nights. Your love shone through.

Table of Contents

List of Tables

List of Figures

List of Symbols

A	coefficient used in equation of Goda (1974)
C	wave celerity
C_o	deepwater wave celerity
C_{res}	resultant wave celerity
D	height of reef from toe to crest
E_{reef}	energy dissipation through the reef
H	wave height
$H_{1/10}$	highest 1/10 of the wave heights in a particular record
$H_{1/3}$	highest 1/3 of the wave heights in a particular record
H_o	deep water wave height
H'_o	unrefracted deepwater wave height
H_b	wave height at breaking
H_{max}	maximum wave height
H_s	significant wave height = $H_{1/3}$
H_v	vortex height
H_o/L_o	deepwater wave steepness
H/L	local wave steepness
H_b/L_b	wave steepness at breaking
L	wave length (distance between successive wave crests)
L_b	wavelength at breakpoint
L_o	deep water wave length
L_{reef}	wavelength at breakpoint on reef
S_f	friction slope
S_L	section length
S_{rf}	West-Cowell surf reef factor
T	wave period
X	distance along x axis in SPHysics package
Z	distance along z axis in SPHysics package

a	parameter used by Weggel (1972) in calculation of wave breaking
b	parameter used by Weggel (1972) in calculation of wave breaking
d	water depth from still water level
d_o	water depth in deep water conditions
d_b	water depth at breaking
d_c	water depth on crest
d_{reef}	breaker depth on reef
d_{toe}	water depth at toe

dt	time step
g	acceleration due to gravity
h	smoothing length
l_c	length of the crest (in the direction parallel to shoreline)
l_v	vortex length
m	foreshore slope = $\tan\beta$
q	non - dimensional distance between particles
r	distance between any two particles
r_{acc}	acceleration ratio
r_c	reflection co-efficient
r_{corr}	correlation ratio
r_v	vortex ratio
s	seaward reef slope = $\tan\beta_{reef}$
s'	orthogonal sea bed gradient
t	time
t_v	time at which vortex is fully formed
u_{crest}	horizontal orbital velocity at crest
u_z	orbital velocity at a distance of z from still water level
v_p	peel velocity
v_{ret}	return velocity
v_{rete}	return velocity at end of crest
v_{rets}	return velocity at start of crest
v_s	surfer velocity
v_w	wave velocity (or celerity)
w_c	crest width (in the direction perpendicular to shoreline)
w_v	vortex width
x'	distance along shoreline (non-dimensional)
x_b	distance from start of crest to breakpoint (positive values are seaward)
y'	distance from original shoreline to new shoreline (non-dimensional)
y_{end}	water depth at the end of the crest
y_{start}	water depth at the start of the crest
z	distance from still water level

α	peel angle ($^\circ$)
β	beach or bottom slope
$\beta_{foreshore}$	foreshore slope
β_{reef}	seaward reef slope
β_{orth}	orthogonal reef slope ($^\circ$)
ΔC	change in wave celerity
Δt	time interval
Δu	change in orbital velocity
η_b	setdown due to breaking
η_s	setup due to breaking
μ	free variable used by Longuett Higgins (1982)
θ_v	vortex angle ($^\circ$)
ρ	density of freshwater
σ	standard deviation
ξ_b	Inshore Iribarren number
ξ_o	Deep water Iribarren number

Chapter 1

Introduction

1.1 Outline

Artificial offshore submerged reefs are usually used as a means of beach protection and beach stabilisation. Multi purpose reefs are submerged reefs whose functions include improvements to the local surfing climate, coastal protection and biological amenity, with the added benefits of increasing tourism and economic spin off to the local community. They are thus becoming increasingly popular to coastal managers and engineers. Numerous multi purpose reefs are being planned in countries world wide, including New Zealand, Australia, the USA, India, Bahrain, Japan, Fiji, South Africa and the UK.

One difficulty in designing such structures is predicting the reef configuration required to break waves at a certain intensity (required for good quality surfing waves) under given wave conditions. This would allow the designer to minimise the volume of the reef, and thus keep construction costs to a minimum. Also, being able to predict breaker intensity based on the reef configuration and wave conditions will be useful in assessing the reefs ability to cater for a wide range of recreational wave riding activities.

Reef configuration is essentially the shape of the reef, and for the purpose of this thesis, it consists of the crest width (where the crest width is measured in the direction perpendicular to the shoreline), and the seaward reef slope, which is the slope of the reef on its seaward side.

It is the purpose of this thesis to report on the investigations carried out to ascertain the effect of the reef configuration on the breaking intensity of waves under various wave conditions. A new definition of breaking intensity developed by Sayce (1997), will be used. This definition is more useful in designing recreational surfing waves than the more traditional method using the Iribarren number. As a case study, an assessment will be made of a specific reef's ability to provide suitable surfing conditions based on the wave conditions, bed slope, reef configuration and the breaker intensity. This reef is situated off Kommetjie in Cape Town, South Africa and has been named 'Sunset' by the surfing community. A relationship between minimum reef width, bed slope and wave characteristics, will then be derived based on physical model tests. Design guidelines will be developed to assist in the design of artificial reefs for surfing purposes.

Chapter 2 presents the literature review, with conclusions and recommendations to be employed in the case study.

Chapter 3 presents a simplified theoretical explanation for the effects of the test variables on breaking intensity .

Chapter 4 presents a case study that describes the variables which are used to define surfability of a reef.

Chapter 5 presents the experimental laboratory study, with test results, procedures, graphs and results.

Chapter 6 presents design guidelines developed based on the results of the study.

Chapter 7 concludes the thesis, bringing together elements from the literature review and the case study. Recommendations for future studies are made.

1.2 Aims and objectives

The chief aims and objectives of the investigations are to:

1. Conduct investigations into the theory behind breaking waves, focusing on the estimation of the vortex parameters of a plunging wave;

2. Assess the wave dynamics on an existing, natural reef configuration that results in very large surfable breakers;

3. Assess the usefulness of a numerical modeling package, SPHysics, in the estimation of vortex parameters based on varying reef configurations and wave conditions;

4. Develop a relationship that can assist in the definition of the reef configuration required to cause waves to break at a certain intensity under given conditions, namely wave height, wave period and bed slope, using physical modeling, and site observations; and to

5. Develop design guidelines to assist in the design of surfability aspects of artificial reefs with regards to wave breaking intensity.

1.3 Methodology and structure of study

1.3.1 Literature review

The literature review gives a relevant overview of existing multi purpose reefs, wave breaking and design for surfing amenity. This highlights the early stages of development of multi functional reefs and the relevant challenges with respect to the existing design guidelines.

An introduction to multi purpose reefs is given, highlighting the existing design guidelines for each function of the reef, economic considerations and the main problems and challenges in designing for multi functionality. The fact that multi functional reefs are in an early stage of development compounds these challenges. This is expanded upon.

Special attention is then given to the breaker type, breaker height formulae and breaker depth formulae. A brief analysis of factors that may affect wave breaking such as bottom friction, focusing, shoaling, winds and currents has been included.

Surfability aspects and the relevant design guidelines are discussed. Surfability parameters such as breaking intensity, peel angle, wave height and section length are expanded upon as is their application to surfability and the design process. Types of surf breaks, ideal surf conditions and surfer skill level are included to highlight the importance of these aspects and the interdependence of each of the relevant factors on surfability.

Numerical modeling theory has been discussed, along with the various types of numerical modeling methods. One of the more recently developed methods, Smoothed Particle Hydrodynamics (SPH), has been expanded upon in order to evaluate its potential for studying wave breaking, and more specifically, breaking intensity as defined by Sayce (1997). Details of SPH in coastal engineering applications are discussed, followed by the open source numerical model package, SPHysics. The merit of the package is assessed by means of numerical model runs.

The main findings of the literature review are then summarised and discussed.

1.3.2 Main investigation

The theoretical study involved the qualitative assessment of the effects of the test variables on vortex shape parameters of plunging waves. These parameters are used to describe the shape of the vortex formed when waves break as plungers. Simple theoretical approximations are made based on linear wave theory, breaker depth formulae and breaker height formulae.

The case study was done in order to illustrate how sea bed topography and wave conditions combine to form good quality surfing waves. A reef situated just off the coastline near Kommetjie in Houtbay was selected for the case study. Wave records were obtained on a particular day that provided good quality surfing waves. A qualitative evaluation of the wave refraction and focusing patterns on and before the reef was done. Wave heights and breaking wave vortex parameters were estimated from images obtained from the internet. Bathymetric charts allowed the extraction of the reefs topography. The corresponding seaward reef slope and reef width was then determined, and used to estimate the degree of wave focusing through the West-Cowell surfing reef factor S_{rf}.

Physical model laboratory tests were conducted varying the wave height, wave period, water depth on the crest, seaward reef slope and crest width. The seaward reef slopes ranged from values typically found at the better surf spots and where plunging waves were expected. Breaking intensity was measured using the measurements of breaking wave vortex parameters as described by Sayce (1997). The effects of the junction at the start of the seaward reef slope and the horizontal crest has been discussed.

Guidelines were developed based on the theoretical studies, case study and laboratory test results. These could contribute to the design of submerged reefs for surfing purposes.

Chapter 2

Literature Review

2.1 Introduction to multi purpose reefs

Multi purpose reefs force breaking of waves and create calmer waters on their lee side. Under certain conditions, they can be used as a means of beach protection, harbour protection, recreational amenity creation in terms of beach walking, sun bathing, wave riding, diving, fishing, and other forms of recreational amenity. They are also used in attracting fisheries biomass, and economic benefits make the structures attractive to engineers and coastal managers. Much research has been done in the field, but, at the same time, much still needs to be done in order to improve on inconsistencies in research results, and to standardize current design procedures and guidelines. Artificial multi purpose reefs are in a relatively early stage of development and just one multi purpose reef has been constructed to date. The reef is known as Narrowneck reef and is situated on Australia's Gold Coast. Several more reef projects are currently underway in other parts of the world.

2.1.1 History of artificial multi purpose reefs

The Narrowneck Reef

The first artificial multi purpose reef was built at Narrowneck on Australia's Gold Coast in 1998 (Figure 2.1). It was built to promote stabilisation of the beach and was designed to be used in conjunction with a sand nourishment scheme (ASR 2002b). Traditional methods such as groynes and rip rap were considered at design stage, but the multi purpose reef option was selected because of its ability to cater for recreational activities and the economic spin off it was expected to generate (ASR 2001).

Figure 2.1: The Narrowneck Reef (Ranashinghe and Turner 2006)

Raybould and Mules (1998) , found that for every (Australian) dollar spent on enhancing the beach, Aus$60-80 would be returned via tourism through surf competitions and beach usage. The reef, including feasibility studies and construction, cost a total of Aus$ 8.5m (Ranasinghe et al. 2002).

The reef was constructed from geotextile sandbags filled with 200,000m^3 of sand from a beach nourishment project (ASR 2002b). Blenkinsopp (2003), found some problems in the surfability of the reef caused by the large bathymetric steps formed by placing the bags on top of each other. These produce steps in the breaking wave face which are undesirable for surfing.

The reef was designed in two arms with a deep narrow channel between the two arms (Figure 2.2). The design of the reef configuration incorporated beach protection, surfability and biological enhancements aspects. The deep channel provides a rip current to assist wave riders to return to the point where their ride begins with little effort. Current results from reef surveys show that much sand has settled around the perimeter of the structure, and that many of the sandbags are buried.

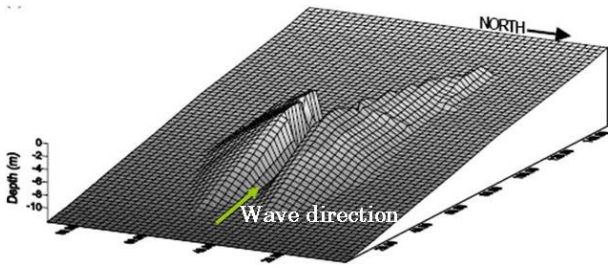

Figure 2.2: The Narrowneck Reef design (Ranasinghe et al. 2002)

Jackson et al. (2005) conducted monitoring of the reef and the Narrowneck Beach and concluded the following:

- In the lee of the reef, seasonal accretion and recession have been noticed and over a period of four years, a beach width of approximately 30m has been attained.
- Biological enhancement (marine ecology) within and on the reef has been better than expected.
- The number of surfers in the water and the occurrence of good surfing waves has increased.
- The reef size could have been reduced, and still have obtained similar results. This would have decreased the construction costs.

The stages of beach accretion and recession noticed on the Narrowneck Reef coincide roughly with the spring/summer and autumn/winter seasons respectively (Jackson et al. 2005). Figure 2.3 shows the extent of the beach profile and the salient that has been created on the lee side of the reef.

Figure 2.3: Beach growth on the lee side of the Narrowneck Reef

From top left, counterclockwise: (a) The beach after storms in March 1999 before the reef was in place, taken at high tide (Mead and Black 2002); (b) The beach after storms in March 2002, after construction of the reef and nourishment, taken at high tide (Mead and Black 2002); and, (c) a view of the salient looking southwards, June 2003 (Jackson et al. 2005))

The findings of Jackson et al. (2005) show that artificial reefs can successfully be used as beach protection and amenity/biological enhancement tools in todays economic driven age. The full beach protection, biological, amenity, economic and social benefits are yet to be realised.

Reefs for surfing purposes alone have been built at Cable Stations, Fremantle, on Australia's West Coast and at El Seguendo, California, in the USA with limited success.

The Cable Stations Artificial Surf Reef

The reef at Cable Stations (Figure 2.4)was built by placing large granite rocks out at sea (Bancroft 1999).

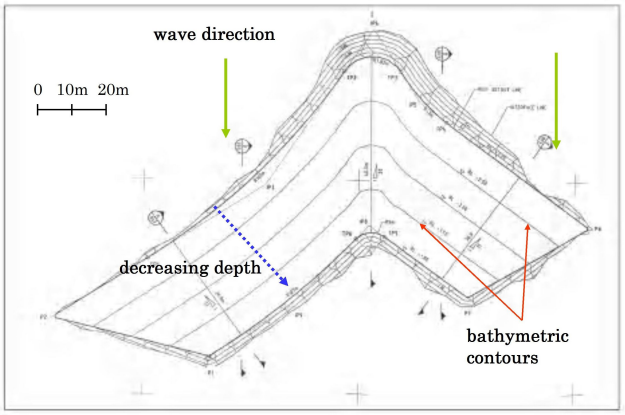

Figure 2.4: Reef design for Cable Stations surf reef (Adapted from Bancroft (1999)).

Two different sizes of stone were used: 1,5 ton units for the reef structure, and 3 ton units for the perimeter of the structure (Bancroft 1999). Construction began in January, 1999, and was complete by December 1999. The reef, including feasibility, design and construction, cost AUS$1,51m (Ranasinghe et al. 2002).

According to *surfermag.com* (2002), it produces ridable waves for more than 150 days a year, and has exceeded expectations with respect to design surfability criteria, (Bancroft 1999). It was built at a site that had no surfing climate, to explore the possibilities of creating good surfing waves. According to (Bancroft 1999), performance of the reef increased significantly after some depressions in the reef structure were filled up with stone units.

Figure 2.5: The Cable Stations reef (left); and surfing conditions on the Cable Stations reef (right) (Bancroft 1999)

Pratte's Artificial Surf Reef

Prattes reef was built in 2001 in El Seguendo, California, USA, to repair damage done to the surfing climate due to coastal development. It did not work because of its small size (Figure 2.6), which was the result of very little funding. In this case, the incoming waves were not significantly affected by the reefs presence (Borrero and Nelsen 2003), and the reef was ineffective.

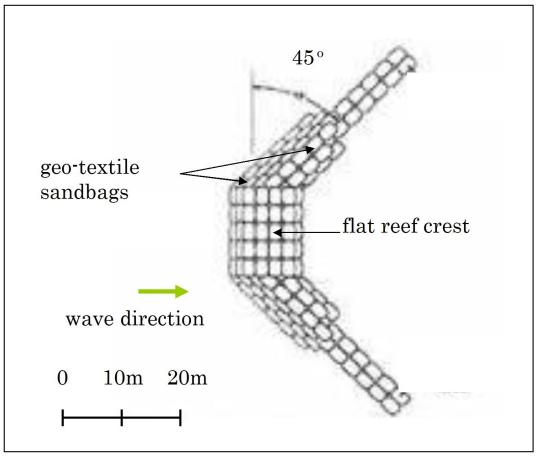

Figure 2.6: Reef design for Prattes reef (Adapted from Borrero and Nelsen (2003)).

Also, dive surveys revealed that the majority of the reef had settled into the sea bed, and were subsequently buried with sand. Furthermore, the reef was constructed from geotextile sandbags, which, in some places became torn, leading to a loss of sand. The initial total volume of the reef was approximately 1600m^3.

Surfers have been seen surfing the waves on the reef, but the reef is deemed as a failure due to the low numbers of good quality waves produced by the reef, caused by its small size. Figure 2.7 gives a good comparison to the performance of Pratte's Reef and the performance of a surf break 2 km to the south. The surfability of the surf break at El Porto (right image in Figure 2.7) has coincidentally been enhanced by a underwater pipeline which assists in orienting the sand in a configuration favourable for the creation of good quality surfing waves.

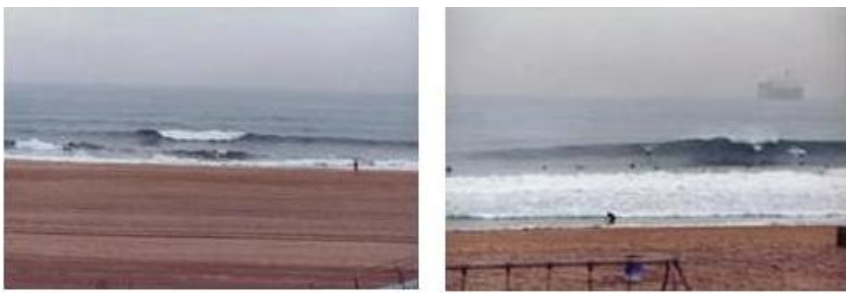

Figure 2.7: Surfing conditions on Prattes reef (left), and 2km south at El Porto (right), on the same day (Borrero and Nelsen 2003)

2.1.2 Multi purpose reefs as a means of beach protection

Annually, millions of cubic meters of sand is moved (longshore and offshore) along the coastlines of the world. It is disturbed by wave action and turbulence, transported by currents, settles, and the process repeats. The beaches retreat and accrete daily, weekly, monthly, seasonally and annually, in varying degrees depending on the local wave climate, which results in very little change over long periods of time. This process is known as a dynamic equilibrium if there is no net loss or gain of sediment along the coastline considered.

At the same time, development (buildings, roads, etc.) occurs close to the sea. In times of large storms, strong winds and heavy seas, these developments sometimes become threatened. Groynes, piers, jetties, reefs, are often used in beach protection measures. Rocks can be dumped as revetments or concrete structures built as seawalls. Sand nourishment schemes are used to feed areas lacking in sand by pumping it from areas where there is an excess of sand. These methods of beach protection all have their own advantages and disadvantages.

Groynes, piers and jetties all trap sand as it is transported by longshore currents. An accreting beach profile is created on the net updrift side of the structure while an eroding beach profile is created on the net downdrift side. These structures are sometimes considered by the public to be have a negative aesthetic appeal.

Rock revetments and sea walls are built on shore as a solid barrier of protection between the sea and the land. They usually accelerate erosion of a beach as they prevent absorption of the water on the beach. In this case, incoming wave energy is not dissipated on the beach, but reflected off the revetments, moving sand back in to the sea. Dyer (1994) found this to be the case in the central areas of the St Clair seawall in Dunedin, New Zealand. They sometimes make it difficult to gain access to the beach and seldom complement the aesthetics of the area, ((Dyer 1994); (USACE 1995)).

Beach nourishment takes sand from one place and relocates it to another to replace sand lost during erosion. The sand is dredged and either pumped or transported by dredger or barge. Beach nourishment is quite attractive to the public as it often results in a wide beach which is favoured by beach users for sunbathing, walking and other recreational sporting activities.

Detached breakwaters (Figure 2.8) are similar to seawalls and breakwaters in that they reflect wave energy, but are situated offshore.

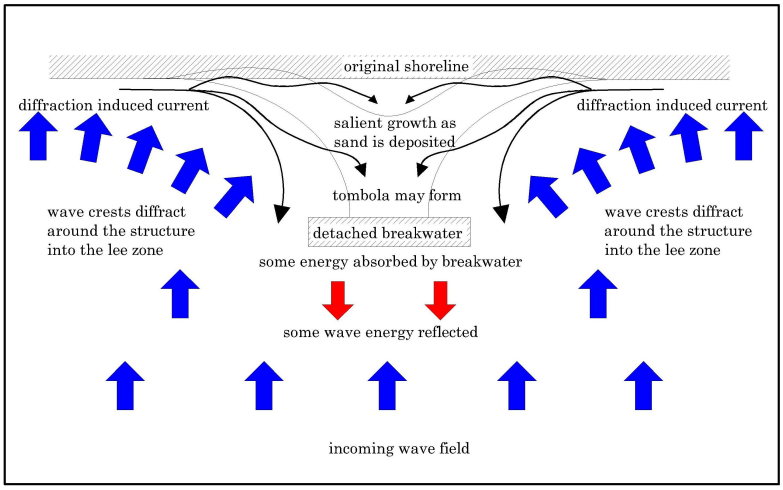

Figure 2.8: Wave and current dynamics around a detached breakwater

Their crests are usually above water level. They block wave energy from passing and so

minimise wave action on their lee side. Here wave diffraction around the breakwater is more prominent than for submerged reefs and more reflection occurs directly off the seaward side of the breakwater. The wave diffraction causes the wave crests to align themselves non-parallel to the original shoreline, as shown in Figure 2.8. A diffraction (radiation stress) induced current is formed, running parallel to the shoreline, which carries suspended sediment with it into the sheltered region on the lee side of the structure. Here it settles because of the reduced wave energy behind the structure. A depositional feature known as the salient will grow seaward, and can achieve equilibrium as either a salient or a tombola (if the new shoreline reaches the detached breakwater).

Reefs promote wave breaking and subsequent dissipation of energy mainly through breaking and bottom friction to a lesser extent, but also through air entrainment. The main difference between detached breakwaters and submerged breakwaters (reefs) is the amount of wave energy allowed to pass over the structure. Detached breakwaters block the majority of the energy while reefs allow a large deal of the wave energy to pass to the lee side of the structure. Reefs create converging current flows on the lee side due to the setup established on either side of the area directly shoreward of the reef. Sand is gradually deposited in this area, and in the longer term a salient forms. Typical wave and current dynamics for a low crested structure are illustrated in Figure 2.9. The reefs are usually not visible as they are, in most cases, situated below the water level.

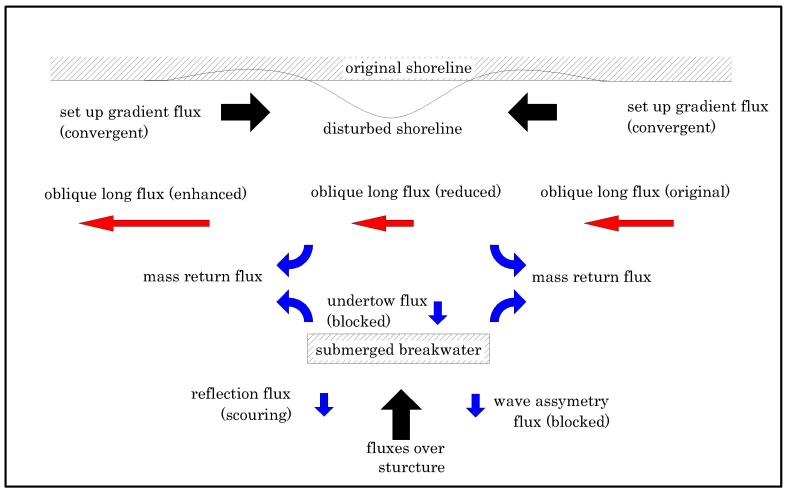

Figure 2.9: Wave-driven sediment fluxes for a longshore uniform beach with a submerged low crested structure . (Adapted from Cáceres et al. (2005)).

Table 2.1, (ASR 2002a), compares four methods of beach protection. It suggests that submerged reefs hold more advantages than the other three methods of beach protection highlighted.

In contrast to Table 2.1, Ranashinghe and Turner (2006) concluded that there is insufficient data to predict the processes that are responsible for accretion/erosion in the lee of the reef and also, whether or not accretion or erosion would in fact occur. They also conducted physical and numerical studies and concluded that:

- shoreline accretion will occur in the lee of submerged structures located on coastlines with significant ambient longshore sediment transport, and
- shoreline erosion will occur in the lee of submerged structures located on coastlines with predominantly shore-normally incident waves.

Table 2.1: Comparison of beach protection measures (ASR 2002a)

	Groynes	Submerged Reefs	Detached Breakwaters	Nourishment
Effectiveness	Most effective when there is a predominant alongshore transport direction (wave-driven or tidally driven). Can result in cross-shore loss of sand if too long due to the jetting of sediment offshore	Most effective in areas where erosion is driven by waves. Can incorporate both wave dissipation and wave rotation principles to retain sediment on the beach.	Most effective in areas with low alongshore sediment transport, unless well-designed to ensure no tombola formation. Good dissipation, but cannot incorporate wave rotation aspects for sediment retention.	Most effective in areas of low alongshore sediment transport,unless used in conjunction with control measures (e.g. submerged reefs, groynes or detached breakwaters). Sustainable issues related to source
Aesthetics	Immediate intrusion on beach aesthetics and natural character. Can block alongshore beach access.	Very low aesthetic impacts, since always covered by water.	Exposed crest reduces the natural character of the coast and from the perspective of persons on the beach replaces the feeling of the open coast with that of being enclosed.	Positive aesthetic impacts, as long as similar colour and grain size is used.
Public Safety	Creates strong offshore directed wave driven circulation currents adjacent to groynes due to compartmentalization. Prevalent for longer groynes at Bournemouth, and further studies are recommended.	Increased public safety, lower waves and currents at the beach (e.g. 67% less rescues in the vicinity of the Gold Coast reef (Jackson et al, 2005)). Any changes to currents are confined to the immediate area of the reef (e.g. Mead et al, 2004) and currents are directed inshore, rather than offshore as can occur with groynes.	Increased public safety at the beach (as long as no tombola formation). Potential safety problems on the structure, since protrudes above water level.	No negative impacts to public safety unless courser grain size is used (can lead to stronger plunging waves).

Cáceres et al. (2005) conducted numerical modelling and from their results formulated a diagrammatic representation of the processes that result in the formation of a salient on a sandy shoreline (Figure 2.9).

In an assessment of shoreline response to submerged structures, Ranashinghe and Turner (2006) examined work done by Black and Andrews (2001b) and Sylvester and Hsu (1997). They investigated the effectiveness of submerged reefs as a means of beach protection. The study of Black and Andrews (2001a) involved natural submerged reefs. They formulated an empirical relationship (Eqn. 2.1) by curve fitting and sensitivity analysis between reef dimensions and shoreline response. They studied a large number of naturally occurring salients from aerial photographs. The growth of the shape of the salient was proposed as follows;

$$y' = -0.052 + \frac{1.187}{\left\{1 + \exp\left[-\frac{(x' - 0.606 ln(2^{1.65} - 1) - 2.649)}{0.606}\right]\right\}^{0.606}} \tag{2.1}$$

where x' is the distance along the shoreline and y' is the distance from original shoreline to the new shoreline. Both x' and y' have been normalized with the respective maximum salient dimensions, and so the equation predicts only the shape of the salient. The profile takes on the following shape (Figure 2.10):

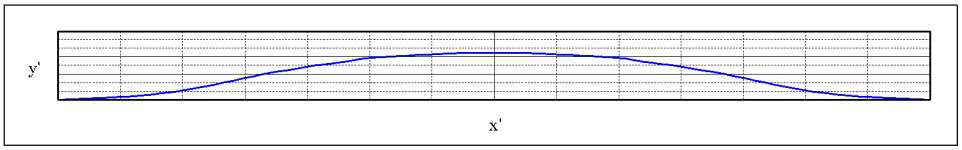

Figure 2.10: Normalized salient shape: Eq. 2.1 (Black and Andrews 2001a)

Sylvester and Hsu (1997) developed a similar relationship for emergent (low crested) breakwaters. Ranasinghe et al. (2002) compared these relationships with natural and man made prototype submerged structures and found inconsistencies in erosion/accretion trends with respect to changing environmental parameters such as wave height and period, direction, tidal range, beach slope, length and width of structure, crest level, structures accompanied by shoreline nourishment programs and longshore sediment transport rates. They state that with emergent structures, accretion is always expected to result on the lee side of the structure.

Ranashinghe and Turner (2004) then conducted physical and numerical modelling of a submerged structure and concluded that a structure very close to the shore resulted in erosion while one farther resulted in accretion. They mention that wave incidence angle and crest level have important effects on the magnitude of the shoreline response, but not on the mode of the response, i.e., accretion or erosion. They developed Figure 2.11 and Figure 2.12 to describe the wave and current dynamics on the lee side of the structure. They also found that the flow over the structure at a particular point is proportional to the wave height over that point (Ranashinghe and Turner 2004).

Cáceres et al. (2005) have similar conclusions. Ranashinghe and Turner (2006) and Ranashinghe and Turner (2004) concluded that more research into shoreline response is necessary to develop a means to predict the level of accretion and erosion at a particular site based on easily measurable environmental conditions. This is essential for the design phase. Cáceres et al. (2005) mention that the breaking of waves with varying freeboard and wave height can have the effect of modifying the mode of shoreline response, i.e., from accretion to erosion or vice versa.

Ranashinghe et al. (2006) then developed an empirical method (based on figures) to be used in the design process. The relationship is based upon numerical and physical model tests, and is to be used as a tool in the design process. The graphs they developed give a relationship between the anticipated magnitude of shoreline response and the distance to the apex of the structure crest from the undisturbed shoreline, the alongshore length of the structure, and the natural surf zone width. They recommend more tests to provide additional data points in their data set to increase the robustness of their empirical relationship. They also recommend that the relationship should only be used as a preliminary engineering tool.

Thus, in order for a multi purpose submerged structure to be successfully designed for beach protection, one needs to asses carefully the effect of varying wave heights with varying freeboard (tidal variation), and possibly even the effect of breaker intensity on the energy dissipation over the reef.

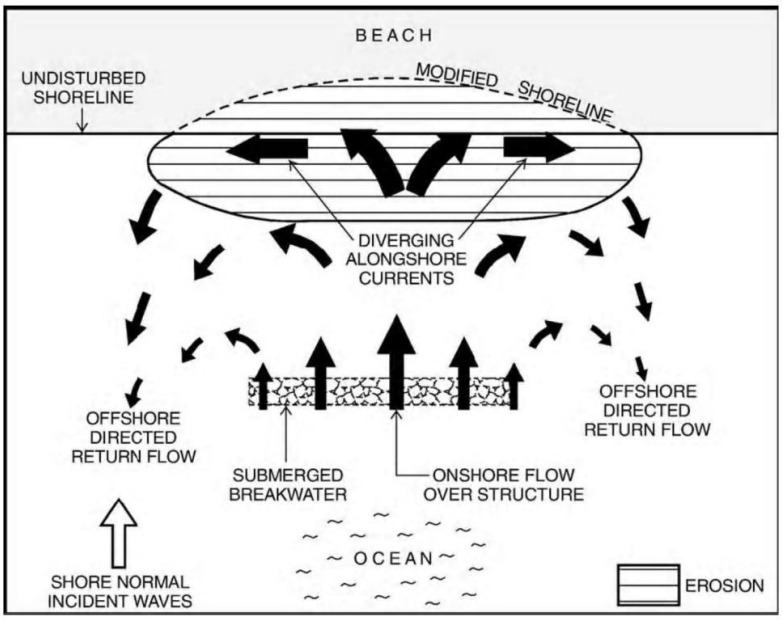

Figure 2.11: Schematic depiction of expected nearshore circulation patterns and associated nearshore erosion pattern that may lead to shoreline erosion in the lee of a submerged breakwater under shore-normal wave incidence (i.e. negligible longshore sediment transport)(Ranashinghe and Turner 2004).

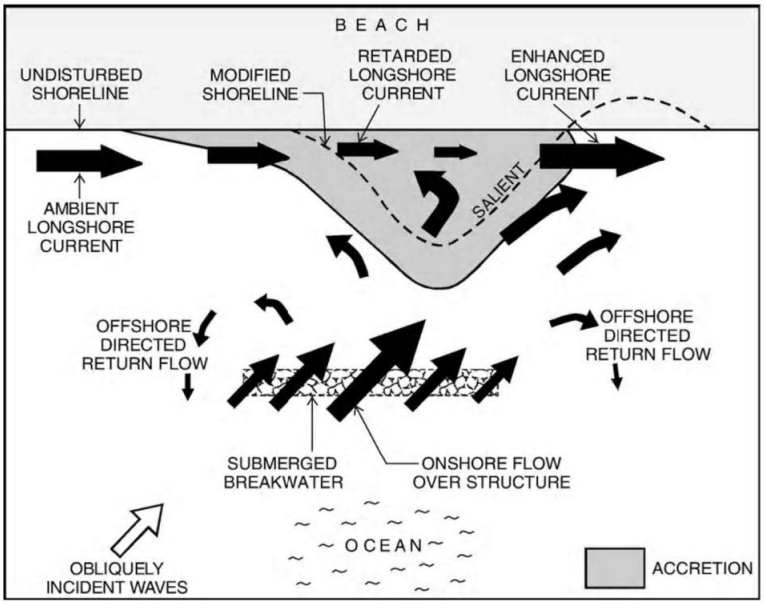

Figure 2.12: Schematic depiction of expected near-shore circulation patterns and associated near-shore accretion pattern that may lead to shoreline accretion in the lee of a submerged breakwater under oblique wave incidence (i.e. significant longshore sediment transport)(Ranashinghe and Turner 2004).

To conclude, changes in energy dissipation over the reef can result in varying energy circulations in the lee of the reef. Based on the work of Black and Andrews (2001a), Ranashinghe and Turner (2004), Ranashinghe and Turner (2006), Cáceres et al. (2005) and Ranashinghe et al. (2006), the intensity with which waves break, may in fact, have an effect on the mode of shoreline response.

2.1.3 Multi purpose reefs as a means of breakwater and seawall protection

Harbour breakwaters are used to protect moored ships from wave and current action and seawalls are usually built to protect the shoreline from wave and current action. Submerged structures on the seaward side of such protective structures can be used to reduce the wave heights at the structures. Generally, larger incident wave heights and periods mean larger and higher structures. Reducing incident wave heights means reducing the sizes of these protective structures. Submerged reefs can reduce wave heights, but they are a separate structure to the breakwater (or sea-wall), with a different construction method and cost. Thus, submerged reefs can reduce the cost of construction of the breakwater or seawall, but whether this will reduce the combined cost of the two structures together, is dependent primarily on the site conditions.

A New Zealand project has included an artificial surf reef as part of a port expansion plan. A multi purpose reef has been planned for the Port of Gisborne, as a means of protecting the breakwater and to provide amenity in the form of diving, snorkeling and surfing (Turnpenny et al. 2003). The reef structure is expected to assist significantly with reinstating the marine biology which is expected to suffer due to the port expansion program.

Practical problems with submerged structures for seawall/breakwater protection have been investigated in some extent by Dean et al. (1997). They constructed a large prototype narrow submerged structure and identified two significant mechanisms which are important in offshore breakwater design. They found that a low crest height may allow so much water to flow over the breakwater that resulting longshore flows will outweigh the benefits of a small reduction in wave height and cause beach erosion landward of the breakwater.

Furthermore, based on numerical model results, they found that the volume of water flow over the breakwater is only slightly affected by the offshore location of the breakwater. They also found that the longshore currents vary inversely with this distance.

They recommended that comprehensive designs must consider the full range of hydrodynamic variables, breakwater variables and sedimentary effects. They attributed the lack of further development of submerged structures as breakwater protection to the lack of understanding of mechanisms that were not fully understood at the time.

2.1.4 Multi purpose reefs as a means of biological enhancement

Much research has been carried out into the area of biological habitation of artificial reefs with respect to biological, environmental and physical conditions. Burgess et al. (2003), list conditions that will affect the degree of colonisation of the reef, namely:

- Depth range of the reef,
- Size of the reef,
- Micro and macro topographic complexity,
- Wave conditions,
- Distance to biological source,

- Direction and current strengths in relation to sources,
- The timing of construction works,
- Nature of fouling assemblage (pollutants), and
- Geotechnical foundation of the reef

The degree of colonization of a multi purpose reef at the design stage seems to be a difficult task to predict. Bohnsack and Sutherland (1985), found that it is unlikely that the artificial reef will mimic a natural reef. They concluded that being able to predict species abundance and diversity associated with an artificial reef will be a function of how the size, shape, complexity, location, and latitude of the reef interacts with particular species and how local species interact among themselves in this environment. The biological enhancement is therefore reliant upon a number of factors and so the nature and extent of colonization will be extremely site dependent. Like surfing reefs, where only occasionally do the factors all come together to make a high-quality surfing break, the same is true of habitat for specific species. There is, however, a degree of uncertainty that artificial reefs do in fact increase the biomass of the marine population. One school of thought is that the reef will only serve in attracting existing marine life from other areas of the ocean. In this way it will not be increasing the biomass, but will only relocate it. Pickering and Whitmarsh (2007), however, note that the majority of species in the oceans are not limited by their number of offspring, but by the availability of habitat for them to colonize and inhabit.

In Indonesia, coral reefs have become threatened by poison fishing, blast fishing, coral mining, over fishing, and sedimentation (Hidayati 2003). These activities are placing these high potential assets for Indonesia at risk. Hidayati (2003) estimates that about US$15,000 worth of coastal products through fisheries and tourism (curio's, coral mining, etc) can be produced from one kilometer of healthy reef per year while from coastal based tourism; the value varies between US$ 3,000/km^2 in low potential tourist areas and about US$500,000/km^2 in high potential tourist areas. Indonesias reefs comprise a total surface area of 75000 km^2 (Hidayati 2003). It should be noted that these high economic potentials, however, are significantly reduced by the degradation of the reefs, in the form of coral mining, blasting and other detrimental activities.

It seems then, that artificial reefs do in fact have a place assisting in biomass habitat creation. For example, the artificial reef off Durban at Vetches Pier, the remains of the first breakwater for the port of Durban, has been declared a conservation area due to the high degree of marine life inhabiting it.

From the results of Narrowneck reef, Burgess et al. (2003) note that reef can be used also as a means of increasing recreational amenity with respect to diving, fishing, boating, etc, and there can be beneficial economic benefits associated with these impacts.

Burgess et al. (2003) recommend that ecological considerations should be incorporated in the designing process to reduce alterations to the local ecology and increase amenity. They also recommend ecological surveys of natural reefs in similar water depths and wave exposure as planned artificial reefs to be conducted to assist the designers in estimating the degree of colonization of future artificial reef projects.

2.1.5 Multi purpose reefs as a means of recreational surfing amenity

In incorporating amenity into their design, multi purpose reefs could serve the purpose of attracting more public to the beaches. Many people enjoy time spent on the beach and public

beaches are often seen by members of the public as places where they can rest, go on holiday, sunbathe, swim, beach walk, play sports games and surf the waves. The wide variety of amenity that the reefs can potentially offer by way of increasing beach width and improving surfing conditions is attractive to coastal managers as it offers a degree of public benefit. The full extent of amenity varies between beach walking and beach combing, playing sports on the beaches, swimming in the sea, sun bathing, diving, boating and surfing.

There are two types of surf reefs that can be used when incorporating surfing amenity into multi purpose reef structures. One is placed in the breaker zone so that it may force breaking of waves in a manner suitable for high quality surfing waves. Much research has been done on these types of reefs. However, there still exists much room for further research into the field. As mentioned earlier, three such reefs have been built with surfing either as the main or one of the main design objectives, these being Narrowneck's multi purpose artificial reef in Australia, Cable Stations surf reef in Australia and Pratte's surf reef in USA.

Another type of surf reef has been proposed by West et al. (2003). Here the shape of the incoming waves is altered (Figure 2.13) prior to reaching the surf zone, so that upon reaching the surf zone the waves break in a manner required for good quality surfing waves. This type of reef refracts incoming parallel wave crests, so that the portions of the wave crests of greater wave height break in deeper waters, while the portions of lower wave height break in shallower waters. These reefs are still in the concept stage, and none have been constructed as yet. Both West et al. (2003) and Black et al. (1997) have noted that these reefs do occur in nature, and very often result in improved surf conditions (refer to the case study in Chapter 4). The main advantage of these reefs over the more conventional reef is a smaller reef size which reduces construction costs. Also, they are placed outside of the breaker zone, which reduces time spent at sea during the construction process and damage caused by waves breaking on the reef.

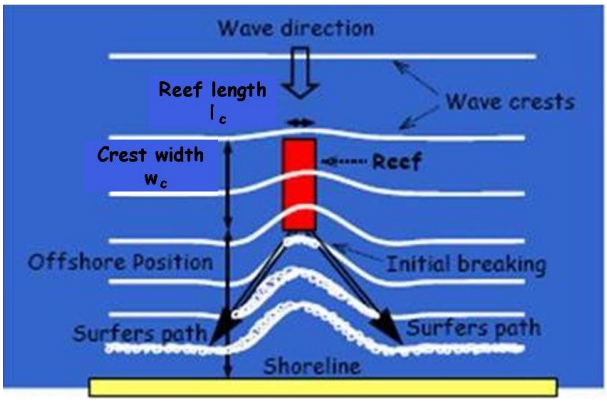

Figure 2.13: The wave focusing reef concept (West et al. 2003)

There are a variety of different types of wave riding disciplines (Figure 2.14). These all require a specific kind of 'board', including surfboards, kneeboards, body boards, kayaks, surf skis and their own bodies. Further subdivisions reflect differences in surfboard design. Longboards are long and wide in comparison to shortboards. Malibus and Mini-Mals form the transition between long and short boards. Tow-in surfing involves motorized craft to tow the surfer onto the wave, this is associated with big wave surfing, where standard paddling is unwise due to the waves rapid forward motion. These surfboards are long and thin in comparison to longboards and are built as such for stability and speed. Some offshoots of surfing make use of the wind. These include kitesurfing and windsurfing. For the purpose of this thesis recreational surfing will be used as a general term that encompasses all wave riding disciplines.

The skill of a surfer is greatly dependent on factors such as equipment, availability of good quality surfing waves, exposure to high levels of surfing skills (such as surf movies and access to world class surf events as competitors and spectators), practise time, and of course, talent. As with any sport, increasing the number of practise facilities should give an increase in the number of people using the facilities. Newer facilities may also make this sport more attractive to people who have not ever experienced the sport, and thus increase the number of people who

Figure 2.14: Various types of wave riding activities
Left to right, from top left: Shortboard surfing; kneeboarding; bodyboarding; longboarding; shortboard surfing on waves of extremely high breaking intensity; tow in surfing; windsurfing a wave; windsurfer using waves as a launching platform; and, kitesurfing a wave.

begin to participate in the sport. This would then increase the skills range of the group, i.e; the most skilled participants are more skilled, because there is now a higher probability of finding a more talented individual.

Multi purpose reefs will also create more surfing locations. This would reduce overcrowding. Overcrowding sometimes results in conflict situations between surfers over 'right of ownership' of waves. Multi purpose reefs would, as discussed earlier, increase the number of people attracted to the sport, and so may in the long run increase the problem of overcrowding.

A reef designed for the full range of recreational wave riding activities would be beneficial as it would cater for the types of wave riding suited to the particular conditions occurring on a certain day. No design guidelines that can be used to estimate the numbers and types of wave riding activities that could use the reef under varying wave conditions have been found in current literature.

2.1.6 Economic considerations

Some concepts of the economy of artificial surf reefs will be discussed briefly here as an introduction to the concepts. In short, it seems that the economical benefits have yet to be fully quantified. Many studies have been done to quantify the economic benefits associated with the construction of an artificial reef at a particular site. These center around the following factors:

- Tourism: The reefs promote widening and stabilisation of the beach in its lee, and creates

highly attractive destinations to members of the public who enjoy using the beaches for sun bathing, strolling, swimming, shell combing and other relaxing pastimes. With more people using the beaches, there are economic spin-offs which benefit nearby businesses and real estate.

- Surfing competitions: These can realise a large proportion of economic spin-offs. Income generated from a single surfing competition has been estimated to be in the order of Aus$2.2m (Raybould and Mules 1998))

- Surf related businesses: Sales and rentals of surf equipment and apparel will increase due to the increase of number of surfers who surf on the reef. Weight (2003), mentions that the construction of reef for surfing will encourage more people to enter the sport and encourage more spectating.

- Marketing oppurtunities: Weight (2003) notes that the reefs should increase the marketing effectiveness and open up new avenues to attract tourists to the surf location.

Cost/benefit ratios have been based on the above four items and are estimated to range from 1:20 in Bournemouth, UK, to 1:70 for the Narrowneck Reef on Australias Gold Coast (ASR 2001). Also, offshore reefs can prove less expensive in the long term than traditional methods of beach protection such as sand bypassing (ASR 2001). In Noosa, Australia and St Francis Bay, South Africa, significant erosion has occurred. Costs to protect properties from the resulting beach erosion has been estimated as millions of US$. With allowance for annual maintenance, the cost/benefit ratio for the Northern Gold Coast Beach Protection Strategy was estimated at 1:80 (MHL 2002). Table 2.2 gives some cost benefit ratios at some locations around the world.

In general, construction costs vary considerably and are very dependent on the location. Availability and costs of mining and dredging sand, quarrying and transporting rock, concrete, labour costs, geotextiles, construction plant, wave conditions all contribute to the large variability in construction costs between the different beach protection options. Typical values from some sites around the world are shown in Table 2.3. These cost values have been shown to give the reader and idea of the relative cost of each of the options. The general trend is that sea walls and groynes seem to be the cheapest options, followed by sand bypassing and then artificial reefs.

Numerous methods have been devised for the construction of artificial reefs. These include pre-cast concrete units, geo-textile containers filled with sand, polyethylene pipes, rock and concrete caissons.

Table 2.2: Economics of some artificial reef construction projects around the world

Location	Country	Estimated Construction Cost (Million)	Cost Benefit Ratio	Reference	Notes
Newquay	UK	£6.0	-	Weight (2003)	For 1 reef only.
Narrowneck	Aus	AUD 8.8	1/70	Boak et al. (2000)	for 1 reef only
Noosa Main Beach	Aus	AUD 5.0	1/20	Jackson et al. (2005)	for 2 reefs
St Francis Bay	SA	ZAR 5.5	-	Mead et al. (2006)	for 1 reef only
Cornwall	UK	-	1/20	Mead and Black (2002)	for 1 reef only
Northern Gold Coast	Aus	-	1/80	MHL (2002)	In conjunction with artificial reefs

Construction costs rise significantly with time spent at sea, so it seems that savings can be made on reef units that are constructed on land such as caissons, pre-cast units, (naturally mined) rock and then placed in the ocean. The use of geotextiles generally requires the filling of the sand bags from dredge material at sea. The sand filled bags are then placed in position from the dredger. Delays in construction due to unpredictable sea conditions and damage to construction plant and equipment during intense storms increase construction costs dramatically. Although there are only a few locations analyzed, Table 2.2 indicates that the benefits of artificial reefs far outweigh the initial construction costs. It should be noted that the data in Table 2.2 has been extracted randomly from a variety of sources and papers.

Table 2.3: Overall construction cost of some planned beach protection projects

			Estimated Cost (Millions)					
Region	Country	Currency	Do Nothing	Sea walls	Sand Nour-ishment	Groynes	Offshore Sub-merged Reef	Reference
Montevideo	Uruguay	US $	23.0	17.1	49.4	-	-	Saizar (1997)
Montevideo	Uruguay	US $	627.2	41.9	118.0	-	-	Saizar (1997)
Strand	South Africa	ZAR	-	2.2	-	-	4.3	Theron (2002)
Waneroo	Australia	AUS $	0.2	1.4	1.6	1.0	1.8	Bohnsack and Sutherland (1985)
Gosford	Australia	AUS $	1.3	1.4	2.1	-	-	MHL (2002)
Gosford	Australia	AUS $	-	0.1	0.2	-	-	WBM (1995)

2.1.7 The challenge of designing for multi functionality

Depending on site conditions, sometimes complete multi functionality is difficult to achieve. Various reefs have been planned world wide in a range of different locations. Some were designed for surfing only, while others have been intended to incorporate biological enhancement, harbour protection, artificial moorings, coastline erosion and flooding protection and additional recreational amenity such as diving and snorkeling.

The Cable Stations Artificial Reef in Fremantle Australia was designed as a stand alone surfing reef. It produces surfable waves more than twice as much as was what it was designed for (Bancroft 1999). This was attributed to the subjective nature of the surfability observations as opposed to the strict criteria for surfability that was imposed on the reef in the design phase. Bancroft (1999) concluded that the reef was successful in obtaining its design objectives.

A reef in Dubai was planned on the Jumairah section of coastline. This reef was designed as a means of coastline protection and to increase recreational surfing amenity (Mocke et al. 2004). They noted that under the site conditions, it proved difficult to combine the two design objectives into one structure. They attributes this to the fact the narrower form of the reef designs that suit surfing were providing only limited wave sheltering for the adjacent coast.

ASR Ltd, a New Zealand based multi purpose reef company, conducted the design process for a reef in Mt Manganui in New Zealand. The primary objective of this project was the enhancement of the local surfing conditions. The extent of shore protection offered by the reef to the adjacent coastline was unknown, and one of the objectives was to form a basis for research into the coastal protection, amenity enhancement, biological response, and social and economic aspects (Black and Mead 1999).

Weight (1990) conducted a multi purpose reef study in Newquay, UK, and investigated a number of issues but essentially the key questions were regarding surfability, effects on environ-

mental parameters such as sand movements and rip currents, and additional benefits such as fisheries biodiversity and educational opportunities for under and post graduate students in the field.

In Ireland, O'Leary et al. (2003) conducted feasibility study into multi purpose reefs. In his study, no surfing amenity was incorporated. The study focused on fisheries protection, increasing biomass, recreational fishing, diving and snorkeling and reducing coastal erosion. In Scotland, Nautilus (2003), also included reduction in flooding and enhancements to surfing amenity. Both reports were feasibility studies to ascertain the pros and cons of multi purpose artificial reefs.

Another multi purpose reef has been planned at Orewa Beach in New Zealand. Mead and Black (2005) found that increasing the distance from shore would increase bio-diversity but decrease amenity enhancement. Also, the large tidal range relative to the wave conditions resulted in most of the waves passing over the reef without causing breaking. This complicated the design process.

Some tidal related advantages were discovered in Pondicherry, India, with the proposed offshore, submerged reef for coastal protection, recreation and public amenity (Neelamani and Sundaravadivelu 2003). The chief objectives here were to create a salient to protect the beach, and to enhance coastal amenity value by incorporating multiple use options of fishing, habitat, tourism and water sports such as surfing, diving, water games and sheltered swimming while still preserving the existing beach character and village use. Here the low tide levels reduced the required costs of the reef while not placing any other of the design objectives at risk.

At St Francis Bay in South Africa, a large, integrated project is envisaged whereby sand dredged from the clogged up Kromme river mouth is used to replace the eroding sand (Mead et al. 2006). The erosion problem has been caused by the stabilisation of the dune fields. This now prevents wind blown sand from entering the sea which would otherwise replace the sand lost due to the wave and wind driven currents. Here, sand dredged from the river mouth will be used to fill the sand bags and is also to be used in a beach nourishment program. The sand will be pumped along the coast and reintroduced into the system upstream of the eroded beaches. Surfing amenity is to be incorporated into the design and a dune restoration program is proposed.

It seems then that the current challenges in predicting the success of the design objectives at the design stage are made more difficult by the multi functional intentions of the structure. Also, the apparent lack of engineering design criteria has been made evident by the fact that some of the projects' chief objectives are to assess the effects of the structures on beach profile, the environment, society and economics of the surrounding areas.

Wave conditions, currents, predominant wind direction, tidal ranges, in shore and offshore bathymetry, social and economical state of the nearby community, size and nature of the project, construction materials, availability of dredgers, all contribute to the complexity of achieving the specified design objectives.

2.2 Wave breaking

2.2.1 Introduction

Ocean waves are generated from wind blowing over the surface of the sea. The wind imparts a shear stress to the sea surface which in turn passes the energy from the wind into the waves, The waves begin as capillary waves and slowly increase in height and period according to the strength of the wind, length of the fetch and the time for which the wind blows over that fetch. The size of the wave is also dependent on the depth of the water.

The larger waves to reach the coastline are generated far out in the ocean in deep water. In deep water dissipative forces such as viscosity play a small role (Dean 1990), and so the energy can propagate for enormous distance with no significant losses in energy. Breaking of waves in deep water can occur, with the general rule of thumb being when the wave steepness (wave height/wavelength H/L) exceeds 1/7. In strong winds white-capping often takes place which also serves as a means of energy dissipation.

As the waves move out of deep water they begin to interact with the ocean floor. In shallower waters, the effects of refraction, shoaling and bottom friction begin to play a role. The waves gradually begin to change direction depending on their orientation relative to the bathymetry, their wavelengths become shorter and they generally increase in height. Winds, currents , wave direction and variations in water levels such as tides and storm surge all play a role in the breaking process in different proportions.

2.2.2 Breaker type

Much research into the factors that affect wave breaking in shallow water have been done by a variety of authors. The type of breaker is determined by a number of factors, namely; wave height, period and orthogonal beach slope.

The surf similarity parameter, Eqn. 2.2, is used as a means of estimating breaker type:

$$\xi_o = tan\beta \left(\frac{H_o}{L_o} \right)^{-1/2} \tag{2.2}$$

where $m = tan\beta$ is the bottom slope, H_o is the deep water wave height, and L_o is the deep water wavelength (Battjes 1974) as shown in Figure 2.15.

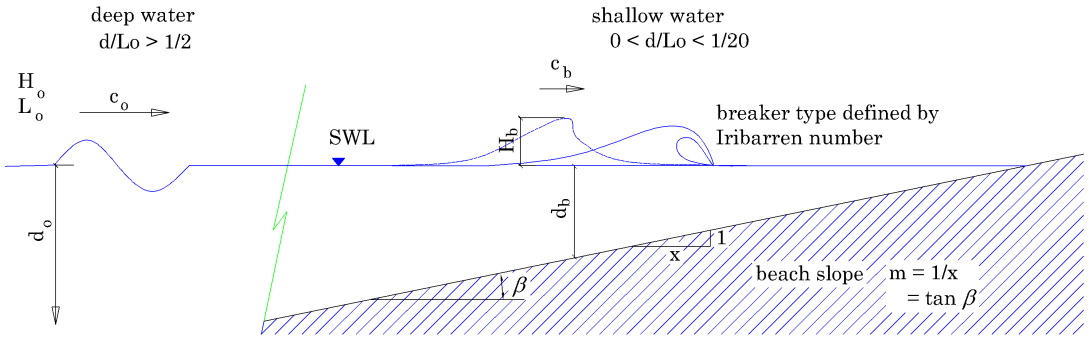

Figure 2.15: Wave breaking parameters in shallow water on a planar, sloping beach

Other factors such as bottom friction, water depth, wind direction and strength, surface tension, currents, focusing due to refraction, and water depth also play a minor part in determining the breaker type.

According to Battjes (1974), Iribarren and Nogales (cited by Battjes (1974)) were the first to use the surf similarity parameter as means of predicting when waves would break. They related ξ_c to the point at which waves would begin to break. ξ_c is the critical limit at which progressive waves becomes unstable and breaks, known as incipient breaking. Battjes (1974) suggests that derivation of the critical value of $\xi_c = 2.3$, even though backed up by experimental data, is perhaps incorrect. He states that ξ_c on its own can be used as a critical ratio of the point at which breaking occurs. He then, based on the work of Galvin (1969), derives the well known critical values for regular waves. In the tests, the waves were breaking on continuous, smooth concrete slopes. It should be noted here that the data used by Galvin (1969) was free from interference from secondary waves, which are waves created from the breaking of the so called 'primary' (original) waves in the wave train.

The section below describes the various forms of breaking waves and has been extracted from the Coastal Engineering manual (2006).

> *"In spilling breakers, the wave crest becomes unstable and cascades down the shoreward face of the wave producing a foamy water surface. In plunging breakers, the crest curls over the shoreward face of the wave and falls into the base of the wave, resulting in a high splash. In collapsing breakers the crest remains unbroken while the lower part of the shoreward face steepens and then falls, producing an irregular turbulent water surface. In surging breakers, the crest remains unbroken and the front face of the wave advances up the beach with minor breaking."*

Figure 2.16: Classification of breaker types, (CEM 2006, Part II-4).
Clockwise, from top left: Spilling, Plunging, Collapsing, Surging

The critical values derived by Battjes (1974) for spilling, plunging, collapsing and surging are as follows, for offshore waves;

$$\begin{array}{rrrl} \text{Surging/Collapsing} & & \xi_o & > 3.3 \\ \text{Plunging} & 0.5 < & \xi_o & < 3.3 \\ \text{Spilling} & & \xi_o & < 0.5 \end{array}$$

For breaking waves, with the subscript ξ_b denoting inshore Iribarren number, with;

$$\xi_b = tan\beta \left(\frac{H_b}{L_o} \right)^{-1/2} \tag{2.3}$$

he derived the limits as:

Surging/Collapsing		ξ_b	> 2.0
Plunging	$0.5 <$	ξ_b	< 2.0
Spilling		ξ_b	< 0.5

The values for barred beaches were somewhat modified by Smith and Kraus (1990);

Surging/Collapsing		ξ_o	> 1.4
Plunging	$0.4 <$	ξ_o	< 1.4
Spilling		ξ_o	< 0.4

as were they for more rougher and permeable slopes by Hedges (2001);

Surging		ξ_o	> 3.3
Collapsing	$2.3 <$	ξ_o	< 3.3
Plunging	$0.4 <$	ξ_o	< 2.3
Spilling		ξ_o	< 0.4

Many authors have mentioned that the critical values for breaking intensity do overlap, especially at the boundary of the spilling-plunging categories.

2.2.3 Breaker depth and breaker Height

In shallower waters, the breaking of waves is no longer limited only by wavelength as it is in deep water. The depth of the water at which breaking occurs also plays a role. Breaker depth is defined as the water depth at which wave breaking begins. This has been referred to as incipient breaking (CEM; 2006) and is defined as the point in shallow water at which a wave reaches its limiting steepness. Other definitions are when the wave reaches its maximum height; where the wave face becomes vertical (for plunging waves); and where the point just before foam begins to form on the wave face (for spilling breakers) (CEM; 2006).

The depth at which breaking occurs and the height of the breaking wave may be predicted with reasonable confidence using empirical relationships. In 1891, McGowan (cited by CEM; 2006) determined the depth at breaking H_b/d_b as 0.78 for solitary waves on a horizontal slope. This is often used as a starting point for determining the point where breaking occurs, but it is simplistic when compared to other breaker depth formulae as it does not take foreshore slope and wave steepness into account. In the 1940's, Miche (cited by CEM, 2006) showed that the breaking wave height for regular waves is limited by its wavelength at which it travels. His work was based on theoretical considerations in linear wave theory, and he based the calculations on the horizontal orbital velocity at the crest being required to always be less than or equal to the forward celerity of the wave, which is, in general, where breaking occurs. He arrived at the following expression;

$$H_{max} \approx 0.14 L tanh\left(\frac{2\pi d}{L}\right) \tag{2.4}$$

Much work was done into breaker indices and breaker formulae prior to 1972. From 1970 onwards, it seems that more data became available to researchers into wave breaking, which assisted in creating more accurate and more reliable formulae.

The following equations are deemed more useful and more accurate for breaker depth calculations. In the equations below, H denotes wave height; L, wavelength; d, water depth; T,

wave period and g, gravitational acceleration, while the subscripts o and b denote the deep and breaking conditions respectively. H'_o represents the unrefracted deep water wave height which neglects refraction. The beach slope $m = tan\beta$, where β is the angle the slope makes with the horizontal.

Weggel (1972) evaluated previously published breaking wave data and developed a relationship between maximum breaker height in terms of breaker depth, breaker steepness and beach slope. He developed Eqn's. 2.5, 2.6 and 2.7 from this data and developed a method to determine the maximum breaker height at the toe of a structure when both the beach slope and depth at the toe is known.

$$\frac{H_b}{d_b} = b - a\frac{H'_o}{gT^2} \tag{2.5}$$

for $tan\beta \leq 0.1$ and $H_o/L_o \leq 0.06$. The parameters a and b are empirically determined functions of beachslope, given by

$$a = 43.8\left(1 - e^{-19tan\beta}\right) \tag{2.6}$$

and

$$b = \frac{1.56}{(1 + e^{-19.5tan\beta})} \tag{2.7}$$

Komar and Gaughan (1973) (cited by CEM, 2006), derived a relationship for the breaker height index from linear wave theory and one laboratory and field data set each. They obtained the following relationship, and after comparing it with solitary wave theory, proposed that it replace previous solitary wave breaking criteria. The empirical solitary wave relationships, were, up to that time, used commonly for breaker depth calculations.

$$d_b = 0.56H_o\left(\frac{H_o}{L_o}\right)^{0.2} \tag{2.8}$$

Goda (1974), (cited by Goda and Morinobu (1998)) re-examined data gathered in a previous study done by himself and proposed an empirical formula for the breaker depth. The formula is based on laboratory data from various sources.

$$H_b = 0.17L_o\left\{1 - e^{\left[\frac{-1.5\pi d_b}{L_o}\left(1+15m^{4/3}\right)\right]}\right\} \tag{2.9}$$

Singamsetti and Wind (1980), cited by Couriel et al. (1998), derived Eqn. 2.10 and Eqn. 2.11 for breaker depth and breaker height respectively.

$$d_b = 0.811H'_o m^{-0.012}\left(\frac{H'_o}{L_o}\right)^{-0.12} \tag{2.10}$$

$$H_b = 0.760H'_o m^{1/7}\left(\frac{H'_o}{L_o}\right)^{-0.25} \tag{2.11}$$

Ogawa and Shuto (1984), in an analysis of runup of breaking and non-breaking periodic waves on gentle, steep, uniform and non-uniform slopes, steps and bars, arrived at Eqn. 2.12. They used the same data that Goda (1974) used to determine Eqn. 2.12. Their equation is only valid under certain beach slopes m and deep water wave steepness H_o/L_o. For $0.01 < m < 0.1$ and for $0.003 < H_o/L_o) < 0.07$, they proposed the following:

$$d_b = 0.46 H_o m^{-0.12} \left(\frac{H_o}{L_o} \right)^{-0.2} \tag{2.12}$$

Dean and Dalrymple (1984), used linear wave theory and derived a relationship for breaking waves. They based their work on energy flux conservation and the breaker height formula of McGowan, where

$$d_b = 0.64 H_o \left(\frac{H_o}{L_o} \right)^{-0.2} \tag{2.13}$$

Battjes and Stive (1985) used Equation 2.14 to describe the rate of energy dissipation of random waves breaking in shallow water. They used a form similar to that of Miche (1944), Eqn. 2.4, and adapted it to include bottom slope and incident wave steepness. This equation was incorporated into their model in order to determine the point at which and the extent at which wave breaking would occur.

$$\frac{H_b}{L_b} = 0.14 tanh \left[0.5 + 0.4 tanh \left(33 \frac{H_o}{L_o} \right) \right] \frac{2\pi d_b}{0.88 L_b} \tag{2.14}$$

Nelson (cited by Goda and Morinobu (1998)), conducted laboratory tests with regular waves. From his results he concluded that the limiting wave height of regular waves on a horizontal slope could not exceed the value of $0.55 d_b$. He then conducted further tests and proposed Eqn. 2.15 for gentle slopes:

For m ≤ 0.01

$$\frac{H_b}{d_b} = 0.55 + e^{\left(-\frac{0.012}{m}\right)} \tag{2.15}$$

In his study of set up, run up and water table, Gourlay (1992), gathered laboratory data of previous studies by seven authors and proposed an empirical formula based on curve fitting. He found that dimensionless breaker height H_b/H_o is insensitive to beach slope, while the opposite was true for the dimensionless breaker depth d_b/H_o. For $0.022 < m < 0.1$ and for $0.001 < H_o/L_o < 0.066$, he proposed

$$d_b = 0.259 H_o m^{-0.34} \left(\frac{H_o}{L_o} \right)^{-0.17} \tag{2.16}$$

Goda and Morinobu (1998) investigated breaker height on horizontal slopes to answer challenges proposed by Nelson ; and to clarify the difference between wave breaking phenomena on slopes, a horizontal bed , in water of constant depth, and the reasons for the differences. They analyzed the latter due to the attention showed by researchers into the field of artificial reefs used for coastline protection. They investigated, amongst others:

a) Laboratory scale effects and breaker height: They conducted small scale physical model tests and found that the water depth at breaking has significant influence on scale effects, which they attributed mainly to the surface tension of the water in the tests. They noticed no scale effects from 75 mm water depth and recommended a breaker depth and breaker depth height greater than 100 mm for waves breaking on a horizontal bed.

b) Approach slope and breaker height: They found that the breaking limit height on a horizontal bed decreased as the approach slope to the horizontal bed became steeper. To cater for this, they adjusted the value of the constant 0.17 in Eq. 2.9 until the closest fit was obtained.

c) Wave profile changes caused by abrupt changes in topography: They attributed changes in the wave profile to the generation of free harmonic secondary (and of higher order) waves at the start of the horizontal bed.

d) Applicability of a breaker depth formula, Equation 2.15, for horizontal slopes proposed by Nelson (1987), cited by Goda and Morinobu (1998): They found that his formula is only applicable for two special cases only, one being for waves at the stability limit of paddle generated waves, and the other for waves that have stabilized after breaking on a horizontal bed.

Rattanapitikon and Shibayama (2000), investigated 24 breaker depth formulae from a variety of authors. Some of these formulae are mentioned above. They found that most of the breaker formulae predicted well for gentle slopes, where $0 < m \leq 0.07$, but unsatisfactory for steep slopes, where $0.1 < m \leq 0.44$. After comparison of the root mean square relative error, ER, of each formula, they discovered that ER increased with increase in the bottom slope m. From the results, they modified the three formulae with the least ER by incorporating a new form of bottom slope effect. They found that the following modified equation of Goda in the form of Equation 2.9 gave the least relative error ER for all cases of bottom slope,

For $0 \leq m \leq 0.44$

$$H_b = 0.17 L_o \left\{ 1 - e^{\left[\frac{-1.5\pi d_b}{L_o} \left(16.21m^2 - 7.07m - 1.55 \right) \right]} \right\} \tag{2.17}$$

Rattanapitikon et al. (2003) developed a new breaker height formula based on 26 sources of breaker height formulae and empirical breaker height data. They found that a power law relationship with the deep water wave steepness H_o/L_o and wave steepness at breaking H_b/L_b gave the closest fit to the data. The wavelength at the breakpoint L_b was calculated from linear wave theory.

For $0 \leq m \leq 0.38$

$$H_b = \left(-1.40m^2 + 0.57m + 0.23 \right) L_b \left(\frac{H_o}{L_o} \right)^{0.35} \tag{2.18}$$

Rattanapitikon and Shibayama (2006) extended their studies on breaker height to propose a formulae for breaker depth d_b. They utilized equations 2.17 and 2.18 to derive the following formula for breaker depth,

$$d_b = \frac{H_o}{\pi(16.21m^2 - 7.07m - 1.55)} \ln \left[1 - \left(58.94m^3 - 43.88m^2 + 7.66m + 3.24 \right) \left(\frac{H_o}{L_o} \right)^{0.8} \right] \tag{2.19}$$

which was validated with the same data set as Rattanapitikon et al. (2003). They found that the equation 2.19 gives reasonable results for gentle slopes but gives unsatisfactory results for steep slopes $m > 0.1$. They then developed equations 2.20 and 2.21 to distinguish between steep and gentle slopes. They recommend caution when using the equations when $H_o/L_o > 0.12$ and $m > 0.38$, as this outside the range of the data used from the 26 different sources.

For $H_o/L_o \leq 0.1$,

$$d_b = \left(3.86m^2 - 1.98m + 0.88 \right) H_o \left(\frac{H_o}{L_o} \right)^{-0.16} \tag{2.20}$$

and for $H_o/L_o > 0.1$,

$$d_b = \left(3.86m^2 - 1.98m + 0.88\right) H_o \left(\frac{H_o}{L_o}\right)^{-0.34} \tag{2.21}$$

In a simple 2D case with constant slope and neglecting such factors as bottom friction, focusing, reflection, winds, currents and tides, breaker depth and bottom slope can be a useful means of determining the minimum reef width required for wave breaking. In nature, there are combined effects of wind, currents, tides, bottom friction and wave focusing that all affect the incoming and breaking waves. These will need to be taken in to account in order to successfully assess the ability for a reef to achieve the desired wave breaking events. It will also then be necessary to determine which of the previously developed formulae are most suitable to the task at hand.

2.2.4 Effect of bottom friction on breaking

As waves propagate from deep to shallow water, they gradually lose more energy as the degree with which the wave interacts with the sea bottom increases. Little data exists on incorporating bottom friction into wave breaking equations. Breaker depth and breaker height formula are based on laboratory tests on smooth (concrete) slopes, where bottom friction is assumed to not influence results significantly.

Symonds et al. (1995) recorded wave driven currents and other wave parameters on the John Brewer Reef 70km NE of Townsville in Queensland, Australia. They found that the site observations of Black and Hatton (1990) suggest that friction co-efficients over coral reefs are significantly higher than for beaches. They further note that this did not greatly affect their results.

CEM Part II-4, (2006), notes that the inclusion of bottom friction into calculations of wave breaking in the surf zone improves estimates, even though the dominant dissipation mechanism is depth-limited breaking. It also states that general guidance on reef bottom friction coefficients is not available. They recommend site-specific field measurements to estimate bottom friction coefficients.

Hedges (2001) notes that the limits for spilling, plunging, surging waves are somewhat modified for rough and permeable slopes. This is more than likely due to the increase in bottom friction reducing the wave celerity at a higher rate than for waves propagating over smoother bathymetry. The limits are shown in Section 2.2.2. Maa (2000)(cited by CEM, 2006) investigated the effects of bottom friction on wave breaking. He used the linear wave refraction and diffraction model RCPWAVE, and found that the inclusion of bottom friction may cause a 30% to 50% reduction in breaker height. His tests considered only friction caused by grain size of a smooth, fixed bed; a sandy bed with ripples and a sandy bed with ripples removed. He also concluded that small waves may experience larger friction factors, while larger waves, especially long period waves, are not subject to large friction factors because the ripples in the bed are wiped out.

2.2.5 Effect of focusing on breaking

As a wave propagates over a shoal, the parts of the wave in shallower waters move slower than those in deeper waters. Wave crests refract around the shoal, tending to align themselves parallel with the depth contours of the shoal. This concept has been explored by West et al. (2003) while developing a wave focusing reef, which alters the wave field before the wave crests reach the breaker zone (Figure 2.17). Because the wave energy is focused at the front of the shoal, the wave height increases. The larger wave heights result in larger breaker depths, and the waves thus break in deeper waters.

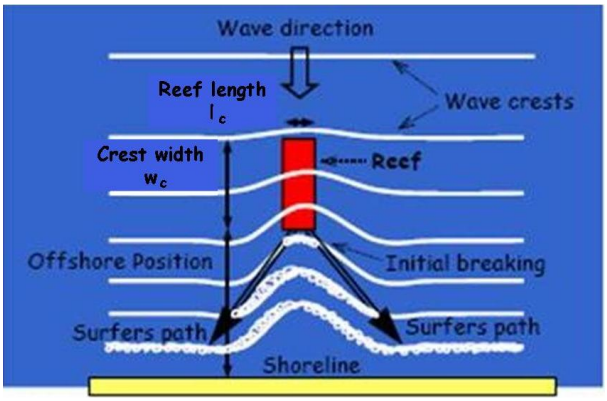

Figure 2.17: Wave focusing over a shoal (West et al. 2003)

The effects of refraction of the wave crests may have an effect on the breaker type. Waves approach the contours from a non-perpendicular direction. Refraction effects can dominate, resulting in slopes gentler than for wave approaching contours at 90°. This is discussed in greater detail in Chapter 2 on peel angle.

2.2.6 Effect of shoaling on breaking

Shoaling, in the process of waves propagating along a bottom slope, increases the wave height at the break point when compared to that of a wave propagating on a horizontal bottom. This would also mean an increase in the breaker depth. This effect is however accounted for in breaker height and depth formula, and can be noted in that all the breaker depth formulae show an increase in breaker height and breaker depth when compared against the case of a horizontal bed. It is not stated in some of the sources whether the slopes were constant from deep to shallow water or if there existed steps, that could have interfered with the transformation of the waves over a non-uniform or a stepped slope.

Goda and Morinobu (1998) found that co-efficient of 0.17 in Eqn. 2.9 increases in value (to the limit of 0.17) as the deep to shallow water slope becomes flatter. They also found that the breaking limit height on a horizontal bed decreases as the approach slope to the horizontal bed became steeper. This could be caused by the fact that a longer flatter slope gives the waves more time to transform and increase in height due to shoaling. Steeper slopes result in more reflection and give less time for the shoaling process to occur. On the other hand, a longer slope results in a longer distance for a wave to propagate. The wave is therefore under the effects of bottom friction for a longer distance, which results in a slightly smaller breaking waves. Goda and Morinobu (1998) attributed this to the formation of harmonic wave components at the junction between the approach slope and the horizontal crest.

2.2.7 Effect of winds on breaking

All of the previously mentioned breaker depth and breaker height formulae show a direct relationship between wave steepness and bottom slope. In nature, however, winds may also play a significant role.

Galloway et al. (1989) mentions that many authors have agreed that wind effects are significant. They conducted field investigations of breaking waves under light to medium strength wind conditions and found that offshore winds tend to delay wave breaking and increase the wave steepness at breaking. This results in a more unstable mode at breaking than if calmer

winds were present, resulting in a more intense release of energy and a more intense plunging wave. For the onshore wind case, they found that micro (capillary) waves were formed by the wind, which created instabilities on the wave face as it approached breaking. The existence of these instabilities resulted in early breaking of the crest of wave. Very often, waves that would otherwise have been plunging, broke earlier as spilling breakers.

For very strong winds, they proposed that more plunging characteristics would be inherent onshore winds while more crest instabilities would promote more spilling on breakers for offshore winds. For offshore winds, they also found that plumes of spray blowing from the wave crest would reduce the crest height at breaking. They also suggest that bottom slope may be more important an effect for breaking waves than wind direction and speed, but add that the effects of wind will still contribute to the breaking wave type. They recommended more detailed laboratory investigations in order to quantify the effect of winds on breaker height and breaker intensity.

Douglass (1990) investigated the effects of offshore and onshore winds on spilling and plunging breakers. He also notes (along with others) that wind has an effect on breaking waves, while some authors believe the effect is minimal even for moderate winds. Douglass (1990) conducted laboratory studies and found that longer period waves feel less of an effect due to winds than do shorter period waves. He found that the surf zone width can increase by 85% for a change in direction from strong offshore to strong onshore wind. He attributed the instabilities in the wave crest under onshore winds to the same mechanism as Galloway et al. (1989). It was concluded that for light to strong winds, the effects on breaker height are minimal while the effects on breaker depth are significant; and that the effect of wind on breaking can be as important as wave steepness and bottom slope.

2.2.8 Effect of currents on breaking

Ocean current are caused by a variety of different factors. Wave current interaction plays an important part in the breaking of waves. Waves propagating into an opposing current will be subjected to a decrease in wavelength, and thus an increase in wave steepness. This results in a larger wave that breaks in deeper water. The opposite is true for waves in a following current.

Currents also have an effect on wave refraction. Wave celerities increase in a following current and decrease in opposing currents. This results in changes in the direction of propagation of the wave crests, similar to that of changes in depth contours. An opposing current has the same refraction effect as the shallower waters of a shoal.

Currents in the surf zone are generally caused by waves breaking in a direction non-perpendicular to the shoreline, which results in a longshore current. Trung (2006) found that reef assymetries can induce larger breaker on one side of the reef, which has the effect of inducing stronger rip currents on that side. This results in increased breaker heights and stronger rip currents until stability is reached where both the wave height and current stop increasing.

2.2.9 Effect of varying water level on breaking

Water levels can vary quite significantly at a surf locations. Deepening water can change breaker types from plunging to spilling, which alters the surfability of a wave. Also, offshore bathymetry can have different effects on refraction and shoaling depending on water depth.

Astronomical tides are the most common causes of varying water levels and are caused by interactions between the earth, moon and the sun. Variations in relative positions of sun and moon, lunar distance and declination of sun and moon contribute to the varying levels of astronomic tides. Tidal variations occur in cycles of approximately 12 hours (semi diurnal tides), 24 hours (diurnal tides) and two weeks (moons fortnightly contribution) (Benassai 2006).

Spring and neap tides occur when the lunar and solar components of the tide coincide (in phase) and cancel (90 ° out of phase) respectively. These occur every two weeks. Land masses, offshore bathymetry and continental shelves all alter the relative sizes of tidal components. Daily tidal variation can vary from as little as 0.5m to as high as 8m at some locations around the world.

Storm surge, caused by wind (wind set-up) blowing in a shoreward direction, can also increase water level. Storm surge can have quite a major influence on water levels. The ocean surface can also be raised slightly by a low pressure cell traveling over it. Setup from breaking waves can increase water levels inshore. The Coriolis effect can cause minor variations in water levels.

Typical South African tidal ranges are in the order of 1m at neap tide, and increase to 2m at spring tides.

2.3 Surfing and surfing design criteria

2.3.1 Introduction

Surfing is defined in the Oxford dictionary as "standing or lying on a surfboard and riding on the crest of a wave towards the shore". The exact origin of the sport is still unknown. It is generally thought that the sport began in the Hawaaian Islands, but some researchers believe its origins are in the Phillipines and Fiji Islands, when local inhabitants used long wooden rafts to travel between the islands, which they then surfed in to the beaches. The sport of surfing almost died out in the Hawaaian Islands due to Christian missionary work, but was revived in the early 1900's, possibly in protest to the illegal overthrow of the Hawaiian Kingdom. The sports popularity gradually grew in America due to work done by the author Jack London and Olympic swimmer, Duke Kahanamoku, and finally made its way to other parts of the world like Brazil and Australia (*wikipedia.org* 2007).

Surfing in South Africa began in the late 1930's and early 1940's when lifesavers on the Durban beach front began to stand on their 18 feet long wooden boards and ride the breaking waves (*wavescape.co.za* 2008). Their boards were copied from Australian designs. After World War II, Durbanite Fred Crocker invented the 'Crocker Ski', a light timber frame covered with canvas and impregnated with aeroplane 'dope' (a resinous liquid that hardens with a catalyst used in aeroplane construction).

Advances in surfboard technology, the formation of surf clubs, the discovery of world class surf spots in South Africa, filming of classic surf movies in South Africa, the construction of piers and groynes (that have enhanced the quality of surfing waves), the reintroduction of South Africa into the world wide community due to the governmental changes in 1994, and the establishment of world class surfing competitions open to international competitors have all led to an increase in the popularity of the sport of surfing in South Africa.

The first surfboards were made up of large shaped planks resembling canoes. Over time, surfboards have changed in shape, size and density, resulting in quite a large number of wave riding disciplines. Generally, the smaller and lighter a surfboard is, the easier it is to manoeuvre. These smaller surfboards are known as shortboards. Shortboards function better in waves where the crest breaks rapidly along its length and in waves that break more intensely. These waves are also more difficult to surf. Shortboard surfers generally prefer plunging waves as opposed to spilling waves.

Parameters such as breaking intensity, peel angle, breaker height and section length are given by Scarfe et al. (2003) as the most important used to define surfing waves. These are addressed in the following sections.

2.3.2 Breaking intensity

The shape of the plunging wave is deemed very important by surfers as it allows many opportunities for a variety of different manoeuvres (Scarfe et al. 2003). Also, if the plunging wave is large enough, the surfer can ride beneath the falling jet (Figure 2.18).

This is known as 'tube riding' within the surfing community. Riding in the tube is a manoeuvre favoured by surfers, and is considered very difficult to perform. High skill levels are required, and tube riding thus is often associated with a high level of accomplishment. In surfing competitions, riding in the tube can produce very high scores, surfers competing in competitions generally perform this manoeuvre over other lower scoring manoeuvres, if the wave shape allows for it.

Prediction of the shape of the plunging wave is thus important when designing for recreational surfing amenity. The ability for a reef to transform the waves in a manner required for

Figure 2.18: Surfers riding beneath the falling jet of a plunging wave (*surfermag.com*).

surfing purposes, and more specifically, for the provision of 'tube rides', is thus deemed very important with respect to:

1. Surfers using the reef for 'social' surfing (outside of competition), and
2. Surfers using the reef for competitive surfing.

With respect to designing for the desired wave shape, many authors have noted that the categories for breaker type as defined by surf similarity parameter (Battjes 1974) are not clearly defined, and has been deemed by a number of authors as unsuitable for design for surfing purposes ((Couriel et al. 1998) and (Sayce et al. 1999)).

A method of predicting the shape of a plunging surfing wave was first developed by Sayce (1997). He fitted curves to the wave shape in profile, and calculated the parameters of vortex length, l_v, vortex width, w_v, wave height at when the vortex is defined H_v and vortex angle θ_v. Figure 2.19 depicts the parameters used. The vortex shape parameters are defined at the point when the falling jet first comes into the contact with the wave face.

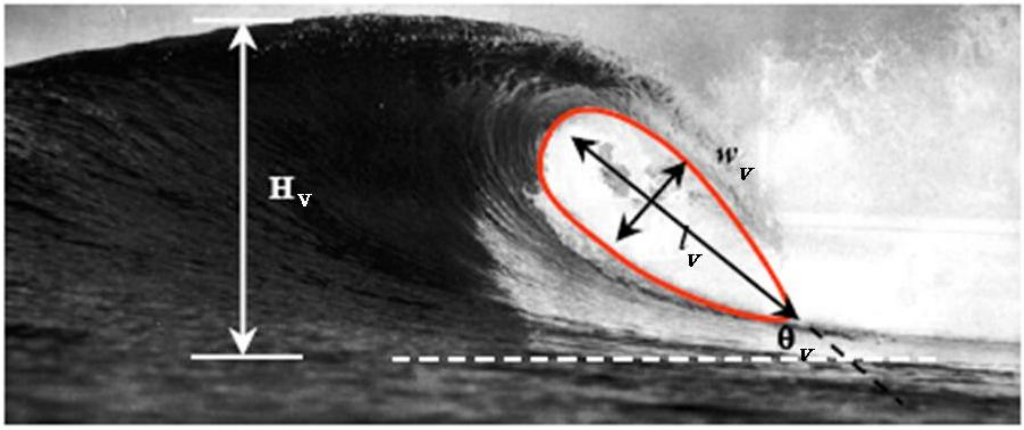

Figure 2.19: Vortex shape parameters as defined by Sayce (1997).

Sayce (1997) employed a method developed by Longuett-Higgins (1982) to fit the curve to the wave profile. Longuett-Higgins (1982) used a parametric description of incompressible, irrotational flow to develop the profile of a plunging wave. He found extremely good agreement

with the forward face of the wave. He proposed Equations 2.22 and 2.23 to describe the shape of the plunging wave mathematically. The derivation of the equations is based on the velocity potential expressed in terms of complex variables

$$\frac{x}{t^4} = 3\mu^2 - 13 \tag{2.22}$$

$$\frac{y}{t^4} = -\mu^3 + 2\mu \tag{2.23}$$

where x and y are spatial co-ordinates measured from an axis of symmetry, t = time and μ is a variable used to separate the real and imaginary parts. The equations were derived for waves breaking in deep water, and suggest a constant vortex angle, which does not reflect realistically what occurs in reality in shallower waters. The time dependency existed in an attempt to describe the wave profile as time progressed, during the breaking process from deep to shallow water to the break point and then to the condition after breaking. The different wave vortex shapes were noted by Vinjeg and Brevig 1981 (cited by Longuett-Higgins (1982)) as a wave evolved from before to after the breaking condition. They noted and quantified the change in the wave vortex shape and the corresponding length to width vortex ratios at different stages of the breaking process.

Black and Mead (2001) surveyed the bathymetry of several high quality surf locations and subsequently analyzed a series of images of waves as viewed in profile at these locations. Parameters such as vortex length, l_v, vortex width, w_v, wave height when vortex is closed, H_v and vortex angle θ_v were extracted from the images. Black and Mead (2001) give their classification of breaker intensity based on vortex ratio, r_v, (Table 2.4), where vortex ratio, r_v, is equal to vortex length, l_v, divided by vortex width, w_v, that is :

$$r_v = \frac{l_v}{w_v} \tag{2.24}$$

Table 2.4: Black and Mead (2001)'s classification of breaker intensity

Intensity	Extreme	Very High	High	Medium/High	Medium
Vortex Ratio, r_v	1.6 - 1.9	1.91 - 2.2	2.21 - 2.5	2.51 - 2.8	2.81 - 3.1
Wave Shape					

Black and Mead (2001) also found that the vortex angle, θ_v, is not useful in defining the breaking intensity of surfing waves. They attributed this to the subjective nature of selecting the two points that define the vortex length l_v, and to the error inherent in the method used to obtain the data, which was based on images found in surfing magazines. There was no certainty in accuracy of the measurements of vortex angle, θ_v, as it was unclear from the images where the horizontal line was and if the images were captured with the camera correctly aligned to the horizontal.

Black and Mead (2001) note that the details of reef shape are the most important factors in the design of surfing aspects of multi purpose reefs. When wave refraction begins to occur, wave crest begin to align themselves with the bathymetric contours. The orthogonal seabed gradient is the gradient taken along a section of bathymetry perpendicular to the wave crest (Figure 2.20). The contour normal bed slope is taken perpendicular to the bathymetric contours. Thus the bed slope value in Equation 2.25 is dependent on the angle of incidence of the wave to the

bathymetry. Orthogonal seabed gradient s' is given by $s' = scos\alpha$ where s ($s = tan\beta_{reef}$) is the contour normal bed slope or reef slope and α is the peel angle. Peel angle is discussed in more detail in the next section. The relationship was proposed by Couriel et al. (1998).

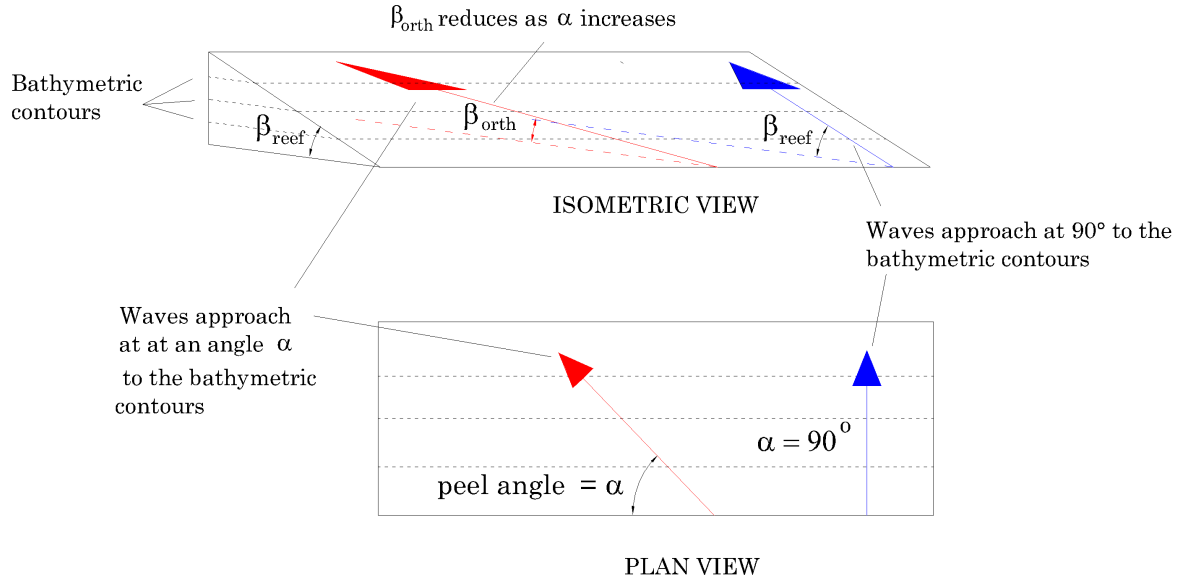

Figure 2.20: Orthogonal seabed gradient (Adapted from Couriel et al. (1998))

Couriel et al. (1998), give typical reef slopes for certain sections of the Narrowneck reef and their orthogonal sea bed gradients are presented in Table 2.5:

Table 2.5: Bed slopes on the Narrowneck Reef (Couriel et al. 1998)

	Contour normal bed slope s, or $\tan\beta_{reef}$	Orthogonal sea bed slope s', or $\tan\beta_{orth}$
Takeoff Section	1:18 to 1:20	1:28 to 1:58
Faster Sections	1:8 to 1:12	1:8 to 1:14
Reef Face	1:12 to 1:15	1:16 to 1:23

The takeoff section referred to in Table 2.5 is the point at which breaking first occurs along the wave crest, and thus where the surfer begins riding the wave. The faster sections are those where the peel angle decreases, which results in faster rides for the surfers.

A relationship between vortex ratio r_v and bed slope was proposed by Black and Mead (2001) through curve fitting. Equation 2.25 shows the fitted relationship between the vortex ratio and the orthogonal sea bed gradient, where r_v is the vortex ratio and s' is the orthogonal seabed gradient.

$$r_v = 0.065\frac{1}{s'} + 0.821 \tag{2.25}$$

Black and Mead (2001) note that Equation 2.25 is the first attempt at quantifying the breaker intensity of plunging surfing waves and is simplistic. They suggest that the method might be improved by incorporating wave height and period. They then assume that the range of surfing wave heights and periods at world-class surfing breaks is not large enough to greatly

affect the general results obtained by using the orthogonal seabed gradient alone to predict breaking intensity.

2.3.3 Peel angle

Breaking waves are surfable when the wave crest does not break entirely along its length at once. A surfer on such a wave must then advance in a direction perpendicular to the shoreline in order to continue riding the wave. Surfers enjoy riding the open face of wave (at angle equal to the peel angle α) as it gives longer rides and more opportunities for more manoeuvres. The peel angle (Figure 2.21) is in essence the angle between the line of advance of the surfer and the crest of a wave. Walker (1974) noted the relationship between the peel angle α and wave, surfer and peel velocity, v_w, v_s and v_p respectively. The parameters are highlighted in Figure 2.21.

Figure 2.21: Peel angle parameters, Adapted from (Walker 1974)

Waves are faster and more difficult to ride for larger peel angles. The surfer needs to be moving faster than v_s to stay ahead of the wave, so that he may continue riding. Peel angle is directly related to the speed at which a surfer must travel to remain in a favourable position on the wave. Because of the vector relationship (Figure 2.22) between α, v_w, v_s and v_p, trigonometric ratios can be used to calculate one value based on other measurable or calculable values. The velocity of the wave, v_w, is wave celerity.

2.3.4 Breaker height

Shortboard surfers generally prefer waves larger than 0.5m in height. It becomes difficult for surfers to ride waves smaller. The limit in wave height for short boarders is probably around the order of 4 to 5m. Waves larger than this can still be ridden, but it becomes difficult (and dangerous) for the rider to keep control.

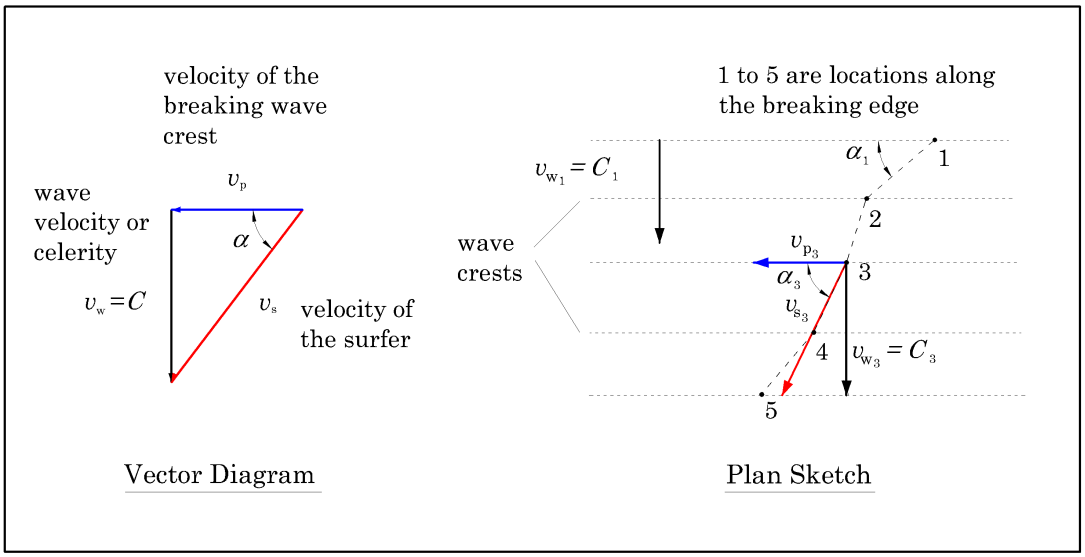

Figure 2.22: Vector relationships between peel angle parameters. Adapted from (Walker 1974)

When waves travel in the ocean, they travel in groups. The speed of the group is determined by the speed of each of the individual waves in the group (CEM 2006). In shallow water, the group velocity closely matches the wave celerity, as wave celerity becomes dependent on depth only. Upon the arrival of the wave groups in shallower waters, surfers ride the larger waves as these are preferred. Hutt 1997 (cited by Scarfe et al. (2003)) recommends using $H_{1/10}$ (a measure of the average of the highest 10% of wave heights in a particular wave record) when estimating the wave heights of surfing waves rather than the more common significant wave height H_s (a measure of the average of the highest 1/3 of the wave heights in a particular wave record). It is assumed that the natural grouping of waves is the reason for the selection of $H_{1/10}$ over H_s.

2.3.5 Section length

When waves break, they rarely break in a consistent manner along their length. A new section begins when there is a change in wave height, peel angle, or breaking intensity, and is given the symbol S_L (Scarfe et al. 2003).

Each surfing manoeuvre is suited to certain wave heights, breaking intensities, peel angles and section lengths. This gives a wide range of possible manoeuvres that can be executed on any specific section. The type of manoeuvre executed is also dependent on the previous section and the type of section that follows. Sections are generally favoured by surfers as it gives more unpredictability and variation to the sport and thus makes the sport more challenging, and thus more rewarding. The section, however, should have a large enough peel angle so that the surfer does not get caught in the broken crest which prevents him from riding the open wave face.

2.3.6 Types of natural surf breaks

Surf-breaks are stretches of coastline where waves break in a manner preferred by surfers. Consistency and predictability of surf conditions are often high on the list of priorities of favoured surf locations, as are the natural beauty, crowd levels and cost of travel and access to the location.

Hugues-Dit-Ciles et al. (2003) developed and distributed a surf destination questionnaire in order to quantify the motivations behind surf tourists. They found that even though surfers prefer uncrowded, perfect waves, consistent swell and beautiful surroundings, the final destination choice is affected primarily by constraints such as cost, accessibility and time.

Locations where the waves on sandy bottoms are known as beach-breaks. Here the breaking intensity can vary considerably as can the peel angle and length of rides. Beach-breaks are generally deemed as inconsistent by surfers because of their unpredictibality, although some locations are considered quite consistent such as the beach breaks of Hossegor in France and the lesser well known of Cape St Francis in South Africa (Figure 2.23). Some beach breaks can be considered man made. These have been created by the construction of piers and groynes or similar human interference that cause the sand to settle in a configuration that induces good quality surf. Superbank in Australia and Durbans Golden Mile are both famous for this. Sand bypassing of the entrance to the river Tweed and the construction of piers for beach widenening are the cause of each respectively.

Figure 2.23: Seals Beach Break (*wavescape.co.za*)

Reef-breaks occur at outcrops of rock just off the coastline or in deeper water that are oriented such that they produce good quality waves. Reef-breaks are generally more consistent and predictable than beach-breaks as the sea bottom is fixed (a rocky or coral seabed) and cannot be placed into suspension and be transported as loose sediment can be. Many good reef breaks exist in the Maldives, Fiji, Tahiti, Pillipines and Hawaii where coral reefs fringe islands and also where hot volcanic rock has solidified upon entering the sea. Sunset Reef (Figure 2.24) in Hout Bay in South Africa is a reef break known for its large waves. The reef crest is at a depth of approximately 10 m and is aligned at approximately 35 ° to the incoming wave crests. The reef produces short intense rides and due to the depth of the reef, waves only break when their height exceeds approximately 4m.

Figure 2.24: Waves breaking on Sunset Reef (*wavescape.co.za*)

Point-breaks are generally situated inside bays and along rocky coastlines that are protected from direct waves. Here wave refraction plays a huge role in the shaping of the waves as the waves generally need to refract around a headland or point (Figure 2.25) before they reach shallower waters in which they can break. These are generally comprised of rocky bottoms although some are a combination of sand and rock. Bruces Beauties in Cape St Francis is an example of a point break. Jeffery's bay in South Africa and Rincon point in USA are very popular point-breaks. The rocky coastline of Supertubes in Jeffrey's bay is relatively unprotected from swell, but is oriented at almost perpendicular to the dominant wave crests. Refraction along the bathymetric contours plays a large

Figure 2.25: Virgin Point (*wavescape.co.za)*

role on the formation of the good quality surfing waves. Rincon point is situated alongside a headland that protects it from head on waves. Here, refraction around the headland is the main cause of the good quality surfing waves.

Reef and point breaks are preferred by surfers because they are more consistent and predictable than beach breaks, although beach breaks can produce some extremely high quality waves when conditions are ideal for it.

2.3.7 Ideal meteorological conditions for surfing

Surfing is unfortunately a sport highly dependent on both weather and wave conditions. High quality waves occur very seldomly in nature because they rely on both the wave and weather conditions to be optimum.

Surfers will generally surf when waves are between 0.5m and 4m. Along certain coastlines wave energy is very minimal and so surfing is uncommon. Counties bordering the Mediterranean have very poor surf conditions, while countries exposed to seas with very long fetches frequently produce waves of surfable height and wave period.

Big wave surfing is popular in countries which, in addition to being exposed to long sea fetches, are near to the latitudes of between 30 and 40 degrees north and south, otherwise known as the 'roaring forties'. Here, extremely large surf is often experienced in the winter months due to the high strength of the winds produced by extra-tropical cyclones. The Hawaiian Islands, Tasmania, California in USA and South Africa are such and are famous for their 'big wave' surf locations.

At the same time, winds conditions can negatively affect surfability at surf breaks. Surfers generally prefer the plunging waves that offshore winds create as opposed to the spilling waves created by local onshore winds. Also, winds along the coast with a speed greater than 20km/hr are usually deemed too strong by surfers for ideal surfing waves, regardless of direction. Surfers thus prefer the winter months when gentle morning offshore winds along the coast usually blow until midday, and the waves are more likely to be large enough and of great enough wave period to make them highly surfable.

2.3.8 Surfer skill level

Surfers prefer waves that match or challenge their abilities (Scarfe et al. 2003). Wave type preferences amongst surfers needs to be allowed for in the design of artificial reefs while incorporating surfabliity into the design of a multi purpose reef. Surfability parameters such as wave height, breaker intensity, peel angle and section length can be estimated from on-site wave records and reef configuration, and can thus be used to estimate the surfability of a proposed reef.

Much research has been done into the design of artificial reefs for surfer skill level. Walker (1974) gave a subjective description of peel angles, breaker heights and corresponding skill level for beginner, intermediate and advanced surfers. Hutt et al (2001) (cited by Scarfe et al. (2003)) reviewed these criteria and made them applicable for standards of modern day surfing, using a rating system of 1 to 10. He also gave criteria for each skill level category between 1 and 10. Moores (2002), (cited by Scarfe et al. (2003)), examined the effect of surfer skill level on surfability with respect to section length. Scarfe et al. (2003) note that the relationship between surfer skill level and breaking intensity is yet to be developed.

Surfer skill level should be considered in the design of an artificial multi purpose reef for surfability, and needs to be taken into account in order to ensure that the reef can provide surfing amenity for surfers of all skill levels. Also, reefs could be designed for surfers of a specific skill level only.

2.4 Numerical Modelling of Breaking Waves

Over the last 30 years, numerical simulation with computers has become increasingly important in engineering and science in solving highly complex and practical problems. With computer power increasing significantly over the past 10 years, more complex and computationally demanding solutions to numerical simulations have been found Liu (2003). This has opened numerous opportunities in the field of engineering, with applications including heat flow (mechanical engineering), nuclear reactor optimisation (chemical engineering), material deflections (civil engineering), electrostatic field applications (electronic engineering) and water wave propagation (coastal engineering). Numerical models complement other design tools and are very often absolutely necessary to design complex engineering systems and to obtain practical and feasible solutions.

Numerical models also provide alternatives to conducting time consuming, labor intensive, expensive and sometimes dangerous experiments in laboratories or on site. The numerical models are often also more useful than experimental methods in that they can provide insightful and more complete data that cannot be measured or observed directly in the experiments, or is simply too difficult to obtain. Furthermore, the connection between numerical models, experimental studies and theories is an important one, ands need to be understood and employed as tools by the engineer in the design process in order to successfully solve the problems at hand.

2.4.1 The numerical modelling method

Essentially, numerical models approximate equations that are extremely difficult or impossible to solve. The approximations result in certain limitations of the numerical models and are a large source of error. A simple flow chart of the procedure to conduct numerical simulations is shown in Figure 2.26.

Once the most important physics has been extracted and simplified from the problem at hand, the equations governing the physics are described. This often involves making assumptions with the goal of simplifying the numerical modeling process. The equations are generally derived from conservation laws, namely mass, momentum and energy.

These physical equations are then discretized into a form which makes it possible to solve the governing equations numerically. Discretization methods may differ between numerical models. The discretization process results in a grid on which various variables are evaluated at the nodes of the grid. This process is known as domain discretization. The accuracy of the numerical method and hence results are closely related to the grid size and grid pattern.

Numerical discretization involves the integration of the governing equations into more usable discrete equations. Together with the domain discretisation, the governing equations are now in the form of numerical equations and can be solved (relatively easily) at the grid points.

The equations are then written into a computer code in some programming language. The code computes the required variables at the required time/distance intervals. Factors that influence the writing of the code include accuracy and efficiency (with respect computer speed and storage) are the most important considerations (Liu 2003). User friendliness and robustness are some other issues code writers need to consider.

2.4.2 Grid-based methods

There are two fundamental methods to discretize these governing equations, namely the Lagrangian and Eulerian methods. The main features of the two methods are highlighted in Table 2.6 (Liu 2003).

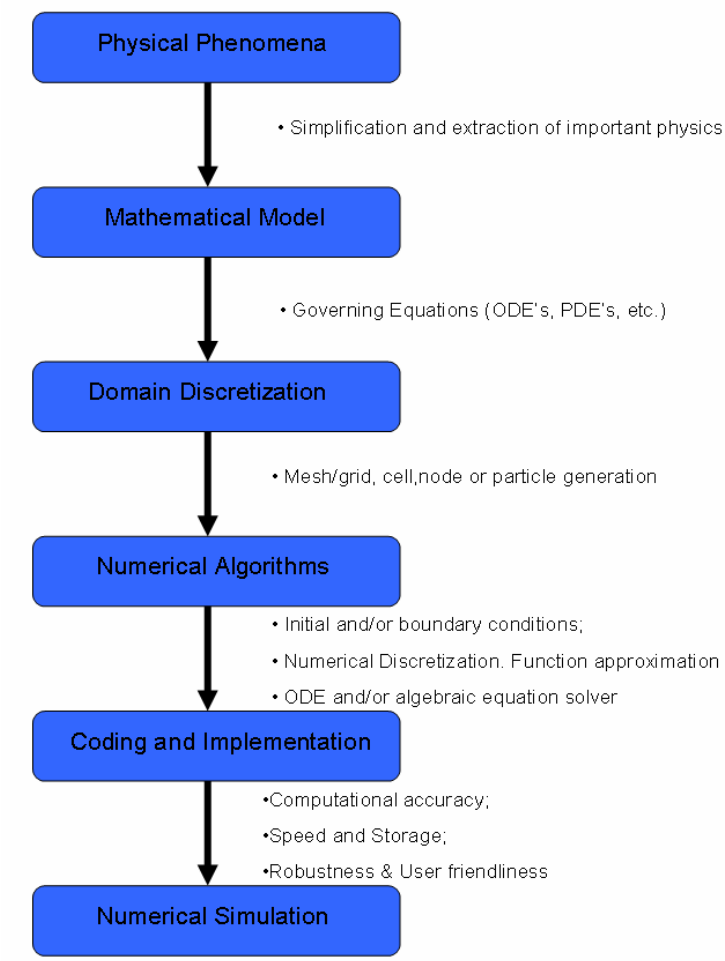

Figure 2.26: Procedure for conducting a numerical simulation (Liu 2003)

Table 2.6: Comparison of Lagrangian and Eulerian based methods Liu (2003)

	Lagrangian	Eulerian
Grid	Attached on the moving material	Fixed in Space
Time history	Easy to obtain time history data at a point attached on materials	Difficult to obtain time history data at a point attached on materials
Moving boundary and interface	Easy to track	Difficult to track
Irregular geometry	Easy to model	Difficult to model with good accuracy
Large deformation	Difficult to handle	Easy to handle

Much work has gone into combining Eulerian and Lagrangian methods into a single method that comprises the best features of each into one new method with limited success.

Problems with using a regular grid to represent irregular or complex geometry, determining locations of free surfaces and moving boundaries have been encountered using Eulerian methods, while Lagrangian methods introduce inaccurate results and time consuming runs due to

required rezoning of the grid. Liu (2003) states that the limitations of grid based methods are especially evident when simulating hydrodynamic phenomena such as explosions and high velocity impacts, when all of the the limitations contribute to the unsuccessful implementations of the method. Also, discrete sets of physical particles are difficult to model with grid based methods (Liu 2003).

2.4.3 Mesh-free methods

Mesh free methods have been developed in order to improve where grid based methods fail. The key idea is to provide an accurate and stable numerical solutions for integral equations or partial differential equations with all kinds of possible boundary conditions with a set of arbitrarily distributed nodes (or particles) without using any mesh to provide connectivity between the nodes (or particles) (Liu 2003).

Mesh free particle methods are different from grid based methods in that they do not require a pre-defined grid for computations. Discrete particles are placed at arbitrary locations in the problem domain and through the numerical code they record the movement of the system. In computational fluid dynamics (CFD) problems, the particles possess a set of field variables (such as, for example, pressure, energy, momentum, velocity and position), and material properties (such as, for example, viscosity and density). The conservation of energy, momentum and mass is fundamental to the evolution of the particles within the system, as it is with grid based methods.

The main advantages of mesh free particle methods over grid based methods is that (Liu 2003):

1. In the mesh free particle methods, the problem domain is discretized with particles without connectivity. Treatment of deformation is relatively much easier.

2. Discretization of complex geometry for the mesh free particle methods is relatively simpler as only an initial discretization is required.

3. Refinement of the particles is expected to be much easier to perform than the mesh refinement

4. It is easier to obtain the features of the entire physical system through the tracing of the motion of the particles. Therefore, identifying free surfaces, moving interfaces and deformable boundaries is no longer a tough task. Time history of field variables at any point on the material can also be obtained quickly.

The numerical solution is formulated in much the same way as for grid based methods (Figure 2.26). The main differences between the two are:

- The domain is discretized with or represented by particles, and
- The functions, derivatives and integrals in the governing equations are discretized through approximating over the particles rather than over a mesh.

Connectivity between particles is supplied by means of an influence domain. Neighbouring particles within a particles influence domain provide all the information for the approximations of the field variables at that particle.

The solution procedure to mesh free particle methods is thus very similar to grid based methods. A typical procedure is as follows, adapted from Liu (2003):

1. Represent the problem domain with particles so that the computational information is known at the discrete particles at an instant t with a proper treatment of the boundary conditions.

2. Discretize the derivatives or integrals in the governing equations with proper particle approximation;

3. From the given velocity or position, calculate the strain rate and/or strain, and then calculate the stress at each discrete particles at the instant t;

4. Calculate the acceleration at each discrete particle using the calculated stress;

5. Use the acceleration at the the instant t to calculate the new velocities and the new positions at time instant $t + \Delta t$, where Δt is the incremental time step;

6. From new velocities and/or positions, calculate the new strain rate and/or the new strain rate at $t + \Delta t$, and then calculate the new stress at time instant $t + \Delta t$. Repeat step 4, 5 and 6 to march forward in time until the final time specified.

2.4.4 Smoothed Particle Hydrodynamics

Smoothed Particle Hydrodynamics (SPH) is a mesh free, Lagrangian, particle method for the modelling of fluid flows. It was first invented in 1977 (Liu 2003) to solve problems in astrophysics and has since been used in modeling of binary stars, supernova, black holes and even the evolution of the universe. It has also been extended to modeling of high velocity impact, heat transfer, shock simulations and underwater explosions (Liu 2003).

Over the last 30 years, many significant improvements have been made to the original code due to its wide range of applications and have thus increased its attractiveness significantly. Presently, the method has proved extremely useful in that it can simulate dynamic fluid flow problems fairly well (Liu 2003).

The SPH method is adaptive in nature, and the particles carry material properties (such as density) with them. Their movements are based on the systems internal interactions and external forces, and function as both approximation points and material components. The name, Smoothed Particle Hydrodynamics, is derived from the smoothed nature in which the influence of the neighbouring particles is weighted for stability, while the term hydrodynamics is the correct niche for the method (Liu 2003).

2.4.5 The SPH method

Once the problem domain has been represented by a set of arbitrary particles and boundary conditions have been implemented, the derivatives and integrals are discretized through approximation of the field functions. The fundamental principle of the SPH method is to approximate any function $A(r)$ by

$$A(r) = \int (A(r)W(r - r, h)dr \tag{2.26}$$

where h is called the smoothing length and $W(r-r, h)$ is the weighting function or smoothing kernel. Essentially, the smoothing length is the size of the domain of influence upon neighbouring particles, while the weighting function is the extent of the neighbouring particles influence. The degree to which the particles have influence over their neighbours is based on the distance to their neighbours. The function approximation (Equation 2.26) is further approximated at a particle a as follows,

$$A(r) = \sum (m_b) A_b / \rho_b . W_{ab} dr \tag{2.27}$$

where the summation is over all the particles within the region of influence. The mass and density are denoted by m_b and ρ_b respectively. $Wab = W(r - r, h)$ is the weighting function.

The particle approximation is performed at every time step, and so the use of the particles depends on the local distribution of the particles at that time. The particle approximations (Equation 2.27) are performed on all terms related to field functions in the partial differential equations, to produce discretized equations with respect to time only. These are then solved with an algorithm to achieve fast time stepping, and to obtain a history of all the field variables for all the particles.

The method of time stepping, moving the particles, computational efficiency, boundary conditions, checking of the limits (extents of the boundaries of the model) and other less general features of the method are dependent on the nature of the physical problem, and implementations thereof vary from application to application (Liu 2003).

2.4.6 Limitations of the SPH method

Although the method succeeds in incorporating the advantages of both Eulerian and Lagrangian models, it is still a long way from being a widely used design tool. Currently, many studies are underway to resolve stability, accuracy and convergence problems of the SPH method (Liu 2003). The causes of these inaccuracies are gradually becoming understood (Liu 2003), albeit that the studies have generally being conducted for very idealized cases and 1-dimensional flows.

The method is, also, not yet as widely used and as robust as the more traditional grid based methods. Liu (2003), note that much work still needs to be done to improve its inherent numerical deficiencies.

2.4.7 Applications in coastal engineering

Due to the fact that SPH has an adaptive nature, can model the free surface, and can also model high velocity impacts, it is very suitable for applications in Coastal Engineering, namely the modelling of water waves. Much work has been done already in the field.

Overtopping (splash and green water) studies, by Gomez-Gesteira et al. (2005), have been conducted to date, as have wave impact studies on coastal structures.

Investigations into overtopping and run up have been done (Shao et al. 2006). Investigations of the use of SPH in modeling of floating bodies in the surf have also been conducted (Rogers et al. 2008).

Recently, and more relevantly, Khayyer et al. (2008) have done work on the improvement of the SPH method in simulation of water waves breaking on smooth planar beach. The models give a good representation of the plunging wave, and a very well defined vortex is defined by the particles. The results have been compared with laboratory studies and show excellent agreement (Khayyer et al. 2008).

2.4.8 SPHysics

SPHysics is a freely distributed and downloadable SPH source code that solves a variety of free surface fluid flow problems. The website, *wiki.manchester.ac.uk/sphysics/index.php*, contains the free source code, along with forums and an upload section where code developers can view and discuss new numerical implementations and shortfalls. The website also contains a link to download the SPHysics User Manual.

The downloadable SPHysics code can simulate five predefined scenarios, that are all run through one Fortran code. The code can be used once it has been loaded and compiled onto a PC. The code can be run through either a windows based or Linux based operating system. Post processing of the output is done through Matlab files provided with the code. Also, the code comes with a user manual and examples of completed scenarios. The scenarios include dam breaks, tsunami generation and waves (generated by a paddle) breaking on a beach. Some include both three dimensional and two dimensional cases.

2.4.9 Evaluation of the SPHysics package

As a part of this study, an extensive evaluation of the SPHysics package was undertaken in order to assess whether it can give good enough resolution of the shape of a plunging wave, and more specifically, to assess whether it could be used as a tool in this study to extract breaking wave vortex shape parameters.

A number of runs were conducted with the supplied package, which was the case of the smooth, planar beach. Results were promising. The source code was then adapted slightly in order to cater for a submerged reef structure. An approximated reef structure (consisting of a reef slope, a reef crest and an absorbing beach) was built in to save on particles. This would have allowed for more particles in the domain to improve the resolution of the plunging jet, and thus a better depiction of breaking wave vortex shape parameters. This was the second problem domain. The original source code proved stable under these conditions, as did the adapted code. Stability was only found with very few particles (approximately 12000), which was insufficient for the required resolution of the plunging jet and thus, also for the extraction of vortex shape parameters (Figure 2.27). A full reef with a rear slope included was then implemented. This third domain proved to be the least stable of the three domains.

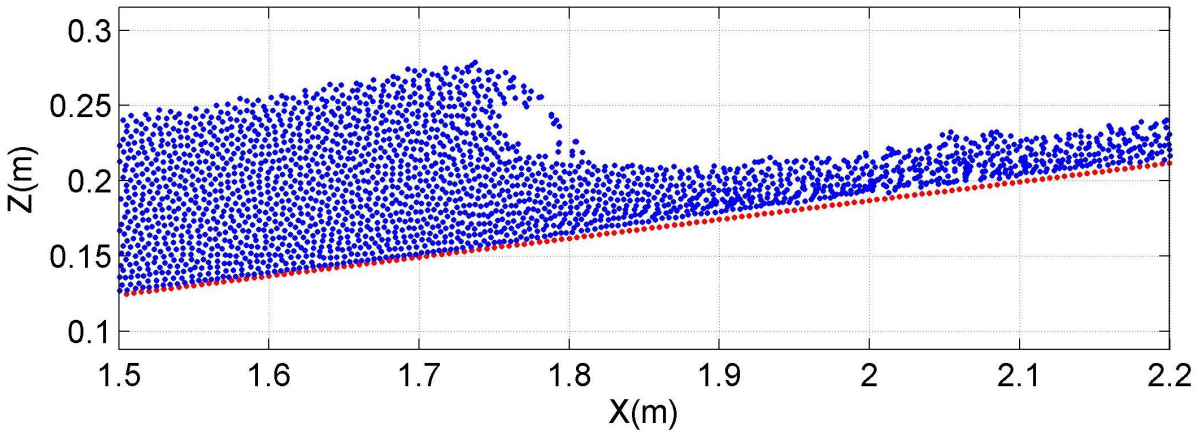

Figure 2.27: Typical resolution of the vortex shape for a wave breaking on a sloping beach with 14185 particles.

A total of 49 test runs were conducted in the process of finding a stable setup for all cases of the three domains. A setup stable enough for wave propagation over a full reef structure was not found due to problems with instability. These problems, such as 'leakages' through a boundary modelled as impermeable and decreasing water level, were found in varying degrees for all cases. The information regarding these runs are presented in Appendix A. The boundary is modelled as impermeable by appyling repulsive forces onto the particles that are in contact with the boundary. There were also many instances on all three of the domains where the

numerical calculations stopped during the simulation. This was another recurring deficiency in the code.

Upon increasing the number of particles in the second domain and in the original SPHysics package to achieve higher resolution, similar instabilities occurred. The SPHysics code, in its current stage of development, does not appear to be able to handle;

1. Number of particles in excess of approximately 50000 on all three domain types - Leakages for all domain types, the extent of which decreases as the domain decreases.

2. Number of particles in excess of approximately 20000 for the full and optimized reef - the water level in the lee of the reef decreases, minor leakages occur through the 'impermeable boundary' in some of the runs, and one random 'underwater explosion' instability occurred.

The SPHysics model is deemed to have deficiencies in the code which prevent, amongst others:

- Usage of high particles numbers,
- Long problem domains, and
- Possibly negative slopes (for the landward slope of the reef structure).

Having said this, the SPHysics package is still in a stage of development. There are links on the web page to a forum and another link where users of the code can upload their modifications and improvements to the original SPHysics code. During the time of this investigation, there were two releases of the package, with the first release being the more stable of the two, even though the second completed the runs quicker.

The SPHysics model gives promising results of the wave vortex shape with plunging breakers, albeit that their are problems with decreasing water level, leakages through the boundaries and random underwater explosions. Due to these deficiencies the SPHysics model was not employed in the investigations for this thesis.

2.5 Summary and conclusions

The following points summarise the most important parts of the literature review which are relevant to the proposed investigations.

- It is evident that multi purpose artificial reef structures are in an early stage of development. One reef with multi functionality as its design objective has been constructed to date. The Narrowneck reef is on Australia's Gold Coast and is functioning better than expected.

- More research into certain aspects is still required in order to develop sound design criteria and suitable standards for design and construction. Such areas of research include beach stability, biomass creation/relocation, breakwater protection and amenity creation.

- Variations in reef size could influence breaking of waves and energy dissipation on the reef. These could effect the biomass creation, beach stabilisation and breakwater protection aspects of the reef.

- A considerable amount of research has been done into the economic benefits of multi purpose reefs. These studies indicate high cost-benefit ratios. The cost-benefit ratios are also very dependent on the site location.

- Breaker depth and breaker height formulae for planar, sloping beaches have progressed to a stage sufficient for realistic design applications. Effects of various parameters such as bottom friction, shoaling, focusing, wind, currents and water level need to be accounted for in the breaker height and breaker depth formulae. The formulae of Rattanapitikon and Shibayama (2006) and Rattanapitikon et al. (2003) were based on a very large data set, are thus deemed the most reliable and accurate.

- Detailed research into the surfability of surf reefs has been conducted taking shortboard surfing into account. Peel angle, section length and breaker height have all been addressed. Design guidelines exist for these surfability parameters. This could be extended to include forms of wave riding other than surfing.

- While design guidelines exist on the effects of most wave parameters on surfability, these need to be extended to include the effects of breaker intensity for all breaker types on surfability.

- Breaker intensity is an important surfability parameter. The 'tube ride', which can only occur with plunging waves, is deemed by surfers to be an important part of surfing, both in the social (non-competitive) situation and in the competitive surfing arena.

- The combined effects of wave height, period, water level, reef crest width and seaward reef slope on breaking intensity through the breaking wave vortex shape parameters, needs to be assessed.

- Meteorological conditions (e.g. wind) play an important part in the surfability of waves.

- Numerical models for modelling the free surface, and, more specifically, for the depiction of the free surface during the wave breaking process, are currently being developed. Studies with these models in Coastal Engineering applications have been done by a number of authors, while others are currently underway. The results look promising.

- The SPHysics package is, at the its current stage of development, unsuitable for modelling of the falling jet of a plunging wave during breaking. Stability only occurs with very small numbers of particles, which results in low resolution and a poor simulation of the breaking wave shape.

Based on the above, the combined effects of wave height, period, seaward reef slope, water depth on the reef and crest width on breaking intensity of plunging waves (as defined by Sayce (1997)), will be addressed in this thesis. Being able to predict vortex shape parameters based on the above mentioned variables will be beneficial to the field.

The study will be done by using a theoretical analysis, a short case study at a local, natural surfing reef, and extensive physical model studies. The SPHysics package will not be used in the study as it is not deemed suitable for the task at hand. The effects of bottom friction, wind and currents will be neglected. Based on the findings, some design guidelines for artificial surfing reefs will be suggested.

Chapter 3

Theoretical Considerations

3.1 Introduction

A sound theoretical background will be needed in order to understand the dynamics that are prevalent before and at wave breaking in a two diumensional scenario. Exact solutions will not be sought, but rather a broad overview with simple approximations to the dynamics occurring before and up to the breakpoint, and how these shape the evolution of the plunging wave profile. Three dimensional effects have been neglected.

In the following text, reference is made to breaking intensity. This is breaking intensity as defined by Sayce (1997), and is defined by the vortex shape parameters. Breaking intensity increases with increasing vortex ratio and decreasing vortex angle, i.e; the plunging jet profile gets more 'round', and the plunging jet is projected further (in the direction of wave propagation) from the breakpoint than for waves with lower breaking intensity.

3.2 Definition of the problem variables

The reef configuration to be investigated is shown below in Figure 3.1.

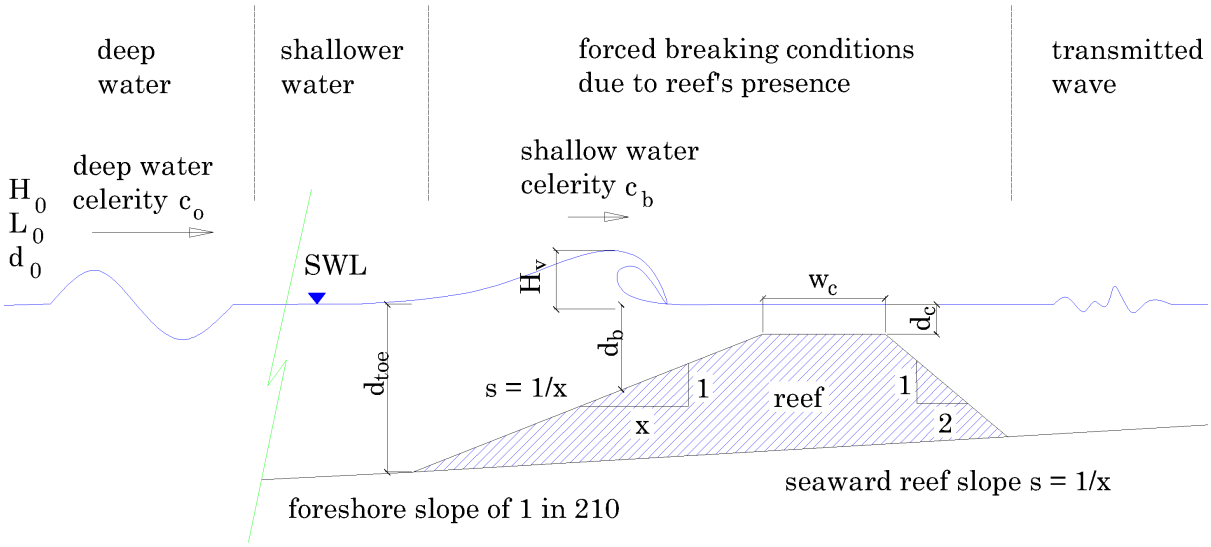

Figure 3.1: Reef configuration variables

The approach slope extends from the toe depth, d_{toe}, to the crest level at a depth, d_c. The crest consists of a horizontal section at a constant depth, d_c, that is of length w_c. This distance, w_c, will be referred to as the crest width in this study. The length of the reef, l_c, is in the direction parallel to the wave crests (for head-on waves). The rear slope will be assumed to be steep. This assumption is based on construction considerations, i.e., that the volume of the material used to construct the reef needs to be as small as possible, and remain stable. Considering that wave breaking should occur on the seaward reef slope and the crest, the assumption should be acceptable.

The method developed by Sayce et al. (1999), as shown in Chapter 2.3, was used to determine the plunging wave shape. This method describes the shape of the plunging wave vortex in terms of its length l_v and its width w_v. The angle that l_v makes with the horizontal is termed the vortex angle, and is given the symbol θ_v. The parameters are shown in Figure 3.2. Incipient breaking shall be taken as the point where the crest of the wave becomes vertical. The point of measurement of the vortex shall be taken as the point when the plunging jet first comes into contact with the front face of the breaking wave.

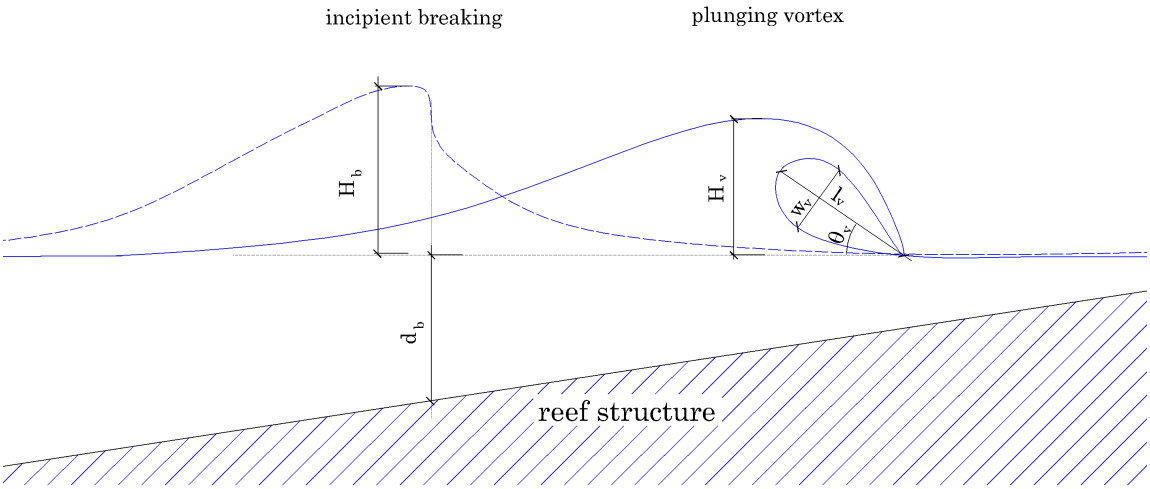

Figure 3.2: Incipient breaking and vortex shape parameters, adapted from Sayce (1997)

3.2.1 Linear wave theory and incipient breaking

The use of linear wave theory in the surf zone has its limitations and is not recommended for the surf zone, CEM (2006). Different wave theories such as cnoidal, stokes 5th and Fenton theory are deemed to be more applicable for orbital velocity, wave profile and energy calculations (CEM, 2006). These theories are, however, difficult to implement easily, and often complex calculations and semi graphical methods are required for solutions (CEM, 2006). Linear theory is thus to estimate the velocities and accelerations, and to give an indication as to the rate of the change of the various wave properties as the wave travels from deep water until depth induced breaking in occurs, with a certain degree of caution of course.

Figure 3.3 shows the plots of changes in depth d, wavelength L and wave height H (with respect to time) of a wave propagating from deep water to breaking conditions, along a planar, sloping beach of constant slope. The plots were calculated from linear wave theory. A MATLAB program was created, that propagates a wave crest, in time, from deep to shallow water conditions, based on the dispersion relation and linear shoaling theory. The most important

observation from these plots is the relative rates of change of the variables with respect to time (as they get close to breaking) and each other. The iterative calculation was stopped when the horizontal orbital velocity at the crest u_{crest} exceeded the wave celerity c, which is shown in Figure 3.3 as the dotted black line. The wave period was 12s with a breaker height of 3m in a water depth of 1.7m.

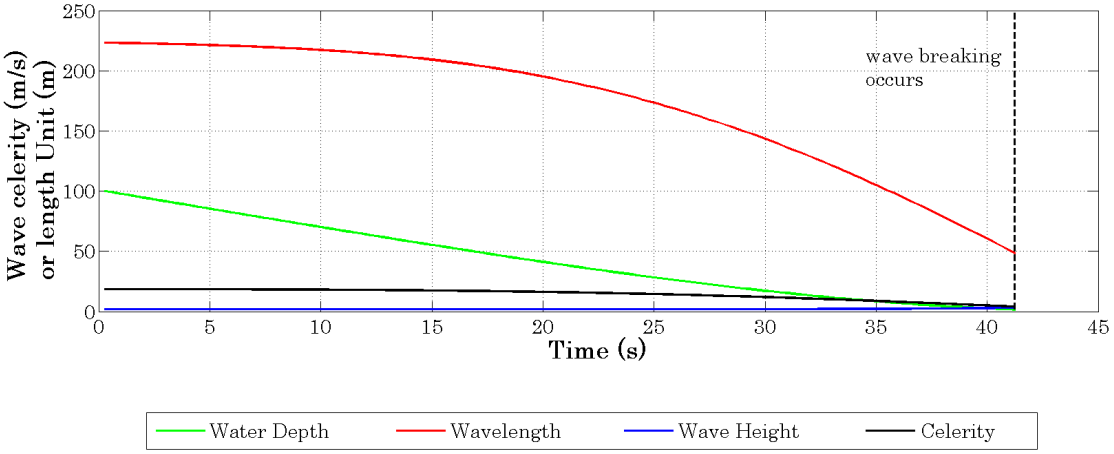

Figure 3.3: Variation of depth, wavelength and wave height from deep water to breaking conditions

The plot shows decreasing water depth as the wave propagates into shallower waters which results in decreasing wavelength (dispersive nature of wave propagation), increase in wave height through shoaling, and a decrease in celerity. The rate of change of wavelength, wave height and celerity all increase with decreasing water depth. This effect is very pronounced in the shallow waters just prior to breaking.

Figure 3.4 shows the increase in orbital velocities at the crest, still water level, near the bottom ($z = -0.1d$) and the wave height H for a wave propagating from deep water to shallow water. Wave celerity has not been plotted on the axes because it is significantly larger than the orbital velocities, and prevents a clear representation of how the orbital velocities and wave height vary with decreasing depth. Again, the dotted black line shows the point at which breaking occurs. The plot suggests that the increase in orbital velocities at the crest is significantly larger than the increase in orbital velocities at other positions from the still water level. The plots also suggests that the orbital velocities of particles near the crest are uniform, while in shallower waters the orbital velocities of water particles nearer the bottom are more uniform, more so at breaking.

The sharp increases in orbital velocities at the crest just prior to breaking indicate high accelerations of the water particles. It is expected that these increases in orbital velocities at the crest and the rate of change of celerity in shallow waters will be the two components significantly affecting the shape of the plunging wave and thus breaking intensity.

Incipient breaking is defined as the point in which the orbital velocities of the water particles at the surface exceed the wave celerity (CEM, 2006). The wave crest then becomes unstable and the wave breaks. Based on this, the breakpoint could then be predicted theoretically. Also, an estimation of the vortex shape parameters could be made. This estimation would be based on the relative rate of change at which the wave slows down upon entering shallower waters and the rate at which the orbital velocities at the crest increase as the wave enters shallower waters, that is, the ratio of the acceleration of the orbital velocities at the crest to the deceleration of

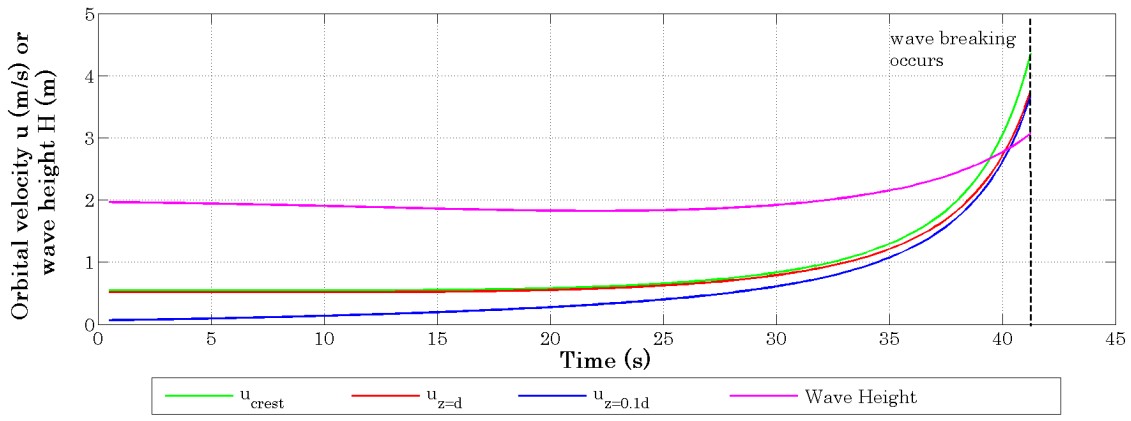

Figure 3.4: Variation of orbital velocity at crest u_{crest}, orbital velocity at still water level $u_{z=swl}$, orbital velocity near bottom $u_{z=0.1d}$ and wave height H from deep water to breaking conditions (z = distance from still water level)

the wave. This ratio shall be termed the acceleration ratio r_{acc}. It is in effect the ratio between the acceleration of the water particles at the crest relative to the propagating wave and the deceleration of the wave immediately prior to incipient breaking, and is equal to

$$r_{acc} = \left\{ \frac{\left|\frac{\Delta u}{\Delta t}\right| - \left|\frac{\Delta C}{\Delta t}\right|}{\left|\frac{\Delta C}{\Delta t}\right|} \right\} = \left|\frac{\Delta u}{\Delta C}\right| - 1 \tag{3.1}$$

where $\Delta u/\Delta t$ is the rate of change of orbital velocity of the water particles at the crest and $\Delta C/\Delta t$ is the rate of change of celerity of the wave. Δt is the time interval over which the changes in u and C are calculated. The ratio r_{acc} has been developed by the author, and is only intended to show how the acceleration of water particles at the crest and the deceleration of the wave can be used to give an idea of the intensity of the plunging wave, and thus it shall be used in this chapter in order to estimate how the various reef configurations and wave parameters can affect the breaking intensity. Higher values of r_{acc} should result in the jet plunging farther from the crest than for smaller values of r_{acc}, with associated lower vortex angles.

3.3 Seaward reef slope and vortex shape parameters

The seaward reef slope provides a means of quickly decreasing the water depth in a controlled manner in order to control wave breaking. Artificial multi functional reefs are generally placed some distance from the shoreline, and so an abrupt, relatively steep seaward reef slope is required to minimise construction costs through reduction of the reef volume, while still fulfilling the design objectives.

3.3.1 Breaker depth and breaker height

Because the orbital velocities are primarily dependent on wave height and wavelength and celerity is primarily dependent on depth, r_{acc} is thus dependent on both water depth and wave height. Breaker depth and breaker height are therefore deemed to very important factors affecting the vortex shape parameters.

With regards to breaker depth and breaker height formulae, Rattanapitikon et al. (2003) developed Eqn's. 3.2 from 26 different sources, while Rattanapitikon and Shibayama (2006) developed Eqn's. 3.3 and 3.4 to predict breaker depth. These equations are shown in Chapter 2.2 and are repeated here for clarity. Eqn's. 3.3 and 3.4 are based on the same 26 data sources as Eqn. 3.2. These equations have been in used this investigation because of the fact they are derived from a very large data set, whereas, the other equations mentioned in Chapter 2.2 are generally based solely upon the data gathered in that particular study. Eqn's. 3.2, 3.3 and 3.4 are thus applicable over a wider range, and contain the least amount of error (Rattanapitikon and Shibayama 2006).

Eqn's. 3.2, 3.3 and 3.4 are applicable over bottom slopes of $0 \leq m \leq 0.38$,
With $0.001 \leq H_o/L_o \leq 0.112$;

$$H_b = \left(-1.40m^2 + 0.57m + 0.23\right) L_b \left(\frac{H_o}{L_o}\right)^{0.35} \tag{3.2}$$

and for $H_o/L_o \leq 0.1$,

$$d_b = \left(3.86m^2 - 1.98m + 0.88\right) H_o \left(\frac{H_o}{L_o}\right)^{-0.16} \tag{3.3}$$

and for $H_o/L_o > 0.1$,

$$d_b = \left(3.86m^2 - 1.98m + 0.88\right) H_o \left(\frac{H_o}{L_o}\right)^{-0.34} \tag{3.4}$$

Figure 3.5 shows plots of varying deep water wave steepness H_o/L_o with constant wave period, thus constant deep water wavelength L_o, i.e., only deep water wave height has been varied. Breaker index H_b/d_b has been plotted against bottom slope m. The breaker depth required for Eqn. 3.2 was calculated using Eqn's. 3.3 and 3.4.

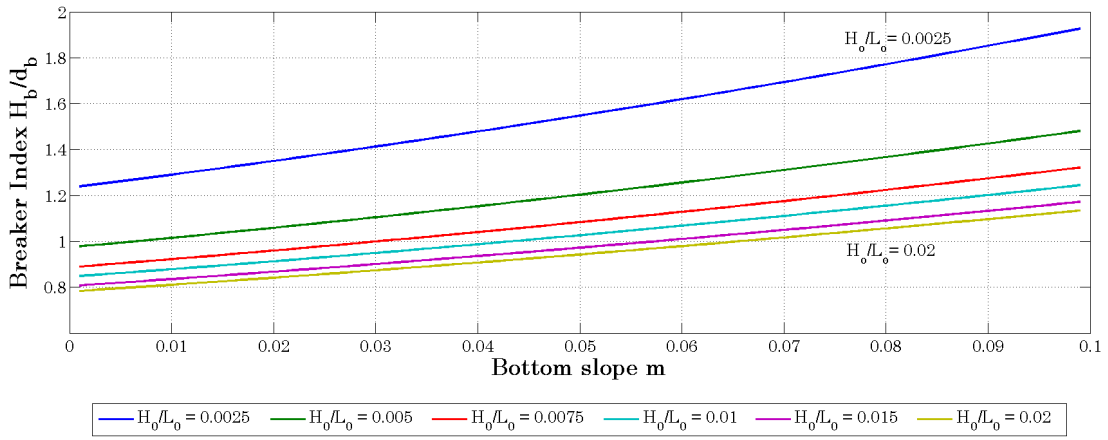

Figure 3.5: Breaker index, approach slope and deep water wave steepness, based on Eqn's. 3.2, 3.3 and 3.4.

The plots show an increase in breaker index for decreasing deep water wave steepness for a given seabed slope, and also for increasing seabed slope at a particular deep water wavelength. This in effect means that for any particular deep water wave height, the approach slope has the effect of increasing wave height at breaking. Along with this increasing wave height with slope, should come and accompanying increase in orbital velocities of water particles at the crest, and

an increase in wave breaking intensity as shown through the vortex shape parameters. From the point of view of breaker depth with constant breaking wave height, the breaker depth decreases with increasing slope. Thus lower wave celerities at the breakpoint, and higher values of r_{acc}. Higher breaking intensity through vortex shape parameters should follow.

3.3.2 Wave period

Linear wave theory shows that u_{crest} is directly proportional to wave height H and inversely proportional to wavelength L and that celerity C is only depth dependent (neglecting setup in the surf zone) in the shallow waters ($C = gd^{1/2}$) just prior to breaking (Figure 3.4). Wave period is also constant at all water depths, thus Δu and ΔC are both unaffected by wave period as waves propagate into shallower waters. This suggests that r_{acc} is independent on wave period. Linear wave theory is, however, an approximation of reality, but it is assumed that the it predicts the minimal effect of wave period successfully.

3.3.3 Iribarren number and vortex shape parameters

Table 3.1 shows various parameters that can be found to be dependent on the Iribarren number (Battjes 1974). The most important of these are deemed to be breaker depth index, H_b/d_b, reflection co-efficient r_c, breaker occurrence and breaker type. The Iribarren number is also useful as it gives an idea of the rate of deformation of waves while they propagate through the surf zone (Battjes 1974). This implies that it may be useful in determining the rate of change of the shape of the wave from deep to shallow water, and thus may be useful in determining the vortex shape parameters of plunging waves.

Table 3.1: Surf similarity in the surf zone (Battjes 1974).

Iribarren number ξ_o (Eqn. 2.2)	0.1	0.5	1.0	2.0	3.0	4.0	5.0
Breaking/No Breaking		breaking				nobreaking	
Breaker Category	spilling		plunging		collapsing/surging		
Breaker Index H_b/d_b	0.8	1.0	1.1	1.2			
Number of waves in surf zone	6 - 7	2 - 3	1 - 2	0 - 1	0 - 1		
Reflection coefficient	0.001	0.01	0.1	0.4	0.8		
Absorbing/Reflecting		absorption				reflection	
Progressive/Standing Wave		progressive				standing	
Setup	setup	dominant			runup	dominant	

Having said this, as discussed previously in Chapter 2.2, the Iribarren number was derived from test results obtained with waves breaking on smooth plane slopes. Its applicability to a submerged structure such as the reef to be used in this study has been shown by Couriel et al. (1998) that there is limited correlation between it and vortex shape parameters.

The most important insights to be gained from Table 3.1, is that the Iribarren number gives an indication of where the transitions between breaker types occur, i.e., at which values waves go from spilling to plunging and from collapsing to plunging. As mentioned in previous chapters, many authors have noted that the transition are not clearly defined, and are thus not very suitable for artificial surfing reef design. The table also shows that low reflection values, increased absorption and lower breaker indices accompany flatter slopes. Iribarren number gives an indication of where the transitions between breaker types occur, i.e., at which values waves go from spilling to plunging and from collapsing to plunging. As mentioned in previous chapters, many authors have noted that the transitions are not clearly defined, and are thus not very suitable for artificial surfing reef design. The table also shows that low reflection values, increased absorption and lower breaker indices accompany flatter slopes.

3.4 The reef crest and vortex shape parameters

When waves are forced to break on the reef structure, the broken wave propagates over the structure into its lee. Assuming that the reef now acts as a kind of surf zone in that waves are breaking over it, the broken wave should result in setup in the lee of the reef. Take the case of an incoming wave field propagating on a reef with s = seaward reef slope. Breaking (assuming breaking occurs) will be forced at a certain depth due to the existence of the approach slope. A certain amount of energy, E_{reef}, will be dissipated through interaction of the wave with the reef. This will result in a setup, η_s, being established on the lee side of the reef (Figure 3.6). The effects of set down due to breaking, η_b, have been neglected.

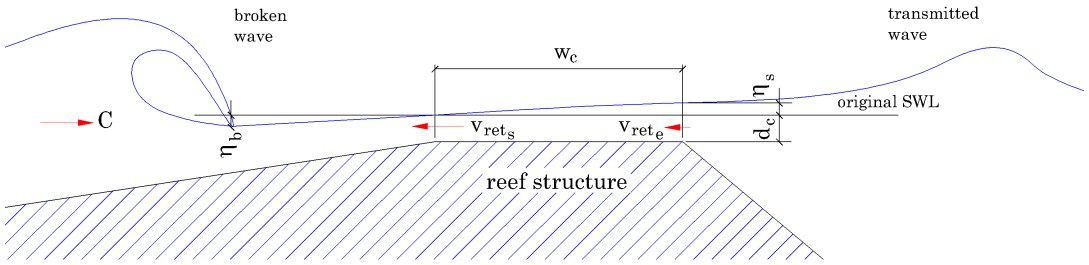

Figure 3.6: Formation of setup and return velocities

If this setup is not removed from the system by means of , for example, a long shore current running in the lee of the reef parallel to the shoreline, a return current will be established over the reef. The velocity of the return current v_{ret} should be proportional to some function of the setup η_s, water depth on the crest d_c, and the reef crest width w_c , that is;

$$v_{ret} = f(\eta_s, w_c, d_c) \tag{3.5}$$

A situation of gradually varied flow over the reef crest will develop as one broken wave crest passes over the crest into the deeper water on the lee side of the reef structure. During the time when the wave is passing over the reef crest, the return current ceases to exist because the celerity of the wave over the reef dominates the flow. Once it has passed over the crest, and prior to the next wave breaking and moving over the reef crest, the full extent of the setup begins to play a part in the return current flowing over the reef.

Assuming then that the water surface elevation at the end of the crest, y_{end}, is equal to the sum of the setup and the original water depth on the crest, that is

$$y_{end} = \eta_s + d_c, \tag{3.6}$$

and that the water depth at the start of the reef crest is not affected by the set down due to breaking, so that

$$y_{start} = d_c, \tag{3.7}$$

It can be shown using Bernoulli's energy equation and unsteady open channel flow theory that

$$v_{ret_s}^2 = v_{ret_e}^2 - \frac{S_f.w_c}{2g} + \frac{(y_{end} - y_{start})}{2g} \tag{3.8}$$

where S_f is the friction slope of the reef crest, and g = acceleration due to gravity. This can be reduced to

$$v_{ret_s}^2 = v_{ret_e}^2 - \frac{S_f.w_c}{2g} + \frac{\eta_s}{2g} \tag{3.9}$$

It should be noted that although η_s is a function of depth at breaking, d_b, and thus related to d_c, the return flow velocity on its own is shown to be independent of the crest depth, d_c. The relationship shows that increasing the setup due to breaking and the decreasing the width of the reef crest will result increasing the return velocity at the start of the crest, v_{ret_s}.

The resultant celerity of the wave, C_{res}, can be shown to be a function of the return velocity at the start of the crest, v_{ret}, and the initial celerity of the wave, C, before its interaction with the return current, as follows,

$$C_{res} = C - v_{ret_s} \tag{3.10}$$

The reduction of the wave celerity due to this return current will have the effect of decelerating the wave, and as such increase the acceleration ratio r_{acc}. This would result in higher breaking intensity as measured through vortex shape parameters.

3.5 The seaward reef slope and the reef crest in combination

Goda and Morinobu (1998), investigated the effects of breaking wave height on a horizontal bed affected by an approach (seaward reef) slope. They found that the limiting breaker height on a horizontal bed decreases with increasing approach slope. They used Eqn. 2.9 and adjusted the constant term ($A = 0.17$ in Eqn. 2.9) in order to fit the laboratory data. Table 3.2 shows the adjusted constants A for each of the respective slopes they tested.

Table 3.2: Adjusted constants for various approach slopes (Goda and Morinobu 1998).

Foreshore Slope	1 in 5	1 in 10	1 in 20	1 in 40	1 in 80
Constant 'A'	0.135	0.136	0.145	0.155	0.159

They found that for the steeper seaward reef slopes of 1 in 5 and 1 in 10, the breaker heights were about 80% of the limiting value, and that this percentage approached 94% for the flatter 1 in 80 slope. The theoretical limiting value is that for the case of waves breaking on the slope, which corresponds to an A coefficient of 0.17. They also found from their tests that increasing the wave period increased the distance of the breakpoint from the start (seaward side) of the horizontal bed. Figure 3.7 shows the relationship between the foreshore slope and the breaker depth for waves breaking on a horizontal slope, and the corresponding decrease in breaker depth on a horizontal bed for steeper approach slopes.

For waves breaking on the horizontal reef crest, steeper seaward reef slopes result in lower breaker heights. The lower breaker heights were attributed to separation of bound harmonics due to the presence of the discontinuity between the foreshore slope and the horizontal reef crest. The free harmonic waves then pre-empted breaking, because they had the effect of increasing the orbital velocities at the crest (Goda and Morinobu 1998). Thus, for waves breaking on the horizontal bed (i.e., the reef crest), in constant water depth, it is uncertain if wave height or the generation of the free harmonic waves is more responsible for increasing the orbital velocities at the crest, to the point that breaking would occur.

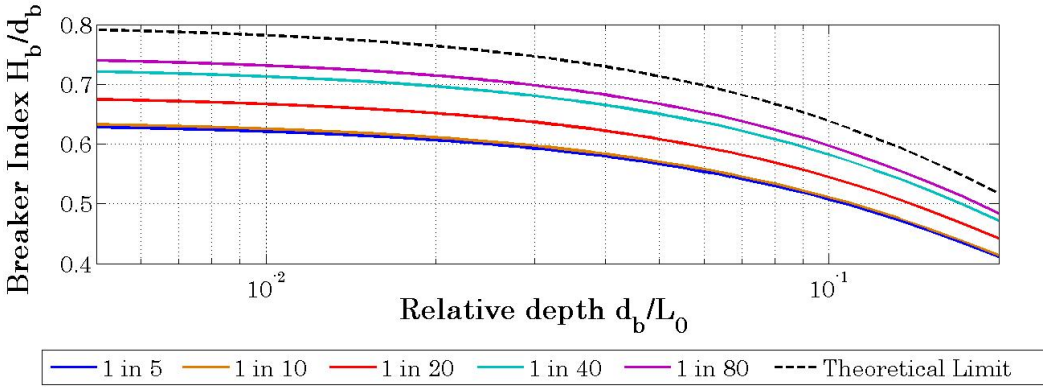

Figure 3.7: Relative depth vs breaker index on a horizontal bed with varying seaward reef slopes

3.6 The discontinuity and vortex shape parameters

Goda and Morinobu (1998) also found that the discontinuity between the foreshore slope and the horizontal reef crest resulted in the generation of free harmonic waves.

They noticed that the forward tilting present in shallow water waves propagating on a sloping bottom disappeared after the waves had propagated on the horizontal section for a certain distance. Furthermore, they noticed that a smaller secondary crest developed at the junction between the crest and the foreshore slope. The magnitude of this secondary crest was found to increase with approach slope. They attributed this to the growth of the non-linear bound components.

The extent to which these bound non-linear components increase in amplitude was found to be higher on flatter slopes than for steeper slopes. The mismatch between the non-linear components prior to the junction and the second and third harmonic formation after the junction, was found to be greater for steeper approach slopes. They attributed this to the fact there was not time for the full formation of the bound 2nd and 3rd harmonic components on the steeper slopes.

Furthermore, they found that the waves on the horizontal bed broke at the location where the bound second and third harmonics reached their full amplitudes. Thus for steeper slopes, there is a lower growth in amplitude of the non-linear bound wave components, resulting in larger bound second and third harmonics, higher orbital velocities at the crest due to the existence of these bound harmonics, and so a smaller wave height is required to cause breaking.

It is presumed that the effects of this phenomenon on the vortex ratio will be as follows:

1. Steeper slopes will result in excessive harmonic wave generation, which, if the crest is long enough, will result in the formation of secondary wave crests, which could negatively influence the shape of the plunging waves in a manner that causes the waves to be undesirable for surfing purposes, and,

2. For waves breaking on the crest, steeper seaward reef slopes will also result in lower breaker indices, thus lower breaker depths and increased r_{acc} and hence increased breaking intensity through vortex shape parameters.

3.7 Conclusions

Based on the previous few sections, the following can be concluded for the case of waves breaking in a 2D scenario, i.e., neglecting 3D effects:

1. Larger wave heights should result in higher breaker intensity;
2. Wave period should have negligible effect on the breaking intensity, within the bounds of say, swell waves with wave periods in the order of 8s to 16s;
3. Breaking waves in shallower waters should result in higher breaking intensity than for waves breaking in deeper waters, with breaker index being equal;
4. Increasing the seaward reef slope should result in higher breaking intensities for the case of waves breaking on the slope;
5. Increasing Iribarren number has the effect of increasing breaker index and reflection coefficients. Previous authors (Couriel et al. 1998) have found little correlation between it and vortex shape parameters, and is thus deemed unimportant;
6. Reduction in the width of the reef crest will increase breaking intensity. With respect to this, the water depth on the reef crest, d_c is deemed to have a greater effect than that due to the friction of the horizontal bed.
7. Harmonic wave generation at the discontinuity between the end of the seaward reef slope and the horizontal crest, will affect the shape of the wave profile, and will thus affect the shape of the vortex during breaking. The extent of this is however difficult to predict from theory.

Chapter 4

Case Study: 'Sunset' - A Natural Surf Reef

4.1 Introduction

Prior to conducting the physical model study (presented in Chapter 5), a case study was done in order to illustrate how sea bed topography and wave conditions can produce good quality surfing waves. This was done by means of a case study of a naturally occurring local surf break. The reef was chosen specifically because of the fact that it is large, and it can be easily identified on bathymetric charts. In addition to this, the reef is situated very close to the Slangkop wave buoy, and thus wave measurements are available.

An assessment was made of the wave dynamics responsible for the formation of good quality surfing waves. These dynamics include wave refraction, focusing, shoaling, and breaking intensity. The shape of the reef was also evaluated.

4.2 Introduction to the reef

'Sunset' is a natural reef that is situated approximately 1km North of the small town of Kommetjie, which lies about 40km SSW of Cape Town in the Western Cape, South Africa (Figure 4.1). The reef is located at a depth between mean sea level and approximately 30m. Due to its shape and orientation, it only produces good quality waves for surfing when extremely large waves are generated by the intense frontal systems in the Southern Ocean, usually in the Winter months between May and September. These large waves refract around the headland due to the shallow water effects, re-enter deeper water, after which they begin to interact with the reef. The refraction is also favourable as it results in consistent orientation of incoming wave crests to the reef, which means that the waves always break consistently along their length.

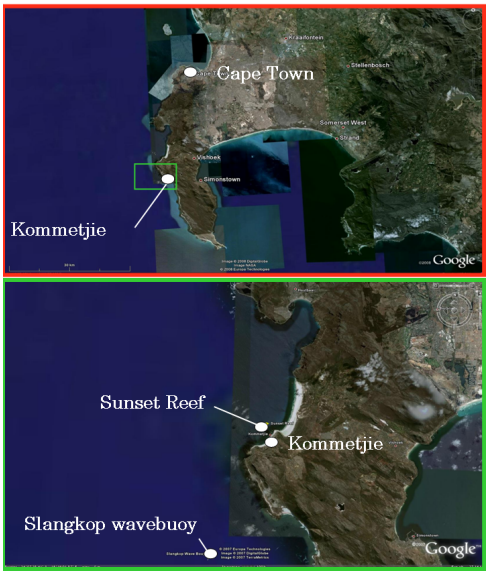

Figure 4.1: Locality map: Sunset Reef

A large degree of wave focusing and shoaling occurs, which amplifies the wave heights. The surfers

are generally towed in with jet-ski's while already standing on the surfboard, because the waves are too large to paddle in to from a lying down position. Very short section lengths also result, caused by the unique shape of the reef.

The reef has been referred to as 'Sunset', as it is known throughout surfing community. There is similarity in the shape of the breaking wave to its Hawaiian counterpart, after which it was named.

4.3 The reef's topography

The toe of the reef starts at approximately the -25m contour line, and the reef rises steadily up for about 1200m where it reaches land. The reef gradually widens from the toe until the crest is five hundred meters wide at approximately the -10m contour line. From this point it widens quickly, and is about 1000m wide by the time it meets the beach. It thus a very large structure, and has significant effects on the incoming waves.

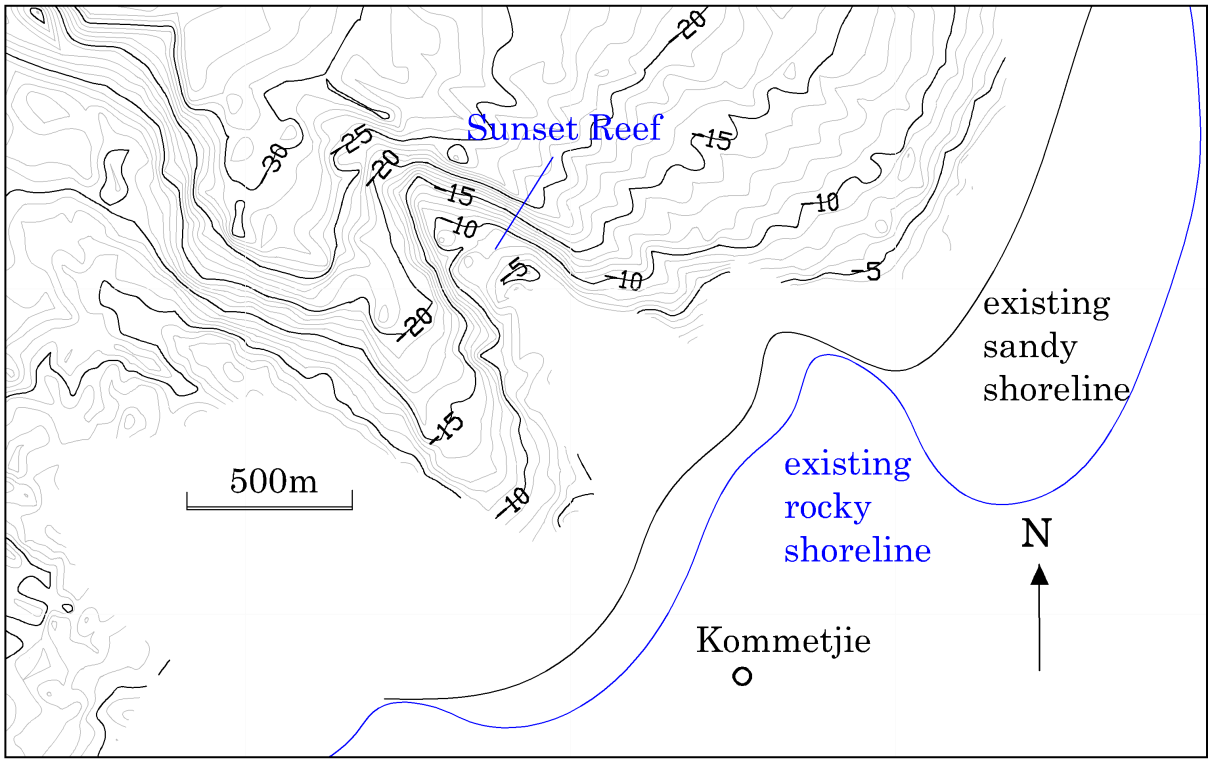

Figure 4.2: Topographic features of 'Sunset' reef

The slope down the longitudinal axis of the reef (starting at the toe) is approximately 1 in 45 until the -25m contour. It continues at about a 1 in 24 slope until the -10m contour, after which it proceeds to the shoreline at a slope of about 1 in 70. The side slopes of the reef are relatively steep, approximately 1 in 10 on the southern side and 1 in 18 on the northern side.

4.4 Wave dynamics before and on the reef

The mean direction of waves in the ocean in the deeper waters off Cape Town is generally consistent from the SW, which is 225 ° relative true North. These waves propagate along the coastal waters and gradually refract in such a way that their crests are oriented more parallel

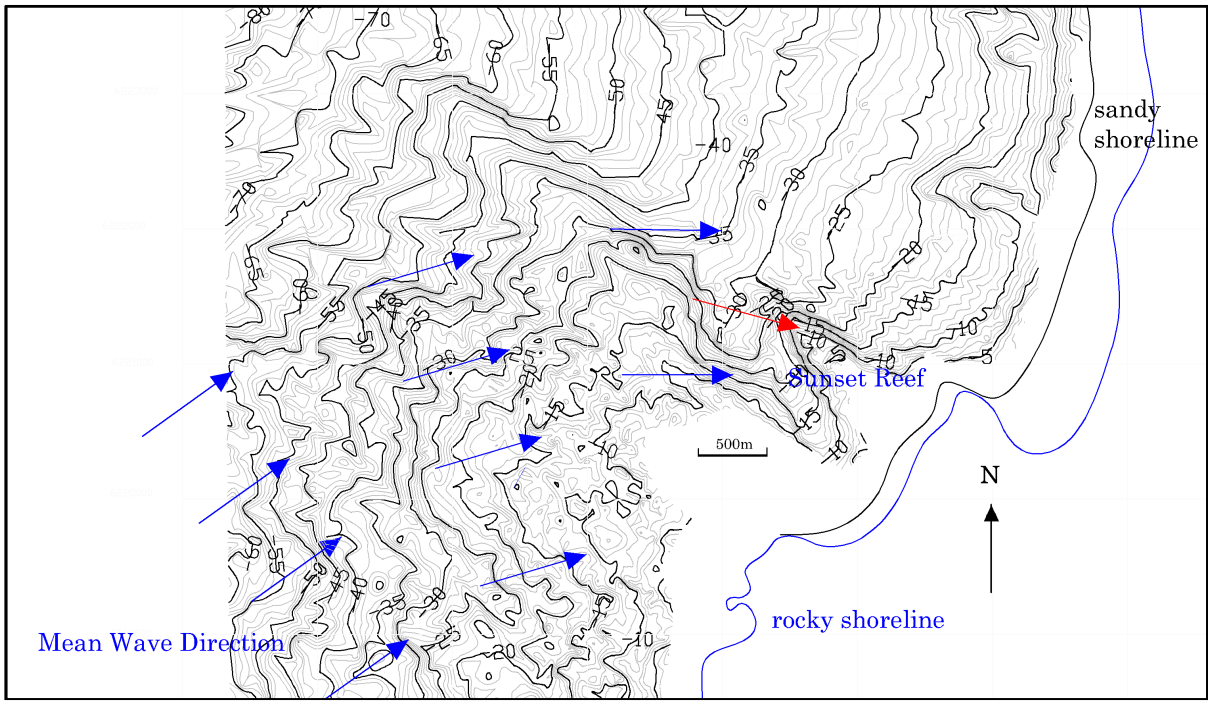

Figure 4.3: Estimated refraction patterns off the coastline at Kommetjie

to the coastline. Figure 4.3 shows a qualitative estimation of the refraction patterns as waves propagate towards the reef. The wave direction is shown with the blue arrows. The degree of refraction increases as the waves begin to interact more with the shelf as they reach the shallower waters.

The wave direction as the waves reach the reef (the red arrow) has been estimated visually from video footage. The reef then acts in a similar manner as a lens (Figure 4.4), focusing the wave energy towards the breakpoint by means of refraction. This results in an increase in wave height due to refraction (focusing) and shoaling.

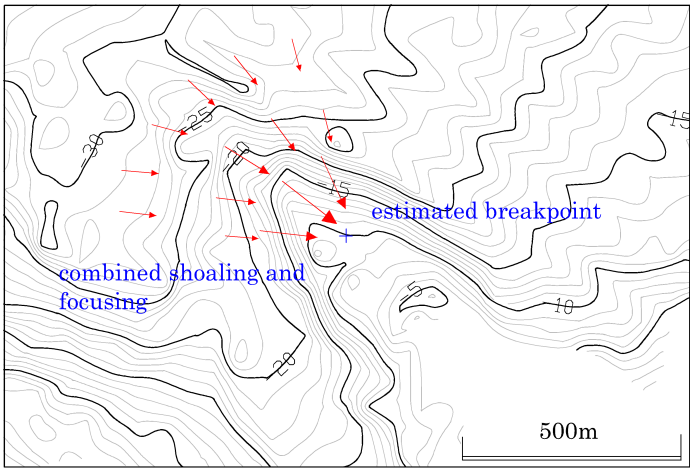

Figure 4.4: Focusing and shoaling at Sunset Reef

The wave focusing effect has been investigated by West et al. (2003). They developed the West-Cowell surfing reef factor S_{rf}, which gives an estimation of the degree of wave focusing that a reef of a certain size has on the incoming wave. The West-Cowell factor (Equation 4.1) is essentially a ratio between the breaker height with the reef present to the breaker height without the reef present. It is based on linear wave theory and numerical models. The West-Cowell surfing reef factor, S_{rf}, is defined by Eqn. 4.1, below:

$$S_{rf} = \frac{D}{d_{reef}} \cdot \frac{l_c}{L_{reef}}, \tag{4.1}$$

where D is the reef height = depth at toe - depth on crest, d_{reef} = breaker depth on reef, l_c the length of the crest, (Figure 4.5), in the direction parallel to the shoreline and L_{reef} is the wavelength at breakpoint.

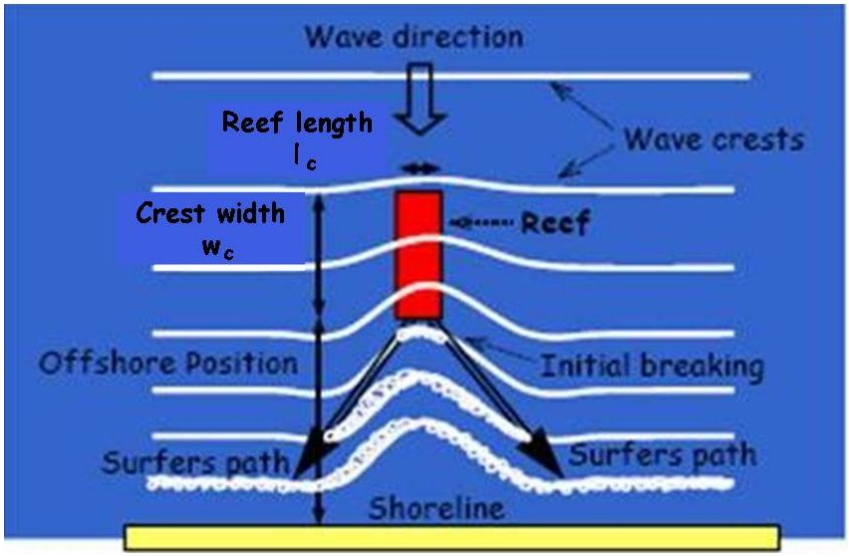

Figure 4.5: The wave focusing reef concept. Adapted from (West et al. 2003)

Thus, S_{rf} relates the shape of the reef to the degree of wave focusing. Equation 4.1 was derived from relationships obtained from simulations with values of crest depth, D, of less than 8m. This is considered to be the limit of the equation's applicability. As an example, it is assumed that:

- D = 25 - 10 = 15m;
- d_{reef} = 9m;
- l_c = 156m (estimated from bathymetric charts) and,
- L_{reef} = 104 (calculated with d_b = 9m and T = 12s),

This results in:

$$S_{rf} = \frac{15}{8.2} \times \frac{156}{113} = 2.4 \tag{4.2}$$

Thus, for a twelve second wave, this reef has the effect of increasing the wave height by a factor of 2.4, assuming that the wave breaks at a depth of 8.6m, which should be the case for a wave of H = 7.2m (assuming $H_b/d_b = 0.8$). Thus, a 3m wave propagating over the 'Sunset' reef should be amplified by a factor of S_{rf} = 2.4 and breaks at a height of 7.2m in a water depth of approximately 9m. This seemingly unrealistic value of the extent of wave focusing is attributed to the limits of the West-Cowell surfing reef factor, S_{rf}.

4.5 Surfing on the reef - 17 May 2008

On the morning of Saturday 17 May 2008, a very large storm swell arrived in Cape Town. Readings from the Slangkop wave buoy, just southwest of Kommetjie (Figure 4.1), measured significant wave heights, H_s, of 6 to 7m with peak wave periods, T_p, in the region of 18s. Maximum wave heights were in the region of 10.5m. The mean direction was measured at 233 degrees, very close to the WSW direction.

Figure 4.6 shows a overhead shot of a wave breaking on the 'Sunset' reef on 17 May 2008. The breaking wave height is estimated at approximately 15m, based on the size of the surfer, boat and helicopter relative to the wave.

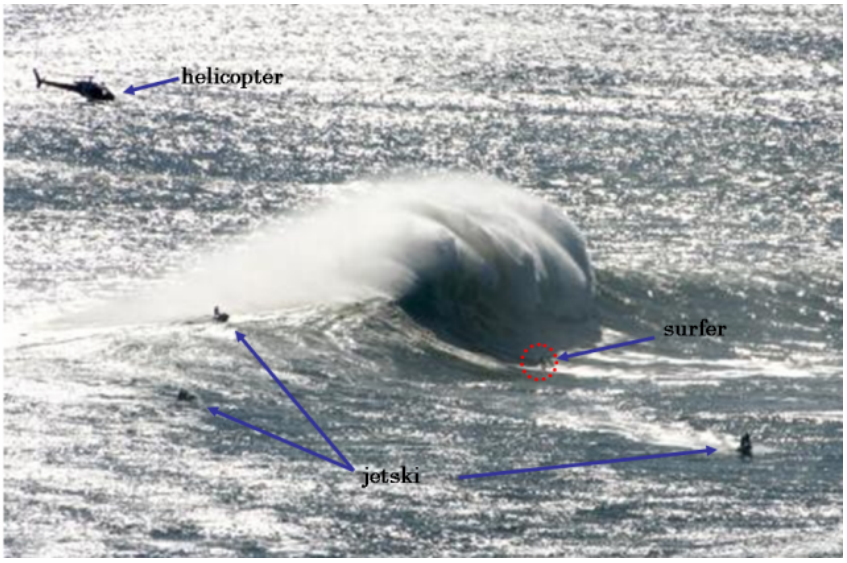

Figure 4.6: Image of wave breaking on 'Sunset' reef - 17 May 2008 (wavescape.co.za)

Assuming this was one of the highest tenth waves, one can estimate the wave height of the wave from relationships shown in the CEM (2006). If $H_{1/10}$ is taken as approximately $1.27 \times H_{1/3} = 1.27 \times 6.5m= 8.2$m and the maximum wave height, $H_{max} = 1.8 \times H_{1/3} = 1.8 \times 6.5$m $= 11.2$m, this wave can be estimated as being in the order of between 8.2m and 11.2m in height before reaching the reef. For these conditions, S_{rf} is calculated as follows:

- Deep water wave height, H_o, was based on the H_{max} from the wave records, $H_o = 10.5$m,
- Deep water wavelength, L_o, $= 505$m,
- Deep water wave steepness, H_o/L_o, $= 10.5 \ / \ 505 = 0.024$,
- From Figure 3.5, with a 1 in 24 bottom slope, H_b/d_b is estimated as 0.83,
- Breaker height, H_b, $= 10.5$m (solved through iterative procedure using S_{rf},
- Breaker depth, d_b, was thus $= 10.5/0.83 = 12$m,
- Wavelength at breaking, $L_{reef} = 190$m from linear wave theory,
- Length of the crest, $l_c = 156$m, as before, and
- Height of the reef from toe to crest, D, $= 15$m as before

Substituting in to equation 4.1 gives,

$$S_{rf} = \frac{15}{12} \times \frac{156}{190} = 1.02 \tag{4.3}$$

This value is clearly not correct as this suggests the reef only amplifies wave height to a very small degree. This is not the case as H_{max} from the wave records is 10.5m, and the estimated breaker height, H_b, is approximately 15m, 1.5 times larger than the maximum wave height in the record and that used in the calculation of S_{rf}. Further work is thus required to assess the usefulness of the West-Cowell factor estimation of focusing effects for reef of complex shapes and also for reef depths, D, in excess of 8m.

With regards to visual observations, one can notice from the images (Figures 4.6 and 4.7)the lack of height (and thus steepness) of the crest adjacent to the plunging vortex on either side. This is attributed to the refraction drawing the wave energy toward the shallower depths on the reef, resulting in increased wave heights at the breakpoint, with subsequent decrease in the height along the length of the crest.

Figure 4.7: Plunging vortex on 'Sunset' reef - 17 May 2008 (wavescape.co.za)

Figure 4.7 shows good detail of a plunging vortex from one of the waves on 17 May 2008. As an indication of breaking intensity, assuming a constant bedslope of 1 in 24 (as mentioned earlier in this chapter) and that the seaward reef slope, s, can give reasonable approximation of the bedslope, β, from deep to shallow water, this wave has a deep water Iribarren number of:

$$\xi_o = \frac{tan\beta}{\sqrt{H_o/L_o}} = \frac{1/24}{\sqrt{10.5/505}} = 0.29 \tag{4.4}$$

and an inshore Iribarren number of:

$$\xi_b = \frac{tan\beta}{\sqrt{H_b/L_o}} = \frac{1/24}{\sqrt{15/505}} = 0.24 \tag{4.5}$$

This means the breaking wave in Figure 4.7 is in the spilling category. A very clear intense plunger is evident in the image. Thus it is assumed that either the current Iribarren numbers are applicable for sloping beaches only, or that the values of Iribarren number for the transitions

between the breaker types are different for waves breaking on reef structures than for sloping beaches. A visual inspection of the vortex shape parameters show the vortex ratio r_v to be approximately 2.2. Based on the classification of breaker intensity by Black and Mead (2001), Table 2.4, this implies high breaking intensity. The vortex angle θ_v is quite low, at approximately 40°.

4.6 Summary and conclusions

The qualitative study of the 'Sunset' reef has shown that:

1. Topography on the sea floor can significantly refract waves and result in improved surfing conditions at a particular surf spot.

2. The reef structure can, depending on its size, orientation and shape, drastically increase wave heights, such that even on relatively flat slopes, they break as plunging breakers with high intensity. Wave focusing effects can result in waves of significantly higher breaking intensity than those expected. This is evident in a wave plunging with medium breaking intensity that was expected to be in the spilling regime.

3. The West-Cowell surfing reef factor relates shape of the reef to the expected increase in wave height. It can give a good indication of the expected increase in wave heights, and is not applicable for crest depths greater than 8m and also for complex reef shapes. Numerical models should give better indications of focusing effects for these cases.

Chapter 5

Physical Model Investigations

5.1 Introduction

Two-dimensional physical model tests in a laboratory flume were conducted for two reasons:

1. To describe quantitatively the manner in which the reef configuration, i.e., seaward reef slope, s, and crest width, w_c, affects the breaking process, but more specifically to establish if the theoretical considerations discussed in Chapter 4 are responsible for affecting the vortex parameters in the expected manner, and

2. To attempt to form a relationship between the wave parameters, namely wave height at breaking, H_b, wave period, T, the water depth on the crest, d_c, and the two dimensional reef configuration variables seaward reef slope, s, and the reef crest width, w_c. Such a relationship could then be used in estimating the plunging wave shape through vortex parameters, and thus provide multi functional reef designers with a means of predicting the plunging shape, to enable more cost efficient and confident designs to be implemented.

Three dimensional effects have been neglected due to cost constraints.

5.1.1 Selection of the test parameters

Time constraints limited the number of tests performed in this study. Reconstruction of the reef structure was kept to a minimum, as this was time consuming. Tests of length of 1min model time were deemed to give sufficient data for the analysis. This resulted in approximately 16 to 25 waves per test. In total, four seaward reef slopes were selected, four wave heights, three wave periods, three water depths on crest, and two crest widths made a total of 288 tests. The selection of each of the values to be tested for the various parameters was based on the following considerations.

Figure 5.1 shows the reef parameters used in the tests.

- ***Wave Height at breaking*** H_b : It was desired to test wave heights in increments from 0.5m to 2.0m prototype. 2m wave heights at breaking are deemed to be close to the limit of waves suitable for shortboard surfing. Wave heights larger than this are assumed to be more suitable to other forms of surfing which require longer surfboards, that are not as manoeuvrable. With these other forms of surfing in larger waves, the shape of the plunging wave is not as critical as it is with shortboard surfing. Also, to construct a reef for extremely large surfable waves is expected to be very expensive, as the reef would need to be placed in deep water (to ensure the waves do not break before they reach the reef), which would require a large volume of construction material.

- ***Wave Period*** T : The wave periods selected were based on typical wave periods generally prevalent at surf breaks. These are in the range of between 8s and 16s. It has been assumed that the wave period greater than 14s can generally be associated with very large winter storms which produce waves that are too large for shortboard surfing, while the sea states with waves of periods below 10s are not fully developed. The waves in these sea state are assumed to be mostly short crested, which are not desirable for surfing as they create relatively short rides. The wave periods between 10s and 14s have therefore been selected based on the fact that these will produce the best quality waves for shortboard surfing.

- ***Seaward Reef Slope*** s : A 1 in 1.5 slope was selected as the first slope to be tested. This would provide an opportunity to assess the potential of a reef with a very steep seaward reef slope to provide a plunging wave suitable for surfing while keep the volume of the reef as small as possible. The 1 in 1.5 slope was based on stability concerns of the reef structure. Couriel et al. (1998), gives seaward reef slopes for certain points along the Narrowneck Reef on Australia's Gold Coast, which are shown in Chapter 2 in Table 2.5. Based on these, a 1 in 10 and 1 in 18 slope were selected as two of the test slopes. Couriel et al. (1998), conducted studies with a 1 in 14 slope, and it was deemed unnecessary to conduct tests of the same nature on the same foreshore slope. A 1 in 6 slope was chosen as the final test slope. This was selected in order to get data for waves breaking on a slope between the 1 in 1.5 and 1 in 10 slopes.

- ***Water depth on the crest*** d_c : The three water depths were based on the tidal cycle of a typical diurnal tidal system, with the maximum difference in tidal elevations between the mean spring high and low tides being approximately 1.5m. This was divided into three test levels, each 0.75m apart, representing a high water spring, mean water level and a mean low water spring tide. It was assumed that other water levels in between this range could be interpolated.

  The lowest water level represented a crest depth of $d_c = 0.75m$. This was chosen based on estimating the crest depths of current literature of multi functional reef structures relative to their tidal range. The crest was thus situated at a depth of -1.5m below the mean test water level.

- ***Reef crest width*** w_c :

  Two reef crest widths were tested, namely 6m and 15m. The effect of the crest width was expected to be minimal, thus only two crest widths were tested.

- ***Summary of test parameters*** :

  Figure 5.1 shows the reef and test parameters employed in the study. Table 5.1 shows a summary of the various parameters used for the test conditions.

Table 5.1: Selected test parameters (prototype values)

	Unit	Prototype Test Values
Seaward Reef Slope s, 1 in x	(-)	1.5 , 6 , 10 , 18
Width of reef crest, w_c	(m)	6 , 15
Water depth on reef, d_c	(m)	0.75 , 1.5 , 2.25
Wave Height at breaking, H_b	(m)	0.5 , 1.0 , 1.5 , 2.0
Wave Period, T	(s)	10 , 12 , 14

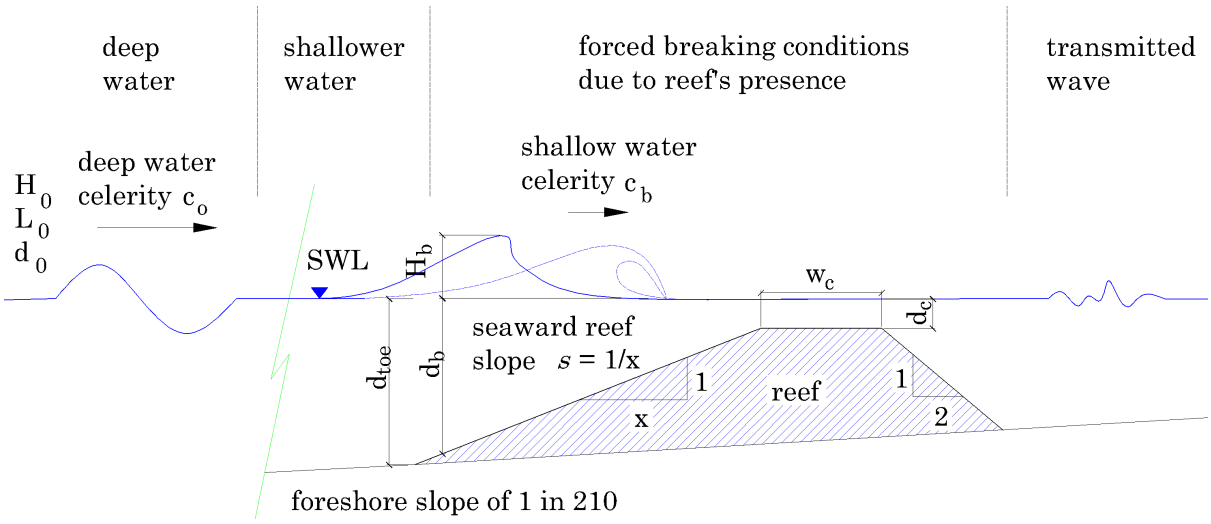

Figure 5.1: Reef configuration parameters

Figure 5.2 shows the Iribarren number plots for the test conditions. Although there is no literature confirming the use of the Iribarren for wave breaking on submerged structures, it has been used to assist in the selection of the test parameters.

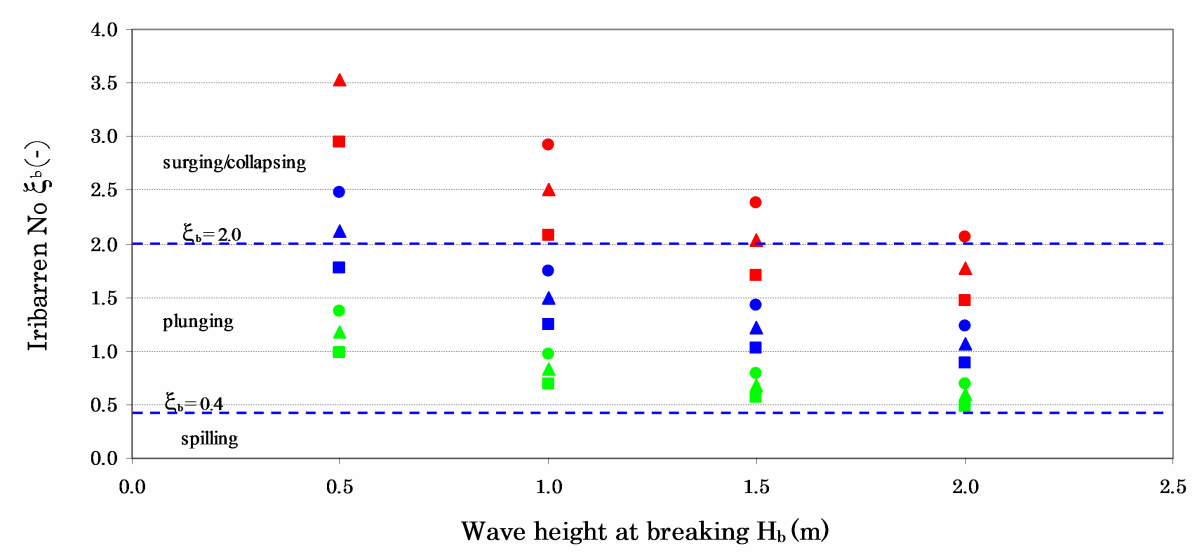

Figure 5.2: Spread of inshore Irribarren No, ξ_b, used in the tests.
The green, blue and red data points represent the 1 in 18, 1 in 10 and 1 in 6 slopes respectively, while the squares, triangles and circles represent the 10s, 12s 14s wave period respectively.

Eleven of the 36 test conditions fall in the surging/collapsing category, 25 into the plunging category, while one condition is into the spilling category.

5.2 Physical model setup

The tests were conducted in a glass flume at the CSIR Hydraulics Laboratory in Stellenbosch, South Africa. The flume is 32m long, 0.75m wide, and 1.2m deep. It was ideal for this investigation because it enabled the test runs to be viewed from the side, which was critical for the measurement of the vortex shape parameters.

The flume was large enough and had sufficient wave generating capabilities for the tests to be conducted at an undistorted scale of 1:15. Due to inertial and gravity forces dominating, the Froude scale law was used to scale from prototype to model conditions. The following derivations result in the length scale N_L and time scale N_T used in the model tests.

$$N_L = \frac{L_p}{L_m} = \frac{15}{1} = 15 \tag{5.1}$$

$$N_T = \frac{T_p}{T_m} = \left(\frac{L_p}{L_m}\right)^{\frac{1}{2}} = (15)^{\frac{1}{2}} = 3.87 \tag{5.2}$$

A long section of the flume is shown in Figure 5.3. Wave measurements were taken for each of the tests at the locations shown as P1 to P10. Probe 10 was a mobile probe placed just seaward of the breakpoint. The reflection off the absorbing beach was estimated at 14%, based on the method of Mansard and Funke (1980).

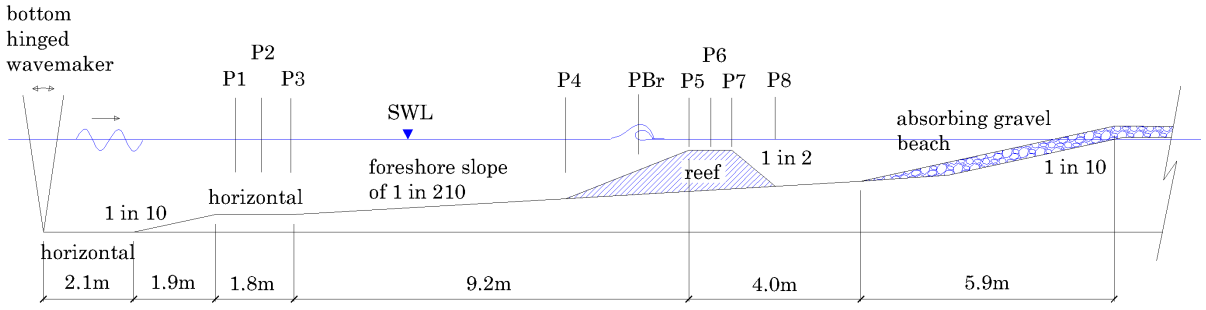

Figure 5.3: Flume long section

The reef crest was situated 15m (in the model) from the wave maker in a water depth of 310mm model (4.65m prototype) below the mean test water level. This depth was based on a study of current multi functional reef projects incorporating surfing as one of the design objectives. In general, these reefs are placed with a prototype toe depth of between 4 and 6 meters relative to mean sea level. For the test conditions, the tidal differences between spring highs and lows are within 1.5 to 2 meters prototype. The final toe depth of 4.65m prototype at mean test water level was based on these current projects and the limitations of wave making capabilities with respect to water depth.

The seaward reef slopes were constructed from lengths of pre-made adjustable slopes. The slopes are in pieces of different lengths. At the ends of each of the lengths is an adjustable thread which alters the elevation of that end. These are fixed to the floor of the flume with weights. The spaces between the walls of the flume and the reef were closed up with plasticine, to prevent any currents from flowing up between the side of the flume walls and the reef, since this can affect the results significantly. The final model test values are shown in Table 5.2.

Table 5.2: Selected test parameters (model values)

	Unit	Model Test Values
Constant foreshore slope ,	(-)	1 in 210
Seaward reef slope, s, 1 in x	(-)	1.5 , 6 , 10 , 18
Width of reef crest, w_c	(m)	0.2 , 1.0
Water depth on reef, d_c	(mm)	50 , 100 , 150
Wave Height at breaking, H_b	(mm)	33 , 67 , 100 , 133
Wave Period, T	(s)	2.6 , 3.1 , 3.6

The relevant literature does recommend avoiding water depths less than 100m and breaking waves less than 100mm (See Section 5.4) in the model due to effects of surface tension. The available wave maker and flume water depth both limited the use of larger scales, with the consequence that two of the breaking wave heights to be tested were less than 100mm in the model.

Tests were also conducted to assess the sensitivity of the vortex parameters to wave height, wave period, water depth and crest width on their own. This was to be used in order to get accurate relationships of the vortex parameters at test values other than those of the main tests. Tests of seaward reef slope were not done due to the long time required for construction of slopes (approximately 5 to 6 hours per slope). The following values were selected for the sensitivity analysis:

Table 5.3: Prototype test values for the sensitivity tests

	Unit	Minimum	Maximum	Increment
Width of reef crest, w_c	(m)	3	15	3
Water depth on reef, d_c	(m)	-0.75	3.00	0.25
Wave Height at breaking, H_b	(% Gain)	10	60	2
Wave Period, T	(s)	6	18	1

The values were chosen on the basis that they would cover the full range of variation in parameters at most surfing reef site in the world.

5.2.1 Test procedure

A total of 288 tests with varying different parameters were conducted. Regular waves were used for all of the tests. This was based on the fact that regular waves provide a constant wave height and period through the test, and as such, enable the collection of a large consistent data set. Wave signals were generated by use of software that converts required wave parameters into an analogue signal that can be read by the wave maker control unit. This is in turn is converted into displacements of the wave maker flap, creating waves. The software calculates the model parameters based on prototype parameters.

Waves were allowed to propagate for about two minutes after the time when the wave maker was switched on to attain steady state conditions in the flume. It was expected that the steady state conditions would provide more reflection within the flume during the test as opposed to obtaining vortex parameters from the time the wave maker was switched on. This was expected to affect results, but it was deemed more important to attain steady state conditions in the flume in order to avoid the measurement of data during the time when the unwanted long

waves were in the process of being generated.

Once steady state conditions had been attained, the recording of data with the video camera began for 1min.

5.2.2 Wave measurement and analysis

Ten twin wire resistance probes were placed in the flume (Figure 5.3) to measure the wave parameters as various points in the flume. Reflection of the reef structure and that due to breaking was measured using probes P1 to P3, using the method developed by Mansard and Funke (1980).

The gravel beach at the end of the flume was used to absorb the incoming waves and thereby prevent reflection back towards the reef. Reflection off the beach was measured in a separate test and estimated at an average of 14% for the three test water levels. P4 was placed at the toe, with P5, P6 and P7 at the start of the crest, center of the crest and the end of the crest respectively. Probe P8 was used at the toe of the rear slope, while P9 was placed at some distance from the end of the reef. Probe P10 was a mobile probe used to measure waves just prior to incipient breaking. The distance from this probe to the break point also varied between tests, and in some cases could not be placed closer to the break point because other parts of the experimental apparatus were in the way. The breaker height was thus measured from the images (the procedure is described in the following subsection) as this was considered to be a more accurate representation of the breaker height.

The wave analysis was done with in-house, CSIR developed software, that calculates average wave heights on a regular wave field, along with the wave period. Typical time-series plots of some of the tests is shown in Appendix B.

5.2.3 Image analysis

A video camera was mounted at 90° to the flume walls in order to capture the vortex shape parameters of the breaking waves. Live video was stored on video tape as it provided far higher quality images than memory card. The video tape was converted to DVD disk format, after which images were extracted in bitmap format. This format provided the highest extracted frames per second, with each image being approximately 1.2MB in size. Approximately 10 frames per second of test were obtained after extraction to be used for analysis.

The images were analyzed in a MATLAB program. The program opens the image of the plunging vortex from which the wave breaking and vortex shape parameters are manually extracted. It allows for user-defined points to be collected from the image. The co-ordinates of these points are then used to calculate the vortex shape parameters.

One adjustment is done for the camera not being set up at 90° (perpendicular) to the walls. Thus if a horizontal line is not horizontal in the camera view, an adjustment is made for this. Also, an adjustment is made for any parallax errors due to distortions of the camera. In some cases the camera was directly in line with the breaking wave, thus lines at right angles to one another some distance from the axis of view of the camera in reality do not appear as though they are at 90° to one another on the image.

The method is illustrated in Appendix C by means of an example, and the code for the MATLAB program is also presented.

5.3 Physical model results

5.3.1 Breaker type classification

A summary of the breaker type classification according to Battjes (1974) is shown in Table 5.4 for the various tests, and a histogram of the breaking events is shown in Figure 5.4. A total of 72 tests were performed for each seaward reef slope.

Table 5.4: Occurrence and percentages of breaker types for the tested slopes

Seaward Reef Slope s	No breaking	Spilling	Plunging	Collapsing-Surging
1 in 1.5	17 (24%)	9 (13%)	11 (15%)	35 (49%)
1 in 6	22 (29%)	12 (17%)	27 (38%)	12 (17%)
1 in 10	17 (24%)	10 (14%)	45 (63%)	0 (0%)
1 in 18	10 (14%)	8 (11%)	54 (75%)	0 (0%)

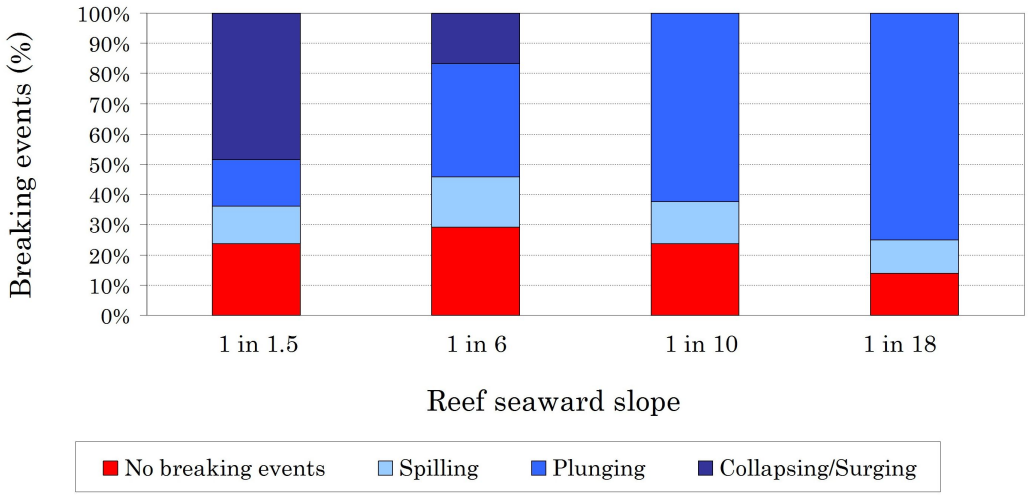

Figure 5.4: Histogram of measured breaking events

A very low occurrence of plunging waves occurs on the steep 1 in 1.5 seaward reef slope. The majority of these waves surge over the crest or collapse before the crest with no breaking. A large flow over the reef is noticed, which flows down the reef slope into the crest of the approaching wave (Figure 5.5). Also, the reef is very near to being exposed, which is unsuitable for surfing conditions. This reef configuration produces very weakly plunging waves only when the crest is long enough and when there is sufficient water depth on the crest to prevent the surging from occurring.

The occurrence of plunging waves increases significantly with the flatter seaward reef slopes. As seen in Table 5.4, the occurrence of surging waves also decreases. An image of the evolution of one of the plunging waves is shown below in Figure 5.6.

Figure 5.5: Surging wave on the 1 in 1.5 seaward reef slope

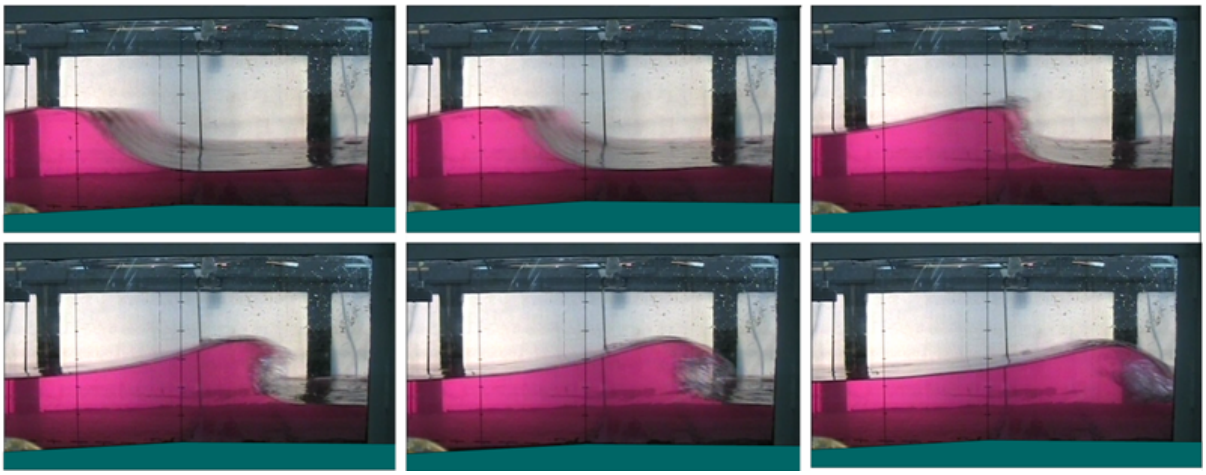

Figure 5.6: Plunging wave for the 1 in 18 slope, model test values of H_b=133mm, T=3.0s, d_c=+100mm above crest, w_c=1m

From left to right, beginning at top left, (i) Approaching the break point, (ii) Just prior to incipient breaking, (iii) Incipient breaking, (iv) The wave begins to overturn, (v) Formation of the vortex, and finally, (vi) a fully closed vortex, which allows the extraction of vortex parameters.

5.3.2 Suitability of vortex ratio r_v and vortex angle θ_v

It has been proposed earlier to use the vortex ratio and vortex angle as an alternate means of measuring the breaking intensity. Black and Mead (2001) found that for site measurements, vortex angle is not useful in estimation of breaking intensity (as discussed in Chapter 2). It was thus necessary to determine if either of these parameters are in fact suitable for defining the breaking intensity through vortex shape parameters.

Figure 5.7 shows the definitions of the vortex shape parameters. The figure has been shown previously, and is repeated for the sake of clarity. First of all, it is necessary to measure the reliability of the process. Three tests were conducted to measure this. The test with a 1 in 18 seaward reef slope, 15m wide crest, low water (at +0.75m above the crest level), wave period of 12s and breaking wave height of 2m was used for the analysis. This test was selected as it gave a good depiction of the plunging wave profile. The error was calculated as the standard deviation for the sample of measurements divided by the mean value of the sample, and is called the standard error.

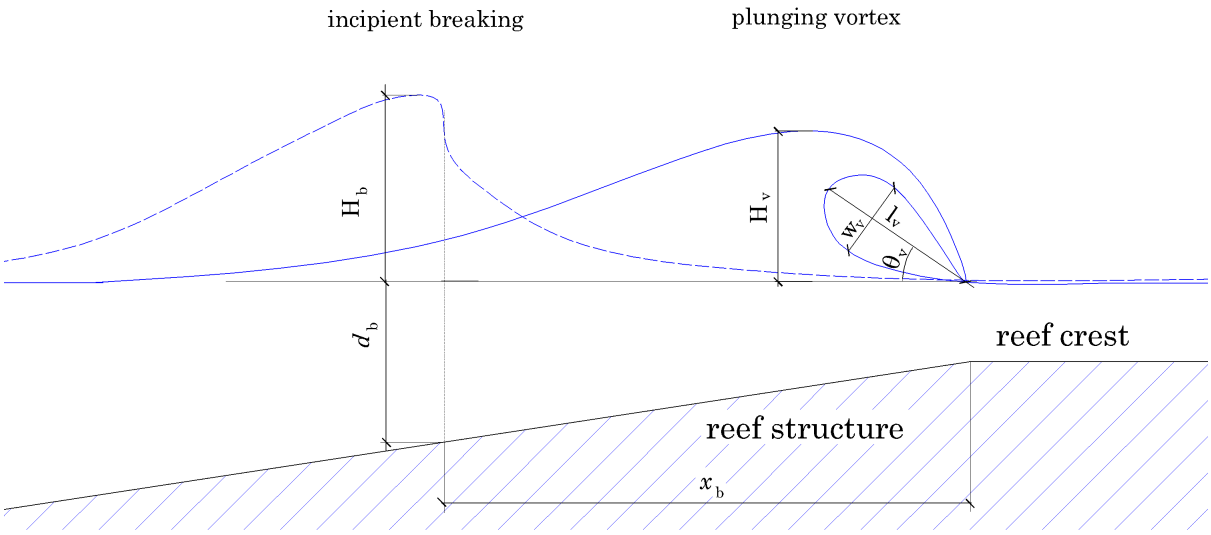

Figure 5.7: Incipient breaking and vortex shape parameters, adapted from Sayce (1997)

1. The first test analyzed the error inherent within the analysis procedure. For this test, the same image was analyzed twenty times using the same method. The results are presented in Table 5.5.

Table 5.5: Results for error test 1: Analysis accuracy

	x_b	H_b	d_b	l_v	w_v	r_v	θ_v	H_v
Mean	4.56	1.07	1.00	0.87	0.46	1.89	45.1	1. 06
Minimum	4.48	1.00	1.00	0.80	0.40	2.00	42.0	1.00
Maximum	4.65	1.14	1.01	0.94	0.52	1.81	48.0	1.10
Std. Dev	0.05	0.03	0.00	0.03	0.03	0.03	1.8	0.03
Std. Error	1%	3%	0%	3%	6%	2%	4%	3%

This suggests that the method of analysis in the MATLAB program is reasonably accurate. The error is less than 6% for all measured vortex parameters. Vortex ratio, r_v, with a standard error of 2%, contains half the standard error of the vortex angle, θ_v.

2. A test to estimate the variations in breaking wave profile inherent during one single test was also conducted. The images of all waves (in one specific test) were analyzed at the point where the plunging jet impacted the front wave face. The results are presented in Table 5.6.

Table 5.6: Results for error test 2: Vortex shape parameter consistency

	x_b	H_b	d_b	l_v	w_v	r_v	θ_v	H_v
Mean	13.76	1.41	1.51	1.13	0.55	2.05	44.0	1.46
Minimum	13.37	1.25	1.49	0.84	0.43	1.95	32.3	1.30
Maximum	14.49	1.52	1.55	1.39	0.67	2.07	53.7	1.58
Std. Dev.	0.34	0.09	0.02	0.15	0.06	0.09	5.0	0.07
Std. Error	2%	6%	1%	13%	11%	4%	11%	5%

Table 5.6 shows the high degree of variation in vortex parameter between waves in the same test. This could be attributed to water depth due to the long wave oscillations in the flume. This would then suggest extremely high sensitivity to water depth. This cannot be the case, because the breakpoint is accurate to within 2%, while the variation in the other vortex parameters is significantly different. It is therefore concluded that there must be some other source of error which results in accuracies greater than 10% for vortex length, l_v, vortex width, w_v and vortex angle, θ_v.

3. The third test was conducted in order to analyse the variation in the estimation of the vortex parameters at three points in time, namely, just prior to the plunging jet impinging the front face of the wave, at the point of contact, and just after wards. Vortex shape parameters were analyzed at these three points (Table 5.7).

Table 5.7: Results for error test 3 : Variation in timing of plunging jet

	l_v			w_v			r_v			θ_v		
	Pre	Impact	Post	Pre	Impact	Post	Pre	Impact	Post	Pre	Impact	Post
Mean	1.19	1.09	1.07	0.58	0.51	0.54	2.05	2.20	1.98	43.6	43.6	45.1
Minimum	0.96	0.86	0.84	0.49	0.43	0.47	1.76	1.97	1.74	36.8	32.3	40.6
Maximum	1.39	1.26	1.25	0.67	0.61	0.62	2.35	2.52	2.13	48.7	53.7	48.4
Std. Dev.	0.14	0.16	0.14	0.06	0.06	0.07	0.18	0.19	0.18	4.2	7.3	3.5
Std. Error	12%	15%	13%	10%	12%	13%	8%	8%	9%	10%	17%	7%

The standard error associated with the vortex ratio, r_v (8%), is again half that of vortex angle, θ_v(17%). This variation in vortex angle is attributed to the return wave which formed due to breaking of the previous wave in the train. Visually, it was noted that this wave is small in magnitude and its frequency of occurrence is not exactly in phase with incoming waves. Also, it is never always the same magnitude. This is attributed to the interactions between the long waves in the flume and the varying degree of air entrainment in the breaker of the preceding wave.

The variation inherent in the standard error of the vortex shape parameters just prior to, at, and just after impact are relatively small, and all measurements at the different timings of the plunging jet are within 2% at the most. This is, however, not the case for the vortex angle. In this case, the point at which the vortex angle is extracted can give standard errors varying up to 10%. This suggests vortex angle is far more sensitive to the reflections in the flume and to the return wave than vortex ratio.

This, coupled with the fact that the errors associated with the measurement of vortex angle are always approximately twice as large as the error inherent in the measurement of the vortex ratios, (Tables 5.5 and 5.6) suggests that vortex ratio, r_v, is a more consistent and reliable means of measuring the breaking intensity than vortex angle, θ_v.

The following subsections are an attempt to identify trends in the data. Due to the large degree of variation in the data set, only linear regression lines have been fitted. Furthermore, only the vortex shape parameters of waves that gave a clear vortex have been included in the study. This includes both collapsing and spilling waves with very small vortex shapes.

The data from the sensitivity tests (Table 5.3) was analyzed and it was found that they also contained a large degree of scatter. This data was therefore included in analysis of the main test data in order to increase the size of the data set, and thus give a more reliable analysis of the relationships between the tests parameters and the vortex shape parameters.

5.3.3 Effects of wave height at breaking, H_b

Figure 5.8 shows the increase of vortex length l_v and vortex width w_v with increasing breaker height. A closer fit to the data was expected, with the correlation ratio for the plots of l_v and w_v measuring 0.71 and 0.72 respectively. The average correlation ratios for the plots suggests scatter in the data, which is a attributed to the high level of variation as mentioned previously.

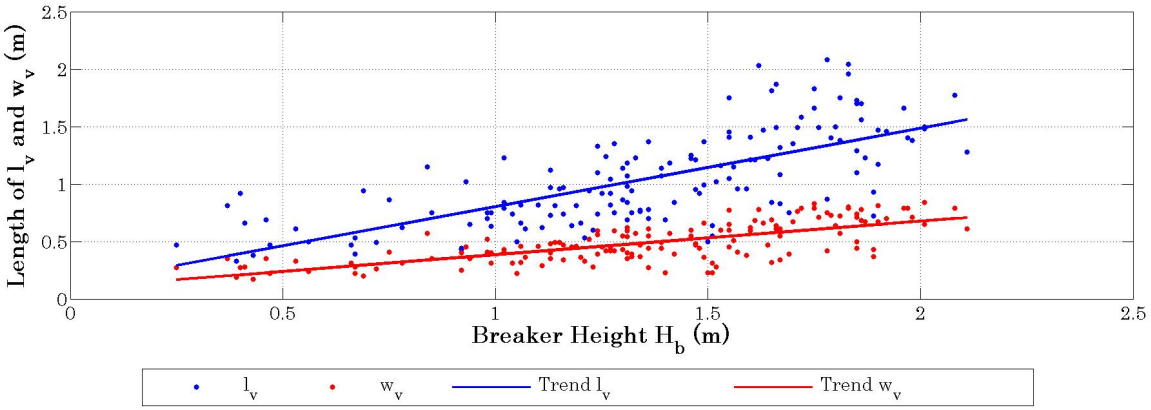

Figure 5.8: Relationship between vortex length, l_v, vortex width, w_v, and breaker height, H_b

Figure 5.9 shows a moderate upward trend of the vortex ratio with respect to breaker height.

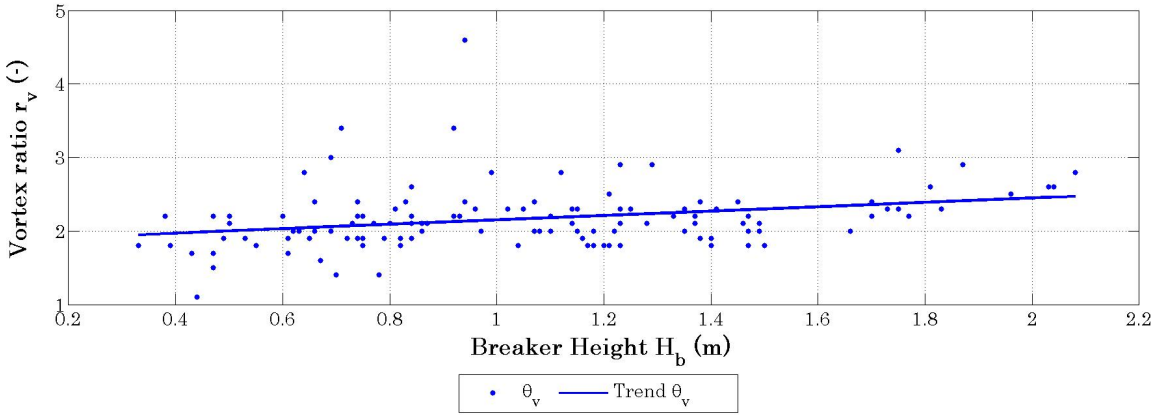

Figure 5.9: Relationship between vortex ratio, r_v and breaker height, H_b

Figure 5.10 shows an appreciable decrease of vortex angle with increasing wave height. One explanation for this is the dependence on orbital velocity on wave height, although there are more dynamics involved.

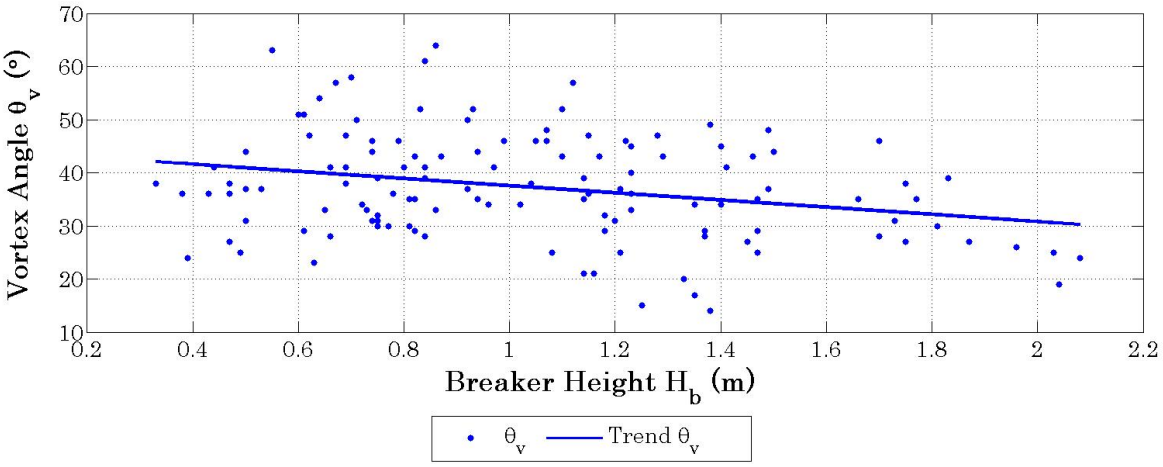

Figure 5.10: Relationship between vortex angle, θ_v and breaker height, H_b

5.3.4 Effects of wave period, T

There appears to be no apparent trend between wave period and any of the vortex shape parameters. Even though Figures 5.11, 5.12, 5.13 and 5.14 suggests that wave period plays a part in the vortex angle, there is no distinguishable relationship between the other vortex shape parameters and wave period, so it is assumed that the apparent relationship does not exist, and, if it does exist, is negligible.

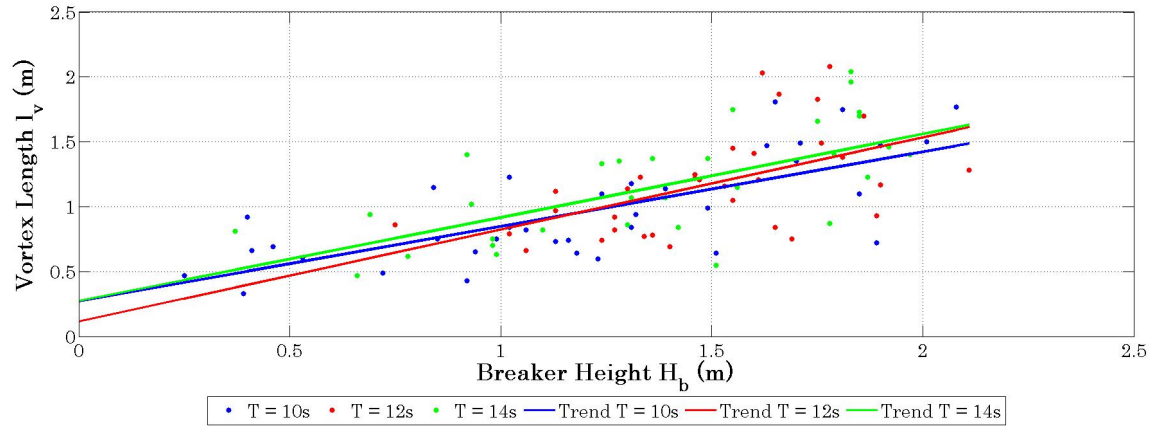

Figure 5.11: Relationship between vortex length, l_v and wave period, T

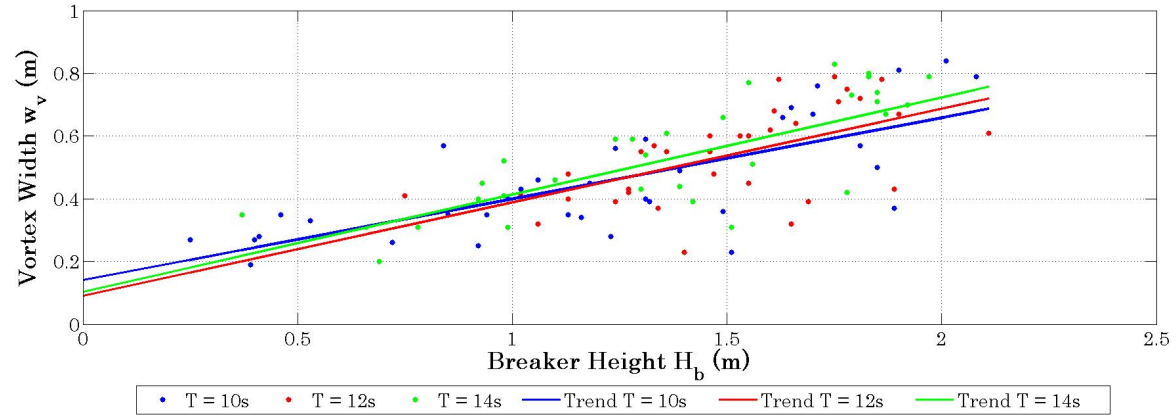

Figure 5.12: Relationship between vortex width, w_v and wave period, T

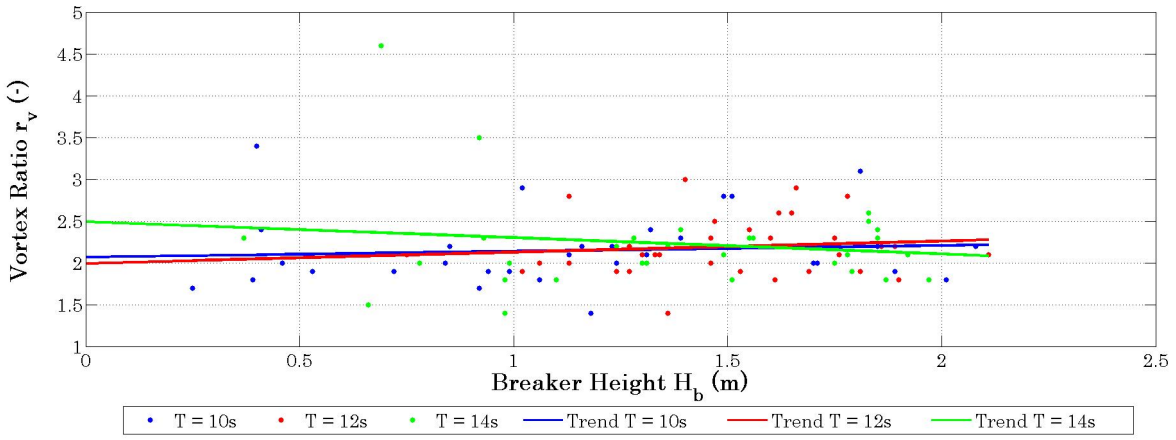

Figure 5.13: Relationship between vortex ratio, r_v and wave period, T

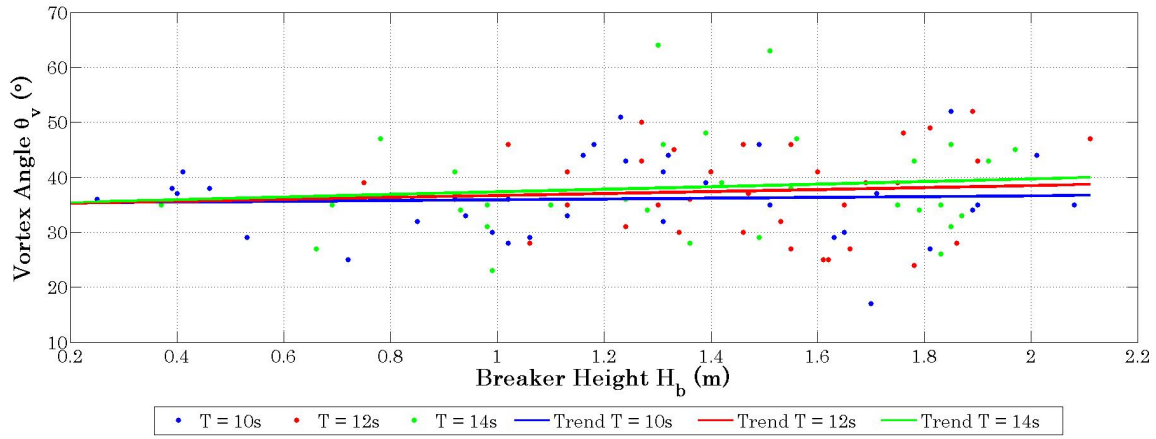

Figure 5.14: Relationship between vortex angle, θ_v and wave period, T

5.3.5 Effects of seaward reef slope, s

Both vortex length and vortex width are affected by the seaward reef slope. For the range of the test conditions, it appears that flatter slopes have the effect of increasing the vortex length and vortex width (Figures 5.15 and 5.16). Again, there is a degree of doubt due to the scatter in the experimental data set. Also, due to the low occurrence of plunging waves on the 1 in 1.5 seaward reef slope, there is very little data plotted for the tests with the 1 in 1.5 seaward reef slope.

Vortex angle appear to be unaffected by the seaward reef slope, even though a slight increase in vortex ratio with slope is evident (Table 5.8).

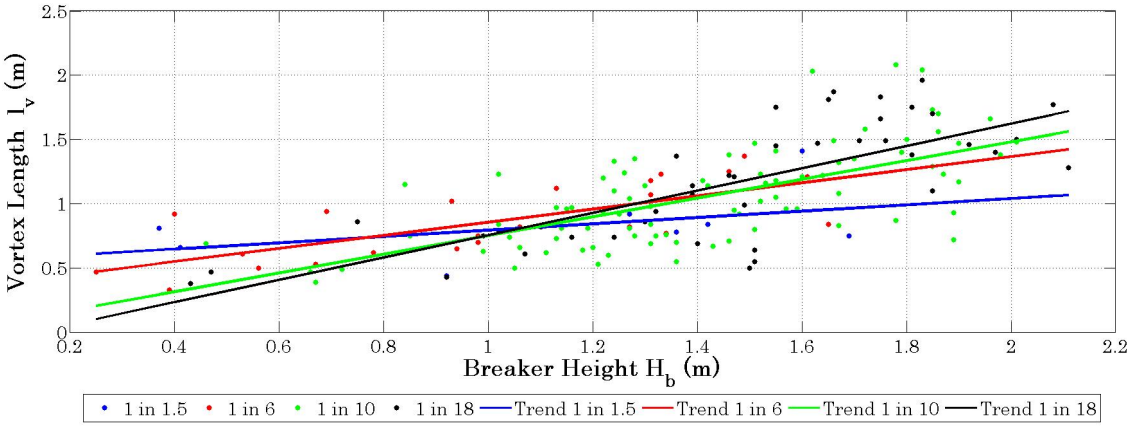

Figure 5.15: Relationship between vortex length, l_v, and seaward reef slope, s

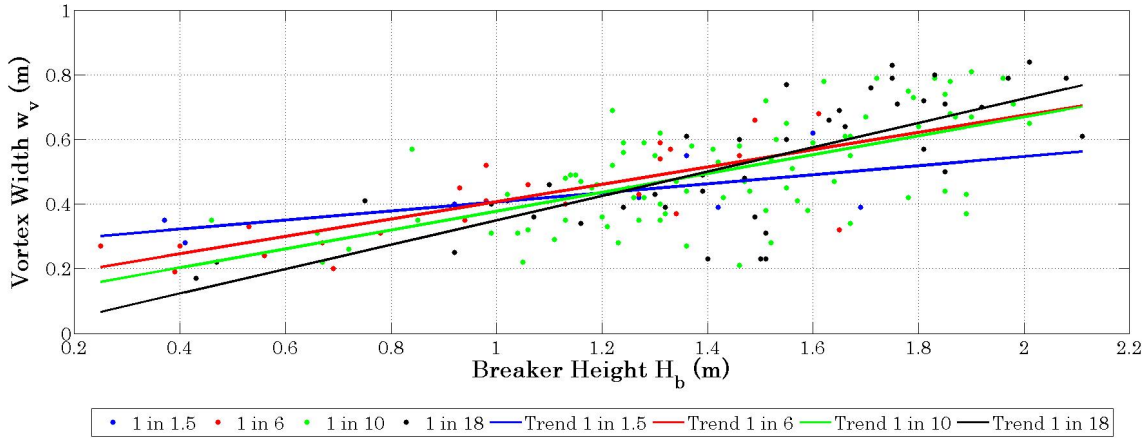

Figure 5.16: Relationship between vortex width, w_v, and seaward reef slope, s

Table 5.8 shows the variation in the slope of the trend lines for each of the slopes. The table contains gradients of the trend line for vortex length, vortex width and vortex ratio.

The data presented in Figure 5.15, Figure 5.16 and Table 5.8 suggests the dependency of the ratio of vortex length to breaker height upon the seaward reef slope. The same is true for vortex width and also vortex ratio (Table 5.8).

Table 5.8: Trendline gradients for vortex length, l_v, vortex width, w_v, and vortex ratio, r_v

	Vortex Length, l_v	Vortex Width, w_v	Vortex ratio, $r_v = l_v/w_v$
1 in 1.5 foreshore slope	0.246	0.140	1.76
1 in 6 foreshore slope	0.511	0.268	1.90
1 in 10 foreshore slope	0.729	0.291	2.51
1 in 18 foreshore slope	0.868	0.377	2.30

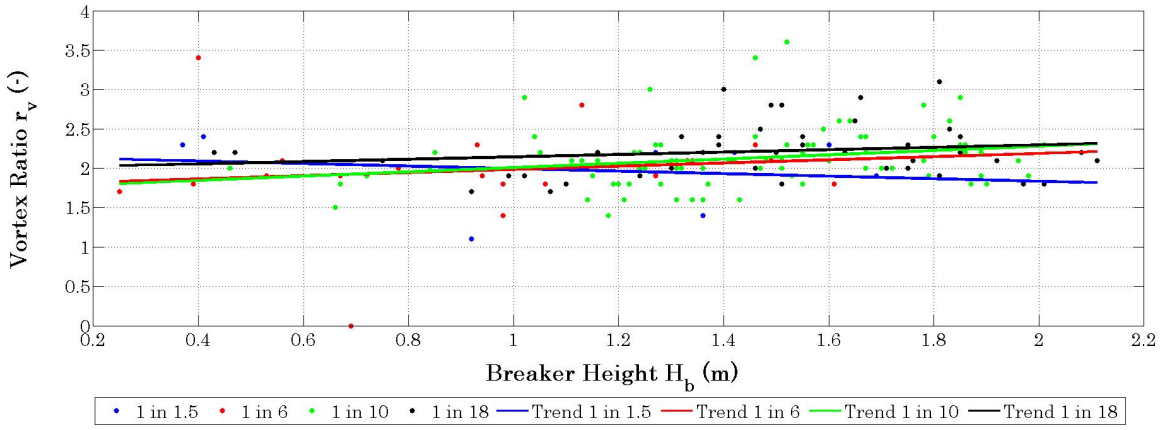

Figure 5.17: Relationship between vortex ratio, r_v and seaward reef slope, s

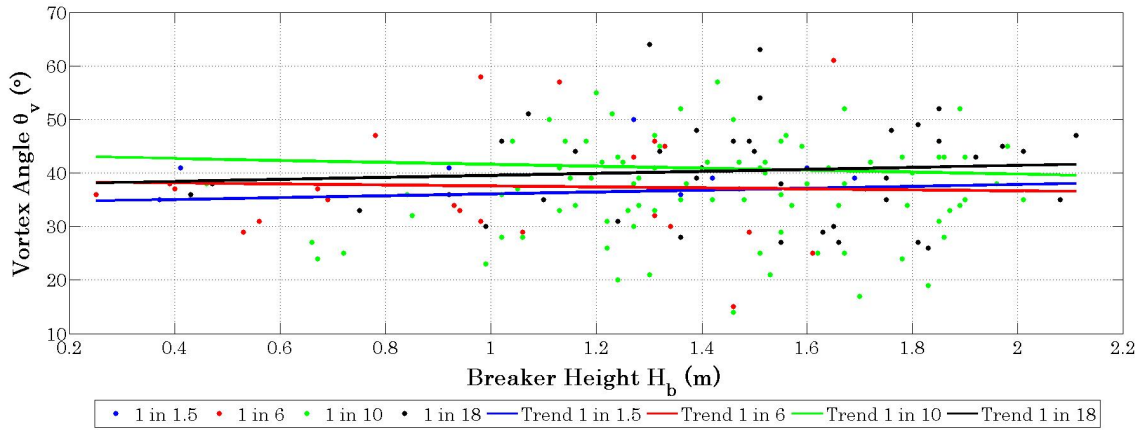

Figure 5.18: Relationship between vortex angle, θ_v and seaward reef slope, s

5.3.6 Effects of width of crest, w_c

Figure 5.19 and 5.20 indicate increasing vortex length and vortex width with decreasing crest width.

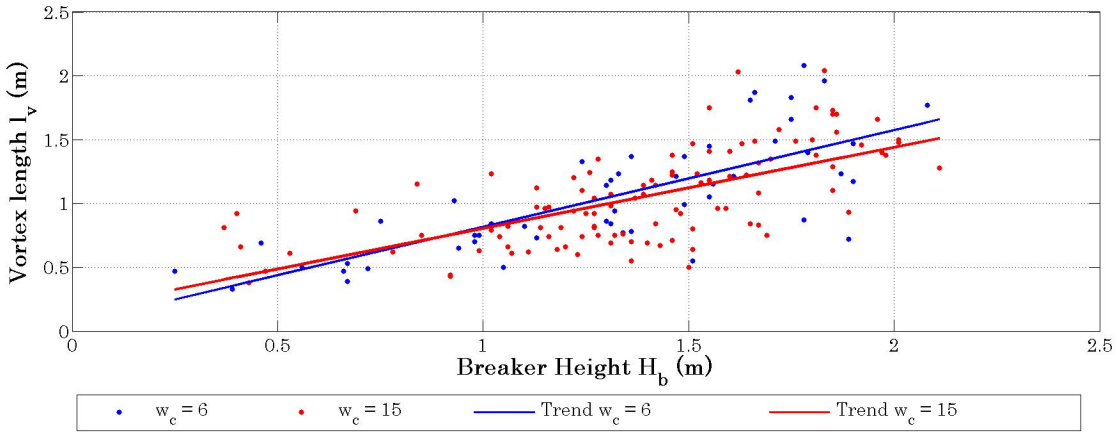

Figure 5.19: Relationship between vortex length, l_v and crest width, w_c

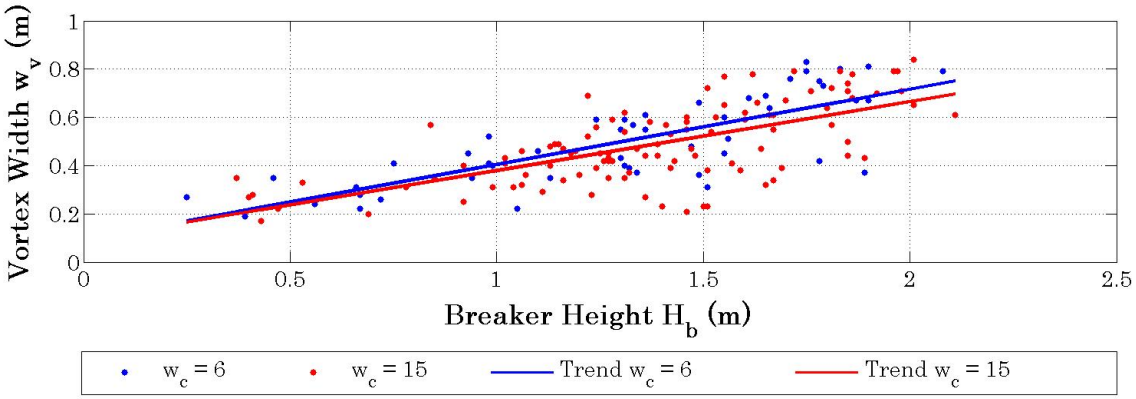

Figure 5.20: Relationship between vortex width, w_v and crest width

With regards to vortex ratio (Figure 5.21), the trend suggests higher vortex's ratios with higher crest width, which does not correlate with the theoretical predictions, where lower vortex ratios were expected. The same is true for vortex angle (Figure 5.22).

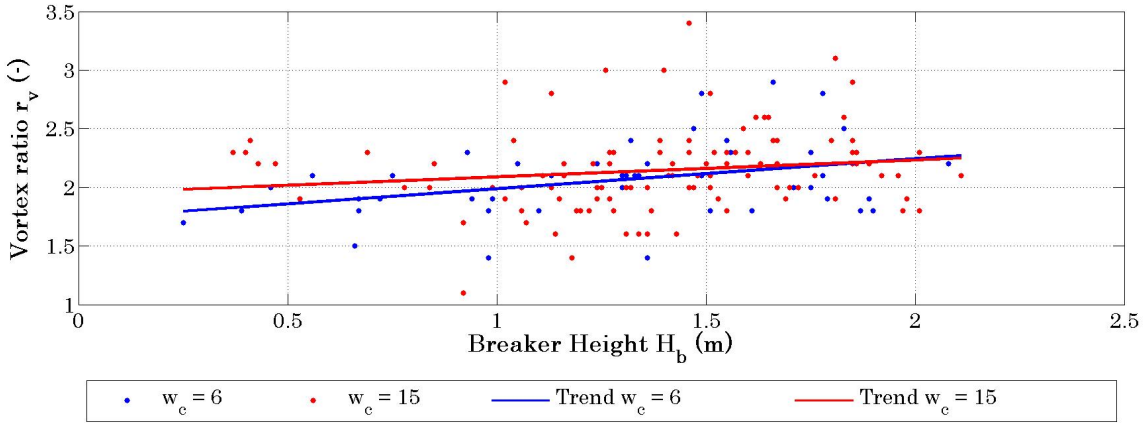

Figure 5.21: Relationship between vortex ratio, r_v and crest width, w_c

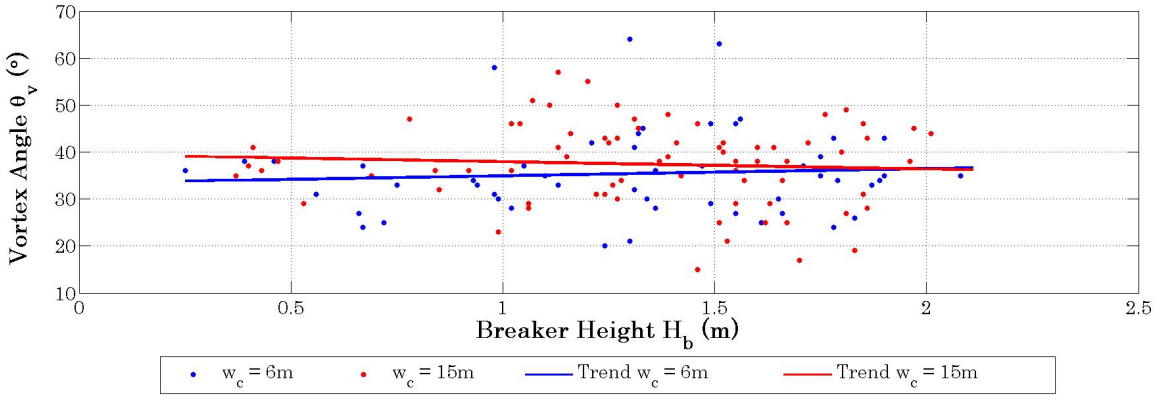

Figure 5.22: Relationship between vortex angle, θ_v and crest width, w_c

5.3.7 Effects of water depth on crest, d_c

Water depth appears to play a significant role in the vortex shape parameters. For the tested conditions, increases in vortex length and vortex width are clearly seen in Figures 5.23 and 5.24. It should be noted here that there was very little data available from the tests where d_c is at +2.25m. Here there are fewer wave breaking events. Also, a large proportion of the wave broke on the crest, where they would be affected by the separation of the bound second and third harmonics (Goda and Morinobu 1998). The effect of this on the vortex shape parameters is unknown, thus due care should be taken while interpreting this data set.

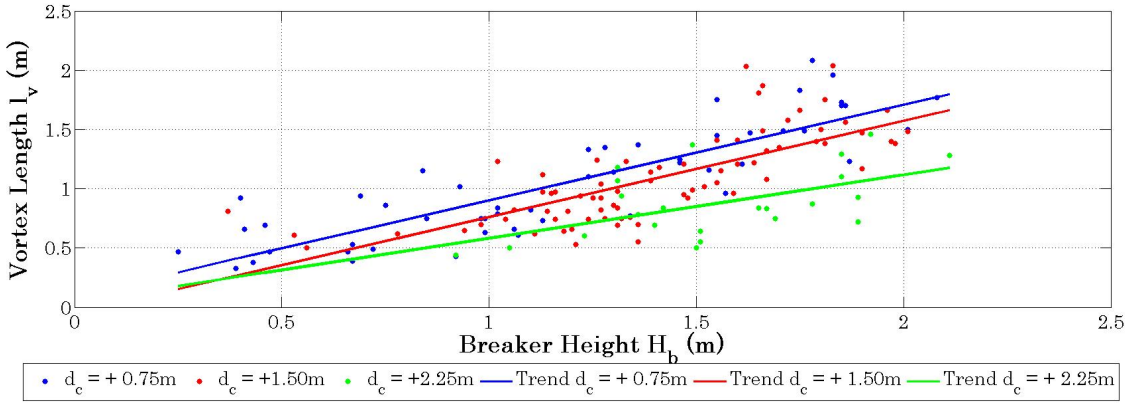

Figure 5.23: Relationship between vortex length, l_v and depth on crest, d_c

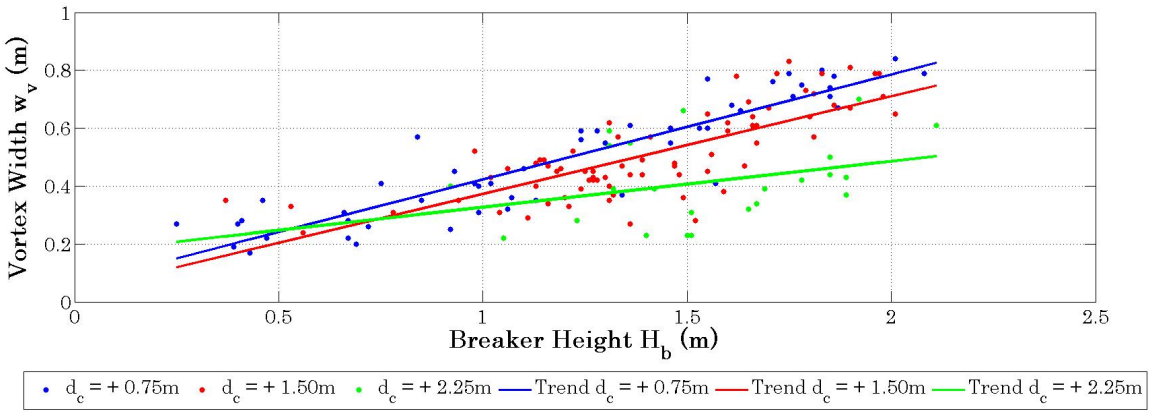

Figure 5.24: Relationship between vortex width, w_v and depth on crest, d_c

Vortex ratio appears to be unaffected by the water depth on the crest (Figure 5.25). Lower vortex angles are noticed at lower water depths (Figure 5.26), which implies higher breaking intensity. The effect of depth was also predicted theoretically in Chapter 3. It was expected that the shallower water would increase the deceleration of the wave, thus increase the acceleration ratio r_{acc}, which would result in an increase in vortex ratio, r_v, and a decrease in vortex angle, θ_v.

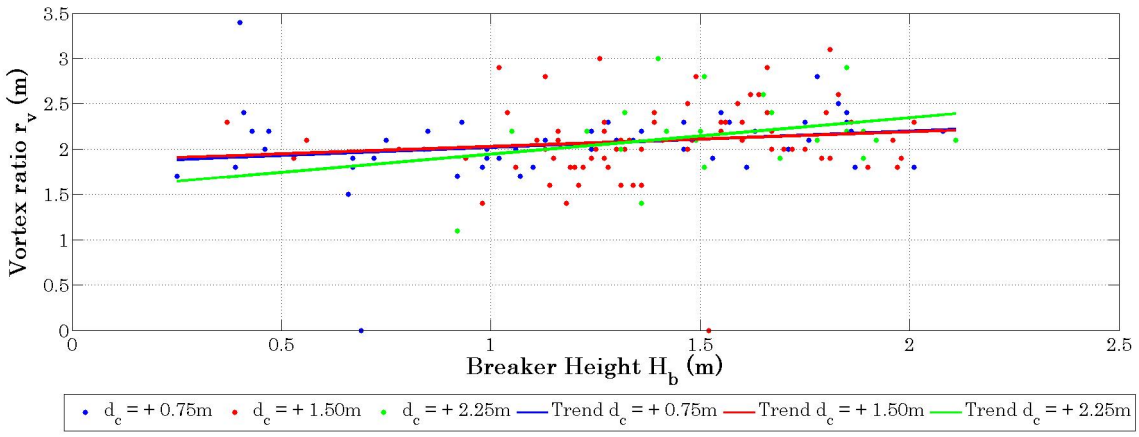

Figure 5.25: Relationship between vortex ratio, r_v with depth on crest, d_c

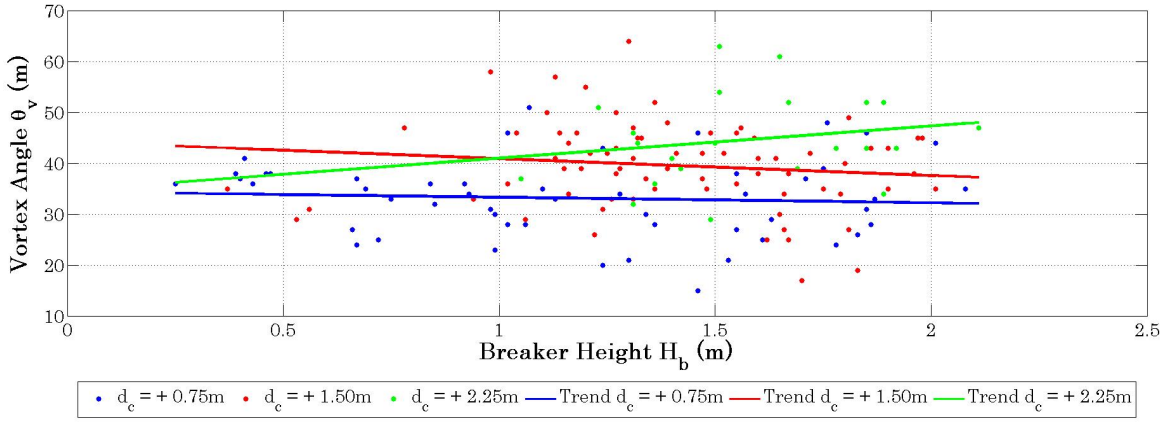

Figure 5.26: Relationship between vortex angle, θ_v with depth on crest, d_c

5.4 Effect of surface tension on breaker intensity

In the preceding sections the relationships between the variables include all the data from the set of tests. This data includes model wave heights of approx 25mm to 150mm. It has been noted by several authors that surface tension can have minimal effects in model studies, but should be taken into account for breaking waves. There is very little available data and relevant research done into surface tension. Few guidelines exist relating the effects of surface tension on the wave breaking process. The general consensus is that it should not be neglected, but exactly how to quantify and account for its effects and presence in still unknown.

Miller (1972) examined periodic, solitary and standing waves found that breaker height and the crest angle are significantly affected by surface tension. He also analyzed samples of water from naturally occurring sources and found significant differences in the surface tension. He concluded that surface tension should not be neglected as a significant factor in the breaking process, especially when conducting small scale physical model tests.

Le Mehaute (1976) recommends that wave periods should be greater than 0.35s and water depths greater than 20mm to be able to neglect surface tension effects when conducting small scale physical model tests. He states that at these values the restoring force of surface tension becomes significant and the model will experience wave damping not present in prototype.

Stive (1985), found that scale effects can be ignored when the undistorted wave height is greater than 100mm.

Goda and Morinobu (1998) recommend a water depth of greater than 100mm for waves breaking on a slope, to avoid any scale effects caused by surface tension in small scale physical model tests.

The test conditions did include breaking wave heights of 33mm and 66mm in the model, and thus the scale effects are expected to play a role, and should therefore be taken into account. The effects of surface tension on the results would then be ascertained. This is, however, outside the scope of this investigation.

5.5 Effect of the discontinuity on wave propagation

The effects of the discontinuity at the junction of the end of the seaward reef slope and the start of the horizontal crest have been discussed previously in Chapter 3. Appendix B gives time series plots of two sets of tests, one with the flatter 1 in 18 slope, shown in Figures B.1 to B.4, and for the steeper 1 in 6 slope, shown in Figures B.5 to B.8.

The probes numbered Probe 0001 through Probe 0010 (in the time series plots in Appendix B) are the probes P1 to P10 (where P10 is shown as PBr, the probe placed at the location of incipient breaking) shown in Figure 5.27 below.

Both sets of plots are performed for the four wave heights, namely the 33mm, 66m, 100mm and 133mm in the model (corresponding to 0.5m, 1.0m, 1.5m and 2.0m prototype). The depth on the crest,d_c, width of the crest, w_c, and wave period, T, remained constant for these eight tests at d_c= +2.25m prototype, w_c = 6m prototype and T = 12s.

The general observation for probes P1, P4 and PBr (Probe 0001, 0004 and 0010 on the time series plots), is a gradual increase in the non-linearies of the wave as the waves propagate along the flume, into shallower waters. This effect is more pronounced for the larger wave heights, as expected, where the troughs become flatter and the crests become sharper and steeper.

Probe P5, P6 and P7 are the probes positioned at the start of the crest, the middle of the crest and at the end of the crest respectively. On each of the eight time series plots through Figures B.1 to B.8, a secondary crest is seen developing, which reaches it maximum height at approximately the center of the crest, very near to probe P6. For the larger wave heights of

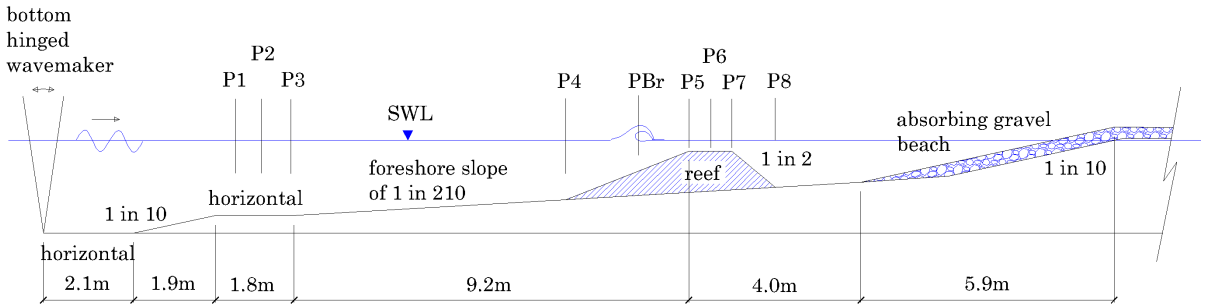

Figure 5.27: Flume long section

133mm model (2m prototype), in figures B.4 and B.8, breaking occurs which manifests itself as three or four smaller wave crests (caused by the turbulence) between the primary crests.

It can be seen in comparing the results of probes P5, P6 and P7 on Figure B.2 with Figure B.6, that the secondary wave crest has developed on the flatter 1 in 6 slope, and that it is larger on the steeper 1 in 18 slope. This disagrees with the theory expanded upon earlier in Chapter 3, where a larger crest should be evident between the primary crests of the waves that propagated along the steeper 1 in 6 slope. A full Fourier analysis should be done on each of the time series plots in order to assess the magnitude of each of the bound wave components. This would give a better indication of the extent of growth of the bound and free harmonic wave components.

5.6 Summary of test results

Table 5.9 gives a summary of the test results for the data analyzed. The tests show little variation of vortex length, l_v, and vortex width, w_v, and breaking intensity in terms of vortex ratio, r_v, and vortex angle, θ_v, for the different tests conducted.

Table 5.9: Variation of vortex shape parameters for the full range of tests

Test Parameter	l_v(m)	w_v (m)	r_v (-)	θ_v (°)
Breaker Height H_b	0.3 - 1.6	0.2 - 0.7	2.0 - 2.5	30 - 43
Wave Period T	0.3 - 1.6	0.2 - 0.75	2.0 - 2.5	35 - 40
Water depth on crest d_c	0.1 - 1.7	0.1 - 0.8	1.8 - 2.3	35 - 44
Seaward reef slope s	0.2 - 1.7	0.2 - 0.75	1.7 - 2.3	35 - 39
Crest width w_c	0.2 - 1.8	0.1 - 0.8	1.7 - 2.4	32 - 44

Table 5.9 shows that when plunging occurs, breaking intensity is generally constant, with vortex ratio's between 1.7 and 2.5, and vortex angles between 30° and 44°. There is of course, a large degree of variation within the entire data set. This is evident immediately in Figure 5.8, but based on the trend lines, it appears that the variation in breaking intensity, ie, vortex ratio, r_v, and vortex angle, θ_v, is consistent for all test conditions.

5.7 Conclusions

The physical model tests, although with a degree of scatter in the data, and subject to a certain degree of surface tension effects, give sensible results. Reflections inherent in the flume during the studies resulted in large variations in the vortex shape parameters. From the results, it appears that the vortex shape parameters are sensitive to these reflections within the flume, and may even be more sensitive to these reflections than they are to the test parameters themselves. The trend lines fitted are based on linear regression, and they indicate qualitatively which factors are affecting the vortex shape parameters. These include:

1. Vortex ratio, r_v, was shown to be a more reliable and consistent parameter in measuring breaking intensity than vortex angle, θ_v. This has been noted by Black and Mead (2001) from measurements obtained during site studies.

2. Plunging occurrences increase significantly with flatter seaward reef slopes. The 1 in 1.5 seaward reef slope had a low occurrence of plunging types, with the majority of the conditions resulting in wave surging over the reef. With regards to the 1 in 6 seaward reef slope, occurrence of plunging waves increase, but there are still large proportion of test conditions resulting in waves surging over the reef.

3. Vortex length, l_v, vortex width, w_v, and vortex angle, θ_v, are affected by wave height. There is a clear relationship between vortex length, vortex width and breaker height, which is expected. A slight increase in vortex ratio, r_v, is noted with increasing wave height, along with a slight decrease in vortex angle. Thus breaker height has the effect of increasing breaking intensity.

4. Wave period, T, appears to have a negligible effect on the vortex shape parameters.

5. Flatter seaward reef slopes tend to result in higher vortex length and widths, while vortex ratio and vortex width seem to remain unaffected.

6. The crest width, w_c, appears to have an effect only with the larger breaker heights, where an slight increase in vortex length and vortex width is seen. The small differences are attributable to friction effects.

7. Water depth, d_c, plays a significant role in the vortex shape parameters. The results indicate that vortex ratio is unaffected, while vortex angle reduces quite significantly. Also, exposure of the reef crest sometimes occurred with the shallow water depths on the steeper slopes. This is unfavourable for surfing purposes as an exposed reef crest can pose a danger to surfers.

8. The discontinuity at the junction of the seaward reef slope and the horizontal crest can result in the generation of free harmonic waves. This manifests itself as a secondary wave crest, propagating in the same direction of the main wave, whose magnitude increases with flatter seaward reef slope. The opposite was expected from theory. Further tests are needed to assess its effect on breaking wave shape and thus vortex shape parameters.

9. The variation in breaking intensity, ie, vortex ratio, r_v, and vortex angle, θ_v, is relatively consistent for all test conditions. This suggests that vortex shape parameters alone may not be very useful in determining breaking intensity.

The large degree of variation of vortex shape parameters, and especially vortex angle, is not attributed to experimental error, but due to the variations in the effects caused by the

interference of the waves in the wave train (which results in a small return wave of inconsistent magnitude) and to reflection in the flume. This reflection consists of both reflection of the short waves reflecting off the reef and the absorbing beach, and to long period oscillations in the 2D flume. Reflection in the flume from the reef structure was measured between 15% and 50%, about 15% of that being attributed to reflection from the absorption beach at the end of the flume.

It is recommended that 3D studies be undertaken in order to attempt to reduce the reflection experienced in a 2D flume. Also, active wave absorption should be used to further minimise the negative effects due to reflection, and tests with a smooth transition in the form of a curve between seaward slope and the horizontal crest should be conducted.

Furthermore, based on the results of the physical model tests, vortex shape parameters alone do not seem suitable for the design of surfing aspects of reefs. Since the findings indicate a small effect of the test variables on the breaking intensity, it is proposed to rather design the reef for surfing purposes based on breaker intensity, breaker type and occurrences of breaking than on vortex shape parameters alone.

Chapter 6

Towards Design Guidelines

6.1 Introduction

In order to design artificial reefs for surfing purposes, various factors need to be taken into account. Breaker height is very important. Very small waves are difficult to surf because the forces these waves create are not great enough to enable the surfer to catch the breaking wave, let alone to perform manoeuvres. Peel angle is also considered very important, as this dictates the speed at which a wave breaks along its crest. Peel angles that are too small result in waves that break too quickly along their length, which makes them unsurfable. Section length defines the length of the section with constant breaking intensity, peel angle and breaker height. Breaking intensity defines the wave face and also the type of section. Waves with high breaking intensity break with a plunging jet, which surfers can use for a variety of manoeuvres, but more importantly, can use to place themselves under the plunging jet, and thus ride the wave while inside the vortex.

Extensive studies of peel angle, section length and breaker height have been done by a variety of authors. Some studies relate these to surfer skill which is another issue designers need to consider when designing for recreational surfing purposes. These issues have not been focused on in this thesis as much work has been done on them already. The focus is on how to estimate breaking intensity based on reef configuration and wave parameters. This will be done by first providing guidelines on estimation of breaking intensity based on the physical model results and work done by Black and Mead (2001), and secondly, to provide a means of predicting breaker height and breaker depth on a submerged reef structure.

6.2 Prediction of breaking intensity

It can be seen from the results of the theoretical investigation and the physical model tests that the measured effects of the test variables on vortex parameters have a small (and sometimes even negligible) effect. Wave period, T, has a negligible effect on vortex shape parameters and crest width, w_c has a small and possibly even neglible effect on the vortex shape parameters. Based on the physical model tests and the work of Black and Mead (2001), Table 6.1 gives a good indication of the expected vortex ratio's based on slope effect.

There is some disagreement between the values of vortex ratios obtained in the physical model tests and from those obtained by the method of Black and Mead (2001). The vortex ratio's from the physical model tests are consistently higher than those predicted by Eqn. 2.25 of Black and Mead (2001). This could be attributed to effects of surface tension, which have been neglected in this study. Also, the data for the 1 in 1.5 slope was collected from a small

Table 6.1: Predicting vortex ratio based on seaward reef slope

Seaward reef slope, s	Vortex Length, l_v	Vortex Width, w_v	Vortex ratio, based on the physical model tests	Vortex ratio, from Eqn. 2.25, Black and Mead (2001)
1 in 1.5	0.246 H_b	0.140 H_b	1.76	0.92
1 in 6	0.511 H_b	0.268 H_b	1.90	1.21
1 in 10	0.729 H_b	0.291 H_b	2.51	1.47
1 in 18	0.868 H_b	0.377 H_b	2.30	1.99

amount of tests (because breaking did not occur in as may of the tests as with the flatter slopes, and should be used with caution.

The most significant observation of the physical model tests is that when plunging waves occur, the vortex ratio is generally between 1.7 and 2.4 (Table 5.9), which is sufficient to create the plunging vortex required for 'tubing' waves, while the vortex angle varies between 30° and 44° (Table 5.9). Eqn. 6.1 of Black and Mead (2001), shown below as;

$$r_v = 0.065\frac{1}{s'} + 0.821 \tag{6.1}$$

(with $s' = s$, for head on waves), predicts vortex ratio's of between approximately 1.0 and 2.0 for the seaward reef slopes tested. This is considered sufficient for the formation of a plunging vortex suitable for creating the 'tubing' wave sought after by shortboard surfers. The effects of wave height and water depth need to be included, but, according to Table 5.9, the vortex ratio's will be between 1.7 and 2.4 regardless, and so these effects will be neglected.

6.3 Prediction of breaker type

The physical model tests showed conclusively that plunging waves occur more frequently on flatter slopes, from approximately 1 in 10 up to the flattest test slope of 1 in 18. Table 6.2 gives a good indication of the effects of seaward reef slope on the breaker type (defined by Battjes (1974)) and the occurrence of the breaker types. Plunging events occur a lot more frequently on the flatter seaward reef slopes. The table is repeated here for the sake of clarity. The histogram of breaker type occurrences, Figure 6.1, shows the relative degree of types of breaking events, and is repeated for clarity.

Table 6.2: Occurrence of breaker types for the tested slopes

Seaward Reef Slope s	No breaking	Spilling	Plunging	Collapsing-Surging
1 in 1.5	17 (24%)	9 (13%)	11 (15%)	35 (49%)
1 in 6	22 (29%)	12 (17%)	27 (38%)	12 (17%)
1 in 10	17 (24%)	10 (14%)	45 (63%)	0 (0%)
1 in 18	10 (14%)	8 (11%)	54 (75%)	0 (0%)

A total of 72 tests were conducted for each case of seaward reef slope. The percentage of plunging waves increases with 15% of plunging waves on the 1 in 1.5 slope, 38% on the 1 in 6 slope, 63% on the 1 in 10 slope, and 75% on the 1 in 18 slope. The number of spilling waves recorded stays more or less constant, These are generally the 33mm (0.5m prototype)

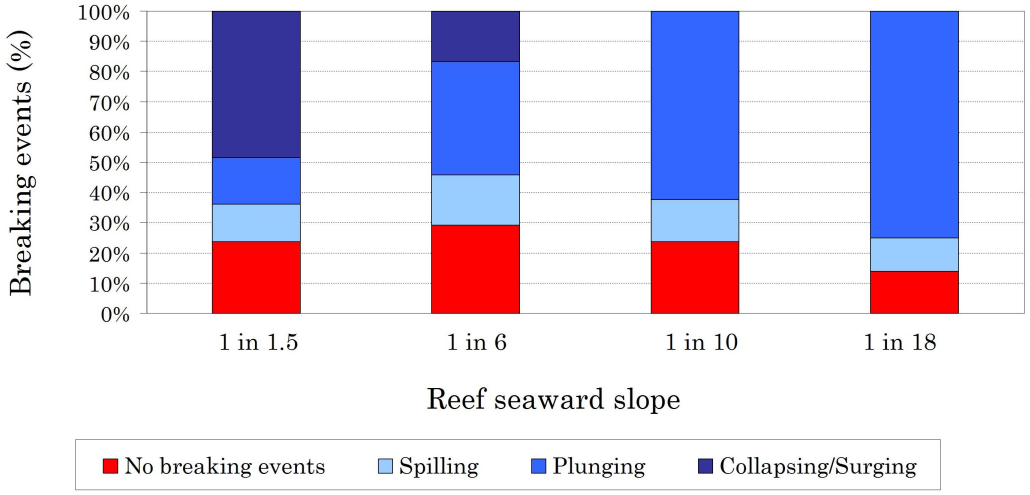

Figure 6.1: Histogram of measured breaking events

waves breaking with depth on the crest at +50mm (+0.75m prototype). These smaller waves are significantly affected by surface tension in the model, and they may in fact plunge under prototype conditions, where surface tension no longer plays a role in defining their breaking intensity. Having said this, the slopes greater than 1 in 10 give a high occurrence of plunging waves, and possibly even higher occurrences if these spilling waves (with no surface tension effects in prototype) are taken into account.

It is therefore recommended to design a reef with the flatter slopes, from between 1 in 10 and 1 in 18, to obtain a high occurrence of plunging waves, rather than to predict the breaking intensity based on the incoming wave conditions. Based on the previous discussion, it can then be assumed that these waves will break with a vortex ratio of between 1.0 and 2.5, which is sufficient to create the plunging vortex required for 'tubing' waves. The vortex angle can be assumed to vary between 30° and 44°. One then needs to determine if and when breaking will occur.

6.4 Prediction of occurrences of wave breaking

As indicated earlier in this thesis, breaker depth and breaker height formulae for the case of planar beaches have been developed sufficiently for prediction of breaker depth and breaker height. Eqn 2.20 of Rattanapitikon and Shibayama (2006) has been developed based on a large set of data, and gives the least error for the full range of experimental data (Rattanapitikon and Shibayama 2006). This equation will thus be used to estimate breaker depth on submerged reef structures.

Deep water conditions were required and were obtained from back-shoaling of the measured wave heights in the physical model tests. This theoretical unrefracted deep water wave height H'_o was used in order to determine a theoretical deep water wave steepness, which is required for calculation of breaker depth from Eqn. 2.20 of Rattanapitikon and Shibayama (2006). A comparison of the calculated breaker depths of Rattanapitikon and Shibayama (2006) and the measured breaker depths from the physical model investigations is shown in Figure 6.2.

The results from the 1 in 1.5 slope have been omitted from Figure 6.2 as they are outside the range of Eqn. 2.20, while the results from the 1 in 6 slope were omitted due to the large

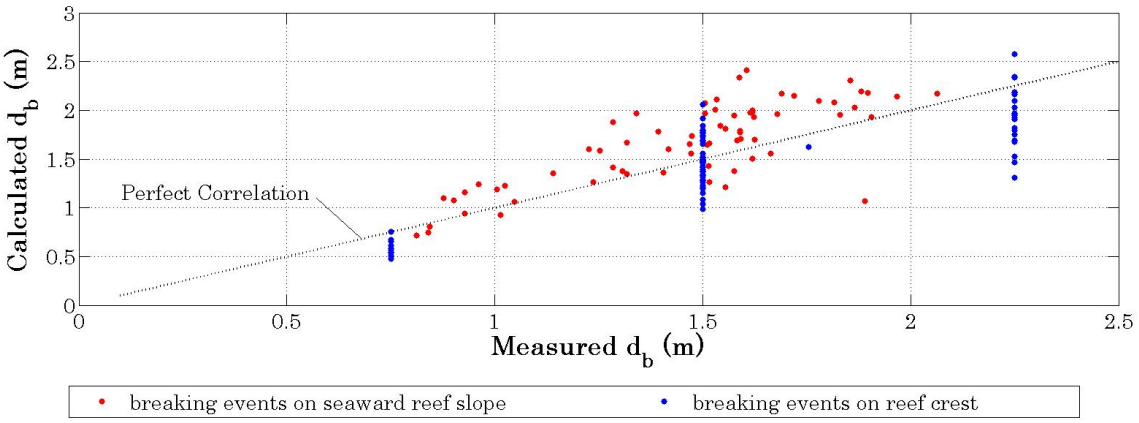

Figure 6.2: Comparison of measured breaker depth and breaker depth calculated from Eqn. 2.20 of Rattanapitikon and Shibayama (2006)

degree of scatter in the data. For the results of the 1 in 10 and 1 in 18 slope, Figure 6.2 shows a significant degree of scatter in the data, and in some cases the calculated breaker depth varies by 0.5m either side of the measured value. The equation gives reasonable prediction of breaker depth, but, due to the amount of scatter evident in the plot, it should be used with caution, especially on slopes steeper than 1 in 10.

6.5 Prediction of breaker height

The breaker height formula of Goda (1974), cited by (Goda and Morinobu 1998), Eqn. 2.9, has been shown by Goda and Morinobu (1998) to give good prediction of breaker heights on a horizontal bed affected by an approach slope. Eqn 2.9 has also been modified by Rattanapitikon and Shibayama (2000) into Eqn. 2.17, with a modified slope effect which gives less error. An analysis of Eqn's. 2.9 and 2.17 has been done in order to assess the applicability of these breaker depth formulae for the case of waves breaking on a submerged structure.

The analysis has been separated into waves breaking on the reef slope and waves breaking on the crest. Figure 6.3 shows the plots of the measured breaker heights and those calculated from Eqn's. 2.9, 2.17 and 2.18 for waves breaking on the seaward slope. The black line is the line of perfect corellation between the two variables. The plots include the data from the 1 in 6, 1 in 10 and the 1 in 18 slope. The data from the 1 in 1.5 slope has been omitted as it is outside the range of both formulae. The data points furtherest from the line of perfect correlation belongs to that of the 1 in 6 slope. This data is distinctly separated from the data from the other slopes, and overestimates the measured breaker height by about 1m, which is quite large.

It is evident from Figure 6.3 that for the 1 in 10 and 1 in 18 slopes, that all of the equations overestimate breaker height by approximately 0.5m, with equation 2.17 of Rattanapitikon and Shibayama (2000) giving the best correlation.

For the waves breaking on the crest, Eqn's. 2.9 and 2.17 were used with modified A values as shown in Table 6.3, which is repeated below. Based on Table 6.3, the A value in Eqn. 2.17 of Rattanapitikon and Shibayama (2000) and Eqn 2.9 of Goda (1974), cited by (Goda and Morinobu 1998), was chosen as 0.136 for the 1 in 10 slope and 0.143 for the 1 in 18 slope.

Figure 6.4 shows plots of the measured values and calculated values for the 1 in 10 and 1 in 18 slope for waves breaking on the crest.

The data from the 1 in 1.5 seaward slope has been omitted. Again, the data from Goda

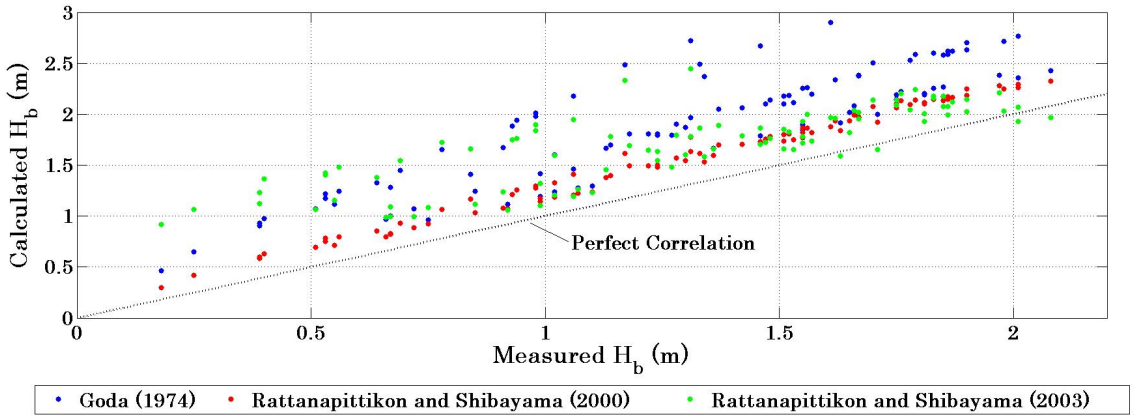

Figure 6.3: Comparison of measured breaker height and breaker height calculated from Eqn's 2.9 and 2.17: Waves breaking on the reef slope

Table 6.3: Adjusted constants for various foreshore slopes

Foreshore Slope	1 in 5	1 in 10	1 in 20	1 in 40	1 in 80
Constant 'A'	0.135	0.136	0.145	0.155	0.159

(1974), cited by Goda and Morinobu (1998), from the 1 in 6 seaward slope over estimates breaker height by approximately 1m, while the data from the 1 in 10 and 1 in 18 seaward slopes overestimated breaker height by approximately 0.25m. Eqn. 2.17 of Rattanapitikon and Shibayama (2000) gives very good estimation of the breaker height for waves breaking on the reef crest.

6.6 Conclusions

Due to the fact that vortex parameters are relatively insensitive to the test parameters (Table 5.9), namely breaker height, wave period, water depth on crest and crest width, it was concluded in Chapter 5 that prediction of breaking and breaker type is more useful than prediction of breaking intensity through vortex parameters. Breaker intensity through vortex shape parameters has been found, based on the two dimensional physical model tests, to be relatively consistent. Vortex ratio, r_v, is primarily influenced by seaward reef slope, s, while vortex angle, θ_v, is primarily influenced by the water depth on the crest, d_c. From the results summarised in Table 6.1, vortex ratio, r_v, can be estimated, with a certain degree of accuracy from seaward reef slope. Conversely, regardless of seaward reef slope and occurrences of breaking, it can be assumed to be between 1.0 and 2.5, while vortex angle, θ_v can be assumed to be between 30° and 44°.

For the test conditions, breaker type can be estimated with seaward reef slope alone, and occurrence of breaking can be estimated reasonably accurately through the breaker depth formulae of Rattanapitikon and Shibayama (2006). It is recommended that seaward reef slopes be flatter than 1 in 10 in order to increase occurrences of plunging breakers, and also to decrease the likelihood of exposure of the crest (on slopes between 1 in 6 and 1 in 1.5), which can be dangerous to surfers. Furthermore, breaker depth and breaker height formulae give better prediction for flatter 1 in 10 and 1 in 18 slopes than they do for steeper 1 in 1.5 and 1 in 1.6

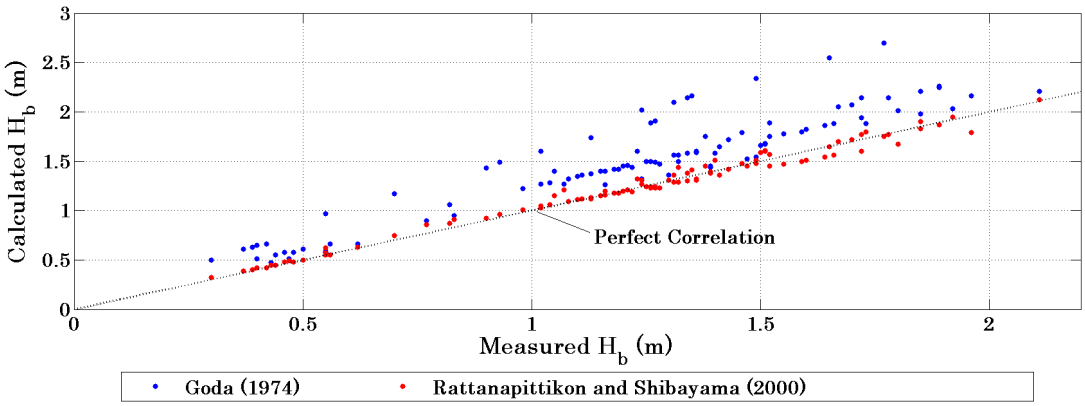

Figure 6.4: Comparison of measured breaker height and breaker height calculated from Eqn's. 2.9 and 2.17: Waves breaking on the reef crest

slopes.

For the test conditions, breaker height can be estimated very accurately by means of existing equations developed for smooth planar beaches. For waves breaking on the reef face, Eqn 2.17 shows good agreement with measured results, while for waves breaking on the crest, Eqn 2.17 of Rattanapitikon and Shibayama (2000) with modified 'A' values gives very good prediction.

Chapter 7

Conclusions and Recommendations

Investigations into the relative effects of various elements of reef configuration on wave breaking intensity as defined by Sayce (1997), have been conducted.

Initially, an extensive literature review was conducted in order to highlight the current stage of development of multi functional artificial reefs. Breaker type categories defined by Battjes (1974) were investigated. The development of breaker depth and breaker height formula for planar, sloping beaches was documented. Studies into the effects of bottom friction, wave focusing, shoaling, winds, currents and water level fluctuations were summarized. Surfing and surfing design criteria was investigated, focusing on surfability parameters such as breaking intensity (as defined by Sayce (1997)), peel angle, breaker height and section length. Ideal meteorological conditions and surfer skill level has also been investigated. An investigation into the applicability of a Smoothed Particle Hydrodynamics method, in the form of the SPHysics package, in estimating vortex parameters was carried out.

For the main study, a theoretical base was established in order to give a qualitative idea of how each of the test variables could influence the breaking intensity (measured in terms of vortex shape parameters). A study of refraction, shoaling and focusing patterns has been conducted and applied to an existing natural surfing reef. Wave breaking intensity has been estimated from images gathered from internet sources. Experimental studies have been conducted in a laboratory wave flume in order to quantify the effects of reef configuration on vortex shape parameters and compare them with simple theoretical approximations. Direct relationships between the variables have not been developed due to the relatively high measured error in the estimation of the vortex parameters. Guidelines have been developed in order to assist reef designers in the design of artificial surf reefs with respect to breaking intensity, one of the parameters deemed important in describing the surfability of a reef.

7.1 Literature review

The literature study provided insight into the current state of artificial reefs, and highlighted the following:

- The SPHysics numerical model package is still in a stage of development and is currently not suitable for the intended study of extraction of vortex shape parameters (thus breaking intensity) for waves breaking on a reef structure. This is caused by instabilities in the current version of the package.

- The combined effects of wave height, period, seaward reef slope, water depth on the reef and crest width on breaking intensity needed to be assessed,

- Guidelines for the effective design of artificial reefs for surfing purposes with respect to breaking intensity needed to be developed.

7.2 Main investigation

The qualitative case study of the 'Sunset' reef has shown that:

1. Natural reef topography on the sea floor can significantly refract waves and result in improved surfing conditions at a particular surfing site.

2. The West-Cowell surfing reef factor relates shape of the reef to the expected increase in wave height. It can give a good indication of the expected increase in wave heights due to refraction and shoaling caused by the reef configuration of reefs of simple shape. Numerical modeling may prove more reliable for estimation of wave focusing for complex reef configurations.

3. The reef structure can, depending on its size, orientation and shape, drastically increase wave heights, such that even on relatively flat slopes, large plunging breakers occur where spilling waves are expected.

The theoretical basis gave good qualitative information on how the breaking intensity would be affected by the test parameters, and, generally, was confirmed by the physical model tests. The following conclusions, based on both the theoretical considerations and the physical model tests, were made:

1. Vortex shape parameters, namely vortex ratio, r_v, and vortex angle, θ_v, are sensitive to reflections inherent in two dimensional wave flume studies, resulting in a large degree of scatter in the data set. It is thus very difficult to elucidate any reliable numerical or graphical relationships. This could be due to the use of regular waves in the physical model tests. Furthermore, it was found that vortex ratio, r_v, is a more reliable means of measuring breaking intensity than vortex angle, θ_v. This confirms results from previous studies based on site investigations.

2. Occurrences of plunging waves increases with flatter seaward reef slopes. Very steep slopes (approximately 1 in 1.5) do not provide a large number of occurrences of plunging breakers, and also may introduce occasions where the reef crest is exposed, which can create unsafe surfing conditions,

3. Vortex length, l_v, vortex width, w_v, and vortex angle, θ_v , are affected by wave height. There is a clear relationship between vortex length, l_v, vortex width, w_v and breaker height, H_b, which is expected. A slight increase in vortex ratio, r_v, is noted with increasing wave height, along with a slight decrease in vortex angle. Thus breaker height has the effect of increasing breaking intensity.

4. Wave period , T, has an insignificant effect on the vortex parameters.

5. Flatter seaward reef slopes tend to result in higher vortex lengths, l_v, vortex widths, w_v, and vortex ratio's, r_v, while vortex angle, θ_v, remains relatively unaffected.

6. The crest width w_c appears to have an effect only with the larger breaker heights, where a slight increase in vortex length, l_v, and vortex width, w_v, is noted. The effect of the crest width is deemed to be negligible.

7. Water depth d_c plays a significant role in the vortex parameters. The results indicate increasing vortex length, l_v, and vortex width , w_v, with increasing crest depths. Vortex ratio, r_v, is unaffected, while vortex angle, θ_v, reduces quite significantly. Thus the breaker intensity is unaffected in terms of vortex ratio, but significantly increased with respect to vortex angle.

7.3 Design guidelines

Vortex shape parameters alone do not seem suitable for the design of surfing aspects of reefs. Since the findings indicate a small effect of the test variables on the breaking intensity, it is proposed to rather design reefs for surfing purposes based on breaker intensity, breaker type and occurrences of breaking than on vortex parameters alone.

Breaker type can be estimated by seaward reef slope (using Iribarren number), and the shape of the vortex can be estimated through vortex ratio. Vortex ratio can be assumed to be between 1.0 and 2.5, based collectively on these physical model studies and work done on site by Black and Mead (2001). The occurrence of plunging waves (for the full range of conditions) is deemed more important than the small variations in vortex parameters over the same conditions. The occurrence of plunging waves is sensitive to the seaward reef slope, with steeper slopes resulting in a large proportion of surging waves breaking over (and before) the crest. The flatter slope of 1 in 18 gives significantly increased occurrences of plunging waves over the full test range, compared with that for the other extreme of the steep 1 in 1.5 slope.

Prediction of wave breaking on submerged reef structures can be done with existing breaker height and breaker depth formula developed for smooth, planar beaches, and thus breaking occurrences, and more importantly, occurrences of plunging breakers can be estimated taking seaward reef slope into account.

7.4 Recommendations

Three dimensional physical model studies should be done to evaluate all of the surfability parameters in an holistic manner. Surfability of a reef is dependent on a variety of three dimensional affects, including refraction, focusing and shoaling. These work interdependently in affecting the peel angle, section length, wave height and, from the results of this study, breaking intensity.

The SPHysics package requires further development before it is stable enough for the use of estimation of vortex parameters for waves breaking on a reef structure.

Further tests to investigate the effects of the discontinuity at the junction between the seaward reef slope and the horizontal crest are required. A smooth transition between the seaward reef slope and the horizontal crest in the form of a parabola (or some other function) is recommended.

References

ASR: 2001, Multi-purpose reefs and economic growth. Unpublished Article.

ASR: 2002a, An assessment of coastal protection options to reduce erosion on exposed coasts. Unpublished Article.

ASR: 2002b, The development of multi-purpose reefs for coastal protection. Unpublished Article.

Bancroft, S.: 1999, *Performance monitoring of the Cable Station artificial surfing reef*, Master's thesis, University of Western Aurtralia.

Battjes, J.: 1974, Surf similarity, *Proceedings of the International Conference on Coastal Engineering, ASCE*, pp. 466 – 480.

Battjes, J. and Stive, M.: 1985, Calibration and verifictation of a dissipation model for random breaking waves, *Journal of Geophysical Research* **90**(C5), 9159 – 9176.

Benassai, G.: 2006, *Introduction to Coastal Dynamics and Shoreline Protection*, WIT Press.

Black, K. and Andrews, C.: 2001a, Sandy shoreline response to offshore obstacles part 1: Salient and tombolo geometry shape, *Journal of Coastal Research* **29**, 92 – 93.

Black, K. and Andrews, C.: 2001b, Sandy shoreline response to offshore obstacles part 2: Discussion of formative mechanisms, *Journal of Coastal Research* **29**, 94 – 101.

Black, K. and Hatton, D.: 1990, Dispersal of larvae, pollutants and nutrients on the great barrier reef, at scales of individual reefs and reef groups in 2 and 3 dimensions, *Technical report*, Great Barrier Reef Marine Park Auth.

Black, K. and Mead, S.: 1999, A multi purpose, artificial reef at Mt Maunganui Beach, New Zealand, *Journal of Coastal Management* **27**, 355 – 365.

Black, K. P., Andrews, C., Green, M., Gorman, R., Healy, T., Hume, T., Hutt, J. and Sayce, A.: 1997, Wave dynamics and shoreline response on and around surfing reefs., *Proceedings of the 1st International Surfing Reef Symposium, Sydney, Australia*.

Black, K. P. and Mead, S.: 2001, Predicting the breaking intensity of surfing waves, *Special Issue of the Journal of Coastal Research on Surfing.*, Vol. 29, pp. 103–130.

Blenkinsopp, C.: 2003, The effect of micro-scale bathymetric steps on wave breaking and implications for artificial surfing reef construction, *Proceedings of the 3rd International Surfing Reef Symposium, Raglan, New Zealand*, pp. 139 – 155.

Boak, L., McGrath, J., Maffey, A. and Jackson, L.: 2000, Northern Gold Coast Beach Protection Strategy, *New South Wales Coastal Conference, Yamba, Australia*.

Bohnsack, J. and Sutherland, D.: 1985, Artificial reef research: A review with recommendations for future priorities, *Technical Report 37*.

Borrero, J. and Nelsen, C.: 2003, Results of comprehensive monitoring program at Pratte's Reef. Unpublished Report.

Burgess, S., Black, K., Mead, S. and Kingsford, M.: 2003, Considerations for artificial surfing reefs as habitat for marine organisms, *Proceedings of the 3rd International Surfing reef Symposium*, pp. 289 – 303.

Cáceres, I., Sánchez-Archilla, A., Alsina, J., Gonzlez-Marco, D. and Pau-Sierra, J.: 2005, Coastal dynamics around a submerged barrier, *5th International Conference on Coastal Dynamics 2005*, pp. 158 – 162.

Couriel, E., Horton, P. and Cox, D.: 1998, Supplementary 2d physical modelling of breaking wave characteristics, *Technical Report TR98-14*, Water Research Laboratory.

De Wit, L.: 2006, *Smoothed particle hydrodynamics: A study of the posibilites of SPH in Hydraulic Engineering*, Master's thesis, Delft University of Technology, Faculty of Civil Engineering and Geosciences.

Dean, R.: 1990, *Coastal processes with engineering applications*, Cambridge University Press.

Dean, R., Chen, R. and Browder, A.: 1997, Full scale monitoring study of a submerged breakwater, *Journal of Coastal Engineering* **29**, 291 – 315.

Douglass, S. L.: 1990, Influence of wind on breaking waves, *Journal of Waterway, Port, Coastal, and Ocean Engineering* **116**(6), 651–663.

Dyer, M.: 1994, *Beach profile change at St. Clair beach, Dunedin*, Master's thesis, University of Canterbury.

Galloway, J., Collins, M. and Moran, A.: 1989, Onshore/offshore wind influence on breaking waves: An empirical study, *Journal of Coastal Engineering* **13**, 305–323.

Galvin, C.: 1969, Breaker-type classification on three laboratory beaches, *Journal of Geophysical Research* **73**(12), 3651 – 3659.

Goda, Y. and Morinobu, K.: 1998, Breaking wave heights on horizontal bed affected by approach slope, *Coastal Engineering Journal* **40**(4).

Gomez-Gesteira, M., Cerqueiro, D., Crespo, C. and Dalrymple, R.: 2005, Green water overtopping analyzed with a SPH model, *Proceedings of the International Conference on Ocean Engineering, ASCE*, Vol. 32, pp. 223 – 238.

Gourlay, M.: 1992, Wave setup, wave runup and beach water table: Interaction between surf zone hydraulics and groundwater hydraulics, *Journal of Coastal Engineering* **17**, 93–144.

Hedges, T.: 2001, Wave breaking and reflection. Lecture Notes: Dept of Civil Engineering, University of Liverpool.

Hidayati, D.: 2003, Coral reef rehabilitation and management program in indonesia, *Proceedings of the 3rd International Surfing Reef Symposium, Ragland, New Zealand*, pp. 303 – 319.

Hugues-Dit-Ciles, E., Glegg, G., Findlay, M., Carroll, N. and Hatton, E.: 2003, Factors affecting the choices of surf tourists, *Proceedings of the 3rd International Surfing Reef Symposium, Raglan, New Zealand*, pp. 258 – 258.

Jackson, L., Tomlinson, R., Turner, I., Corbett, B., D'Agata, M. and McGrath, J.: 2005, Narrowneck artificial reef: 4 years of monitoring, *Proceedings of the 4th International Surfing Reef Symposium, California, USA*, pp. 47–61.

Khayyer, A., Gotoh, H. and Shao, S.: 2008, Corrected incompressible SPH method for accurate water-surface tracking in breaking waves, *Proceedings of the International Conference on Coastal Engineering, ASCE*, pp. 236 – 250.

Liu, M. B.: 2003, *Smoothed Particle Hydrodynamics: A Meshfree Particle Method*, World Scientific.

Longuett-Higgins, M.: 1982, Parametric solutions for breaking waves, *Journal of Fluid Mechanics* **121**, 341 – 349.

Mansard, E. and Funke, E.: 1980, The measurement of incident and reflected spectra using a least square method, *Proceedings of the International Conference on Caostal Engineering, ASCE*, p. 154172.

Mead, S. and Black, K.: 2002, Multi-purpose reefs provide multiple benefits amalgamating coastal protection, high-quality surfing breaks and ecological enhancement to maximise user benefits and development opportunities, *SASIC 2*.

Mead, S., Black, K., Borrero, J., Frazerhurst, J., Anderson, D., Phillips, D. and Krammer, I.: 2006, Reef feasibility study at St. Francis Bay beach, South Africa. Unpublished Proposal.

Mead, S. T. and Black, K. P.: 2005, Development of a multi-purpose reef at Orewa Beach, New Zealand, *Proceedings of the 17th Australasian Coasts and Ports Conference, Adelaide, 20-23 September 2005*.

MHL: 2002, Gosford city beach nourishment feasibility study: Stage two deatiled assessment of potential sand sources, report no. 929, *Technical report*, Department of public works and services, (NSW), Manly Hydraulics Laboratory.

Mocke, G., Smit, F. and Zahed, K.: 2004, Evaluation of a novel: Multi-functional artificial reef for Dubai, *Proceedings of 29th International Conference on Coastal Engineering, Lisbon, Portugal*, pp. 1971–1983.

Nautilus: 2003, Artificial reefs, Scotland: Benefits, costs and risks report, *Technical report*, Nautilus Consultants Ltd.

Neelamani, S. and Sundaravadivelu, R.: 2003, Plans to win back a sandy beach in Pondicherry, South-east coast of India, *Proceedings of the 3rd International Surfing Reef Symposium, Raglan, New Zealand*, pp. 375 – 377.

Ogawa, Y. and Shuto, N.: 1984, Run-up of periodic waves on beaches of non-uniform slope, *Proceedings of the 19th International Conference on Coastal Engineering, ASCE*, pp. 328–344.

O'Leary, E., Hubbard, T. and O'Leary, D.: 2003, Artificial reefs feasibility study, *Technical report*, The Marine Institute, Coastal Resources Center national University of Ireland Cork.

Pickering, H. and Whitmarsh, D.: 2007, Artificial reefs and fisheries exploitation: a review of the attraction versus production debate, the influence of design and its significance for policy, *Journal of Fisheries Research* **31**, 39–59.

Ranashinghe, R. and Turner, I.: 2004, Process governing shoreline response to submerged breakwaters: Multi-function structures - a special case, *Coastal Engineering* **53**, 1984 – 1986.

Ranashinghe, R. and Turner, I.: 2006, Shoreline response to submerged structures: A review, *Coastal Engineering* **53**, 65 – 79.

Ranashinghe, R., Turner, I. and Graham, S.: 2006, Shoreline response to multi-functional artificial surfing reefs: A numerical and physical modelling study, *Coastal Engineering* **53**, 589 – 611.

Ranasinghe, R., Hacking, N. and Evans, P.: 2002, Multi-functional surf breaks: A review, *Technical report*, New South Wales Department of Land and Water Conservation.

Rattanapitikon, W. and Shibayama, T.: 2000, Verification and modification of breaker height formulas, *Coastal Engineering Journal* **42**(4), 389–406.

Rattanapitikon, W. and Shibayama, T.: 2006, Breaking wave formulas for breaking depth and orbital to phase velocity ratio, *Coastal Engineering Journal* **48**(4), 395–416.

Rattanapitikon, W., Shibayama, T. and Vivattanasirisak, T.: 2003, A proposal of a new breaker height formula, *Coastal Engineering Journal* **45**(1), 29–48.

Raybould, M. and Mules, T.: 1998, Northern Gold Coast Beach Protection Strategy: A benefit cost analysis, *Technical report*, Gold Coast City Council.

Rogers, B., Dalrymple, R. and Stansby, P.: 2008, SPH modelling of floating bodies in the surf zone, *Proceedings of the International Conference on Coastal Engineering, ASCE*, p. pages.

Saizar, A.: 1997, Uruguay climate change country study: Assessment of impacts of a poential sea level rise on the coast of Montevideo, Uruguay, *Climate Research* **9**.

Sayce, A.: 1997, *Transformation of surfing waves over steep and complex reefs.*, PhD thesis, University of Waikato, New Zealand.

Sayce, A., Black, K. and Gorma, R.: 1999, Breaking wave shape on surfing reefs, *Proceedings Coasts and Ports '99*, Vol. 2, pp. 596 – 603.

Scarfe, B., Elwany, M., Mead, S. and Black, K.: 2003, The science of surfing waves and surfing breaks - a review, *Proceedings of the 3rd International Surfing Reef Symposium, Raglan, New Zealand*, pp. 37–59.

Shao, S., Ji, C., Graham, D. and Reeve, D.: 2006, Simulation of wave overtopping by an incompressible SPH model, *Proceedings of the International Conference of Coastal Engineering, ASCE*, Vol. 53, pp. 723 – 735.

Smith, E. and Kraus, N.: 1990, Laboratory study on macro - features of wave breaking over bars and artificial reefs, *Technical Report CERC-90-12*, Department of Army, USACE.

surfermag.com: 2002, http://www.surfermag.com/features/oneworld/cablesreef.

Sylvester, R. and Hsu, J.: 1997, *Coastal Stabilization*, World Scientific Publishing Co. Singapore.

Symonds, G., Black, K. and Young, I.: 1995, Wave driven flow over shallow reefs, *Journal Of Geophysical Research* .

Theron, A.: 2002, Solutions to wind blown sand and beach wall overtopping problems at the Strand, South Africa, *Technical Report ENV-S-C-2002-085*, CSIR.

Trung, L.: 2006, *Interacting artificial surf reefs*, Master's thesis, Delft University of Technology, Faculty of Civil Engineering and Geosciences.

Turnpenny, B., Tahata, B., Black, K., Healy, T. and Beamsley, B.: 2003, Planning Port Gisborne's surfing reef within the proposed port expansion, *Proceeding of the 3rd International Surfing reef Symposium, Raglan, New Zealand*, pp. 268–227.

USACE: 1995, Design of coastal revetments, seawalls, and bulkheads, *Technical Report 20314-1000*, Department of the Army, US Army Corps Of Engineers.

Walker, J.: 1974, Recreational surf parameters, *Technical Report 30*, University of Hawaii, LOOK Laboratory.

wavescape.co.za: 2008, http://www.wavescape.co.za/top_bar/history/history.html.

WBM: 1995, Coastal management study and coastal management plan - Gosford city open beaches, *Technical report*, WBM Oceanics Australia.

Weggel, R.: 1972, Maximum breaker height for design, *Proceedings of the International Conference on Coastal Engineering, ASCE*, pp. 419–432.

Weight, A.: 1990, Artificial reef in Newquay, UK, *The institution of civil engineers municipal engineer 157*, Vol. no. ME2, pp. 87 – 95.

Weight, D.: 2003, Economics of surf reefs, *Proceedings of the 3rd International Surfing Reef Symposium, Raglan, New Zealand*, pp. 351 – 359.

West, A., Cowell, P., Battjes, J., Stive, M., Doorn, N. and Roelvink, J.: 2003, Wave-focusing surfing reefs - a new concept, *Proceedings of the 3rd International Surfing Reef Symposium, Raglan, New Zealand*, pp. 360 –370.

wikipedia.org: 2007, http://en.wikipedia.org/wiki/History_of_surfing.

Appendices

Appendix A

Numerical Model Investigations

Introduction

The numerical model tests were conducted in order to assess the capability of the SPHysics package in modeling the vortex of a plunging wave. The approach was done in two steps:

1. To get the SPHysics package installed on a PC and conduct some initial test runs.
2. To alter the SPHysics code so that a submerged reef structure may be placed in the model domain, and then to conduct numerical model runs with the submerged structure in place. The results from these runs were then to be compared with the physical model results.

The Initial Test Runs

Working with the SPHysics package

The installation is relatively easily to complete. Good instructions are given in the user manual and installation was not a problem. Fortran 90 is required in order to compile the main program.

Once the test parameters are defined, the program that defines the conditions at t=0 is compiled. This program then calls the main SPHyscs program which implements the time stepping algorithm and calculates the variables until the run is complete. The time required for a full run is dependent primarily on the length of the domain, the particle spacing and the time step.

The data is saved in directories unzipped during the installation process, which increases its user-friendliness. The user interface to describe the problem domain, i.e. input for initial conditions, wave parameters, wavemaker options etc. is in a text file, which makes it ideal when altering certain aspects of the original code.

The package complete runs far quicker on the faster PC platform. Runs done on a 2.66GHz processor with 3.25 Megabytes of Random Access Memory (RAM) were complete in about a third of the time as the a similar run (with similar no. of particles) on a 2.2GHz processor with 2 Megabytes of RAM.

The first few runs were conducted with the release SPHYSICS_2D_v1.002, while the remaining runs (the bulk of the work) were conducted with SPHYSICS_2D_v1.2.000, which had been updated with faster time stepping algorithms and a means of restarting runs that were already complete.

Input variables

There are a range of input conditions that can be specified for each run by the user in the input text file. These were kept constant for each of the runs, and are shown below:

- ***The type of kernel for determination of the weighting function*** $W(q,h)$: The cubic spline method as recommended by de Wit (2006) was selected. This is piece wise over its length and for the two dimensional case, with $q = r/h$ being the non-dimensional distance between particles and r the distance between any two particles:

  when $0 \leq q \leq 1$,

$$W(q,h) = 1 - \frac{3}{2}q^2 + \frac{3}{4}q^3 \tag{A.1}$$

  for $1 < q \leq 2$,

$$W(q,h) = \frac{1}{4}(2-q)^2 \tag{A.2}$$

when $q > 2$,

$$W(q,h) = 0 \tag{A.3}$$

- ***A co-efficient for the calculation of smoothing domain***: This was kept at 0.92 as this gave a smoothing domain h of 1.4 times the particle spacing. De Wit (2006) recommends this as a good trade off between accuracy and speed of calculation.
- ***The kind of algorithm for the time stepping procedure***: The predictor - corrector method was selected. This was the pre-set method that was selected after the installation of the SPHysics package.
- ***The type of boundary conditions***: Repulsive boundary conditions were selected as recommended by De Wit (2006). This boundary condition prevents the movements of water particles across it by applying a force on the particles near the boundary. This force is chosen so that a particle experiences a constant repulsive force as it travels parallel to the wall (Gomez-Gesteira et al. 2005),
- ***Other important parameters*** : such as viscosity value, viscosity type, water density and the co-efficient to calculate the speed of sound in water were all held constant.

Other parameters deemed less important are listed in the SPHysics user manual, (Gomez-Gesteira et al. 2005).

Plunging waves on the steeper slopes

The initial test runs were all based upon the initial unzipped input parameter file supplied with the program. An image of one of these run at t=0 is shown in Figure A.1. The domain is quite small and it appears that length and time have been scaled according to the Froude scaling laws.

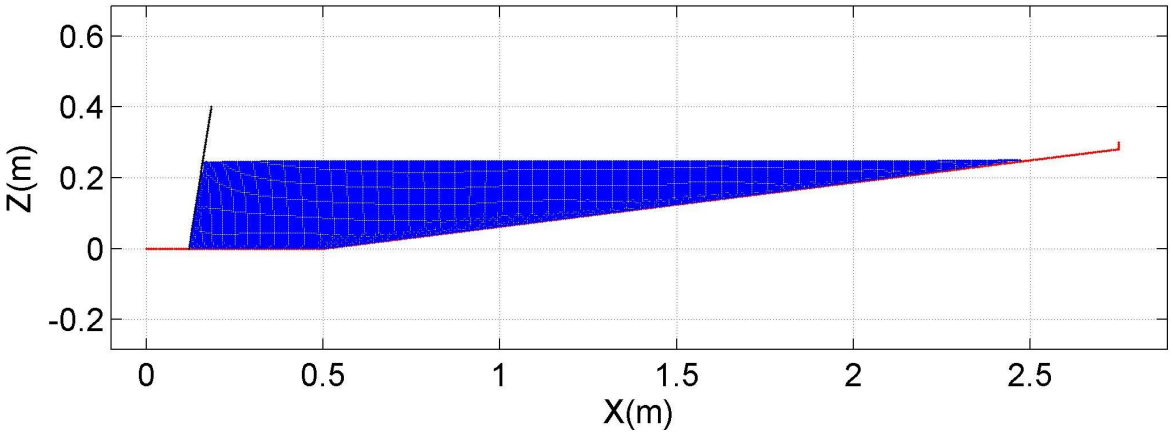

Figure A.1: Unzipped test run at initial conditions dt

Details of one of the first test runs are summarized below in Table A.1. There are many input variables that could be shown such as boundary conditions, but all of these were kept constant during all of the runs.

The runs were designed to give an Iribarren number of between 0.4 and 2.3, to assess specifically plunging breakers on a flat planar beach. This tests corresponds to an Irribarren number of 0.5, and thus a mildly plunging wave close to spilling were expected.

Table A.1: Details of the first run

Foreshore Slope (-)	1 in 8
Wave Height (m)	0.125
Wave Period (s)	1.12
Water depth at wavemaker (m)	0.25
Domain Length (m)	2.75
Particle Spacing (m)	0.005
No. of particles	14185
Smoothing Length (m)	0.0065
Max. Time Step (s)	1.8×10^{-5}
Time Step (s)	0.9×10^{-5}
Total run length (s)	5.0
Computational Time (Approx. hrs)	11
File Size for dt(kB)	1801

Figure A.2, A.3 and A.4 shows selected frames from the run. These initial runs give a good impression of the usefulness of the numerical model. Good development of the wave while propagating up the slope is seen. Good details of the plunging breaker with respect to vortex parameters are visible. One can also clearly see the breakpoint shift and the increase of the vortex angle (as described in Chapter 2 on breaking intensity) as the equilibrium conditions are reached. It should be noted that for these conditions, the inshore Iribarren number, ξ_b is approximately 0.5, which suggests waves close to the spilling category. The wave types in Figure A.2, A.3 and A.4 are clearly plunging waves.

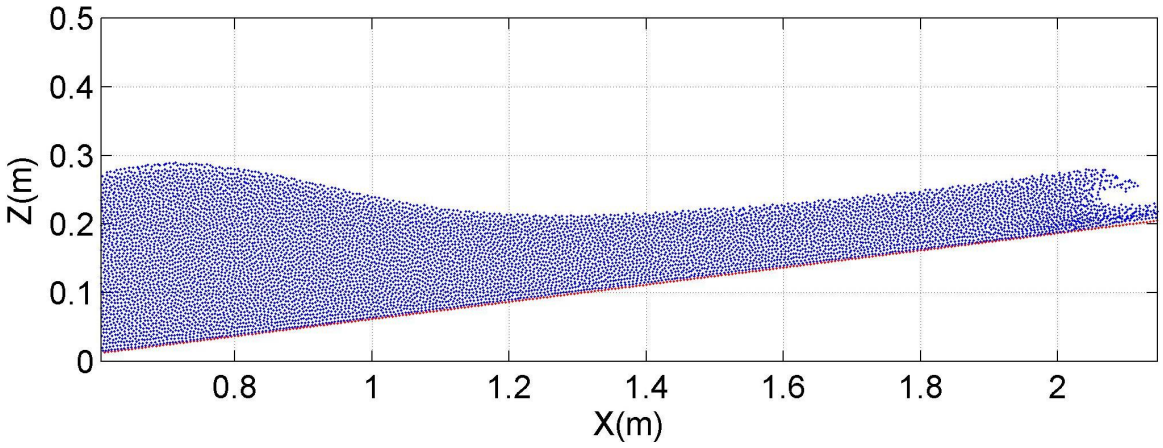

Figure A.2: First plunger of the run at time $t = 2.35s$

One should note the gradual clustering of the particles near the boundary between $X = 1.8$ and $X = 2.2$. This will be discussed further in the next subsection.

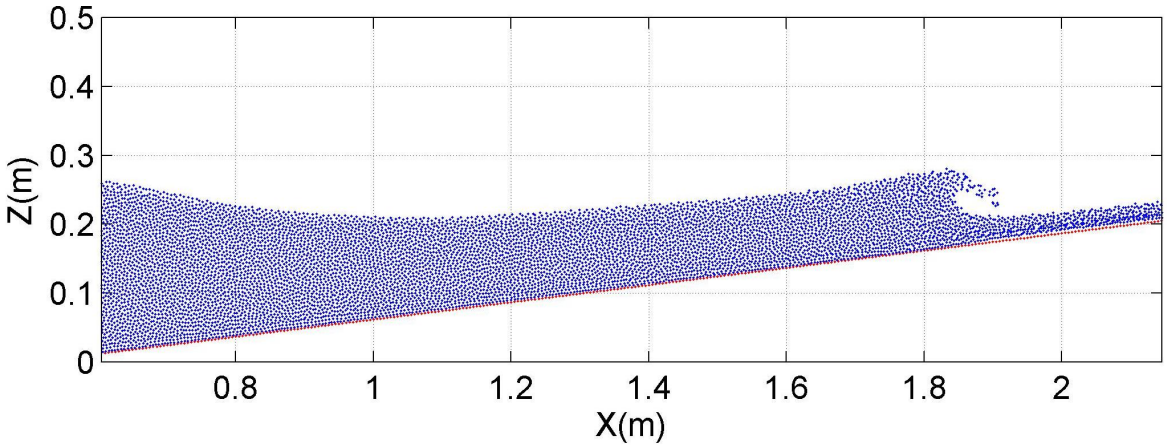

Figure A.3: First plunger of the run at time $t = 3.45s$

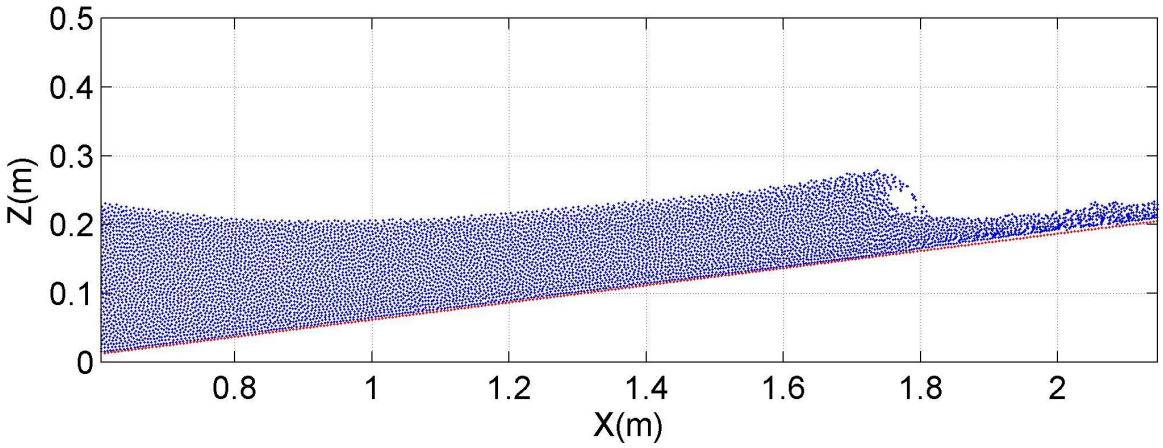

Figure A.4: First plunger of the run at time $t = 4.45s$

Spilling waves on gentle slopes

Further runs were done in order to assess the capability of the SPHyiscs package in wave breaking aspects on a gentler slope. The details of this test run are shown in Table A.2. The long domain requires a large number of particles, and so the water depth at the wavemaker was decreased slightly to allow for a more computationally practical number of particles.

The large computational time here (Table A.2) is due to the extra time required for the wave to propagate the longer distance on the flatter slope.

The initial setup at time $t = 0$ Figure (Figure A.5) shows the long domain required for the spilling breaker. The foreshore slope could have remained at 1 in 8 in order while varying the wave parameters in order to obtain an Irribarren number in the region 0.3 to 0.4, but sometimes the SPHysics package does not work with small wave heights. The exact cause of this unknown, but it is suspected that it due to some numerical error in the calculation or rounding off error.

It should be noted that the spilling case also resulted in some clustering of particles in the area close to the boundary between $X = 3.2$m and $X = 3.7$m (Figures A.6 and A.7). The model run depicts the expected spilling breaker (Figure A.7) as a very weakly plunging breaker.

Table A.2: Details of the 'spilling' run

Foreshore Slope (-)	1 in 25
Wave Height (m)	0.1
Wave Period (s)	1.2
Water depth at wavemaker (m)	0.2
Domain Length (m)	6
Particle Spacing (m)	0.006
No. of particles	15698
Smoothing Length (m)	0.0083
Max. Time Step (s)	2.4×10^{-5}
Time Step (s)	1.2×10^{-5}
Total run length (s)	7.38
Computational Time (Approx. hrs)	22
File Size for dt(kB)	1993

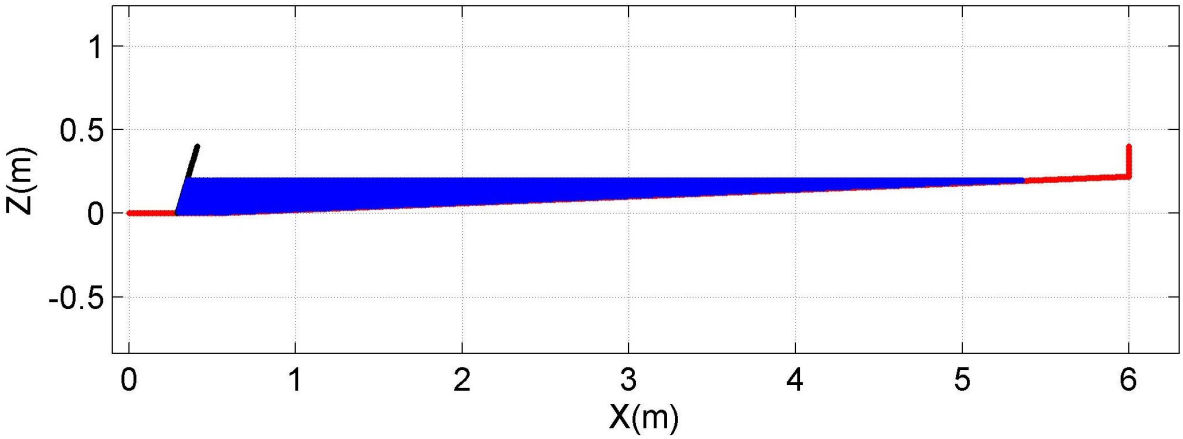

Figure A.5: Spilling breaker case at time $t = 0s$

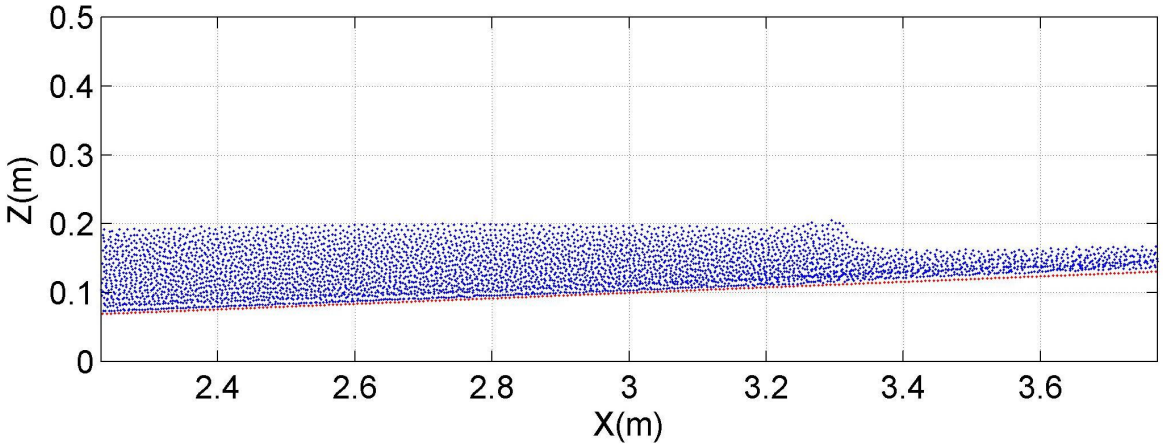

Figure A.6: Snapshot just prior to breaking at $t = 5.13s$

Inclusion of the reef structure

One problem with the very small domain is that the numbers on their are not prototype values. Even though they can be scaled up easily, it makes for easier evaluation of results if everything

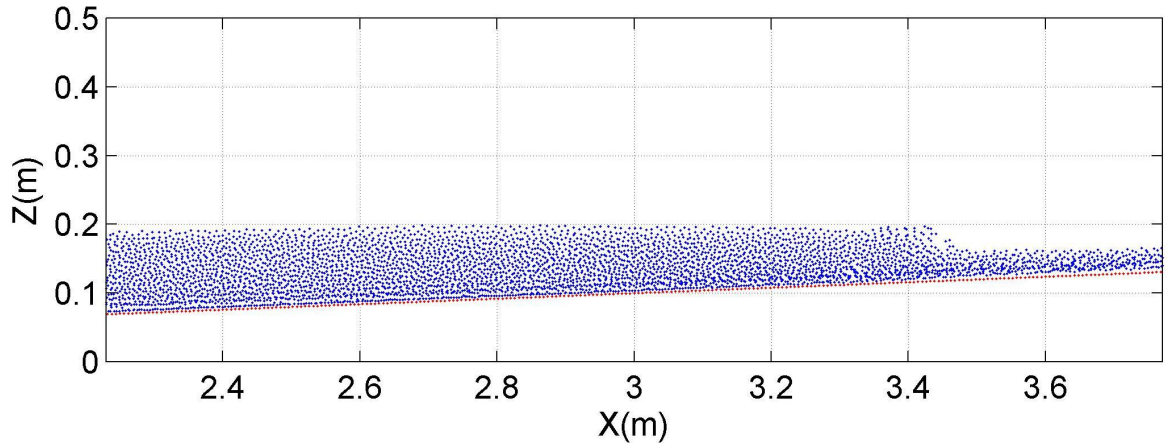

Figure A.7: Snapshot at break point at $t = 5.29s$

is done in prototype values. Prototype values were thus used for the remaining numerical model runs.

Initially, an optimized reef structure was used, in order to reduce computational time. This was then adapted to include a full reef structure.

Optimized reef structure

A reef structure was placed into the domain by altering the input text file and then calling the subroutines that define the bottom boundary and the one that fills particles into each section of the problem domain. Thus the new code simply adds in a two more sections of a bottom boundary. The angle and the length of the boundary are part of the input file.

The first proposal of reef structure was approximated as a foreshore slope, a flat reef crest, which then is followed by an absorption beach. The advantage of this is that the problem domain is made slightly smaller by virtue of not requiring the length in the domain for the back slope of the reef. This saves particles and hence computational time. Also, and more importantly, the slope up to the end of the problem domain, now starts at the end of the reef crest, and not at the bottom of the back slope. This then cuts off about 30% of the required particles for the run, which saves computational time significanlty.

Many runs were conducted with this setup with approximately 12000 particles. The results were satisfactory, however, the vortex was not very well defined.

Full reef structure

The code and the input file was adjusted as before. A full reef structure with rear slope was placed in the domain. An absorption beach ran up from the toe of the rear slope to above the highest runup level. Again, runs with 10000 to 15000 particles were quite stable. Upon increasing the number of particles for increased resolution of the plunging jet, large instabilities were evident. The domain is shown below in Figure A.8, along with the run details in Table A.3.

Figures A.9 to A.10 show the selected run for the 'full reef' case in the lee of the reef. At time $t = 5.0s$, (Figure A.9), the water level has dropped dramatically. Large circular eddy currents are evident that circulate adjacent to the rear slope. Large numbers of large clusters form (Figure A.10) on the bottom boundary on the absorbing beach. These then slowly move

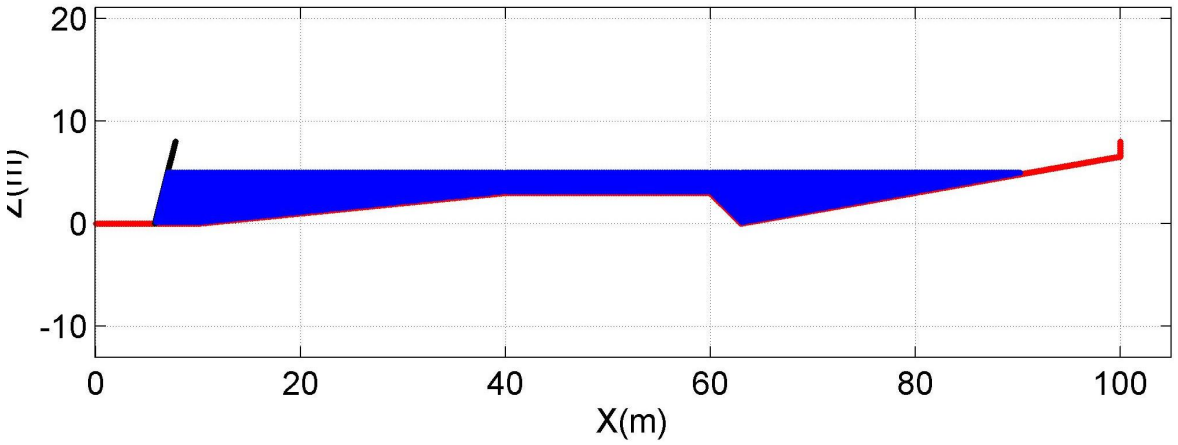

Figure A.8: Full reef at time $t = 0s$

Table A.3: Details of the full reef run

Foreshore Slope (-)	1 in 10
Crest Width (m)	20
Depth on Crest (m)	2
Rear Slope (-)	1 in 1
Absorption Slope (-)	1 in 10
Wave Height (m)	1
Wave Period (s)	10
Water depth at wavemaker (m)	5
Domain Length (m)	100
Particle Spacing (m)	0.0075
No. of particles	42701
Smoothing Length (m)	0.098
Max. Time Step (s)	6.1×10^{-5}
Time Step (s)	3.5×10^{-5}
Total run length (s)	10.3
Computational Time (Approx. hrs)	24
File Size for dt(kB)	5551

though the boundary , until at time $t = 10.0s$ (Figure A.11), an underwater explosion occurs. This is assumed to be caused by the numerical formation of a very large force, accompanied with the small time step. $dt = 3.5 \times 10^{-5}$.

Many other runs were conducted in an attempt to get the model functioning without leakage or other problems like explosions. The closest achieved was with approximately 13000 particles and with the domain scaled down to model values. The vortex of the plunging wave was considered poorly defined for all of these runs with fewer particles.

Optimized reef structure - Additional Particles

Upon increasing the number of particles significantly for increased resolution of the plunger, some problems with clustering of the particles and the boundary conditions were encountered. The initial problem domain for the flat top reef is shown in Figure A.12, and the details of the run in Table A.4.

The following figures detail the run. The figures show the reef crest between the start at $X = 40$ and the end at $X = 55$m, and the absorption slope. The cause of the instabilities in this

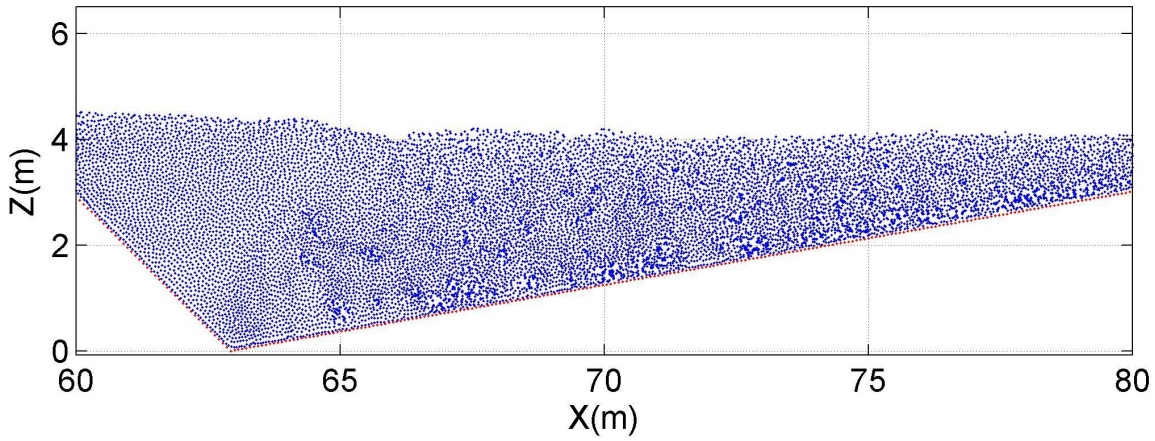

Figure A.9: Full reef at time $t = 5.0s$, illustrating instabilities on the rear slope of the reef

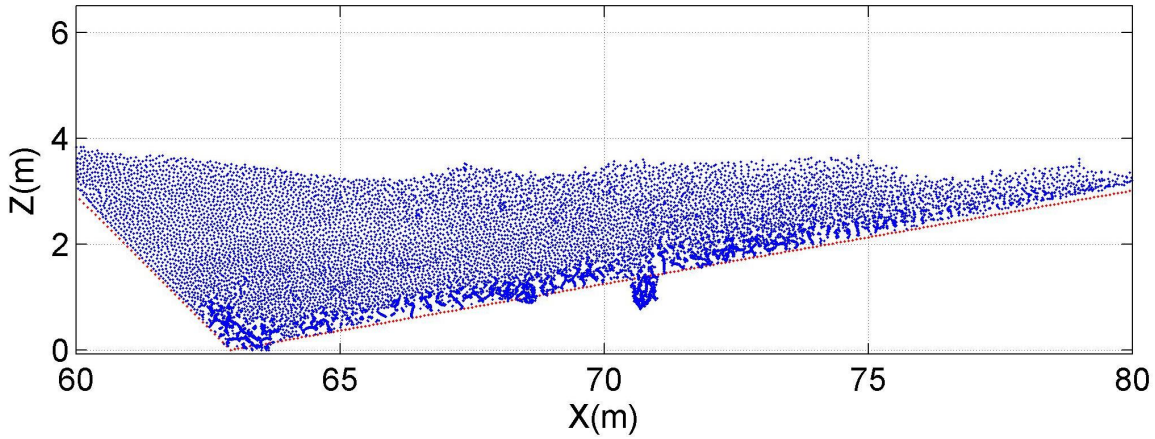

Figure A.10: Full reef at time $t = 7.5s$, illustrating instabilities on the rear slope of the reef

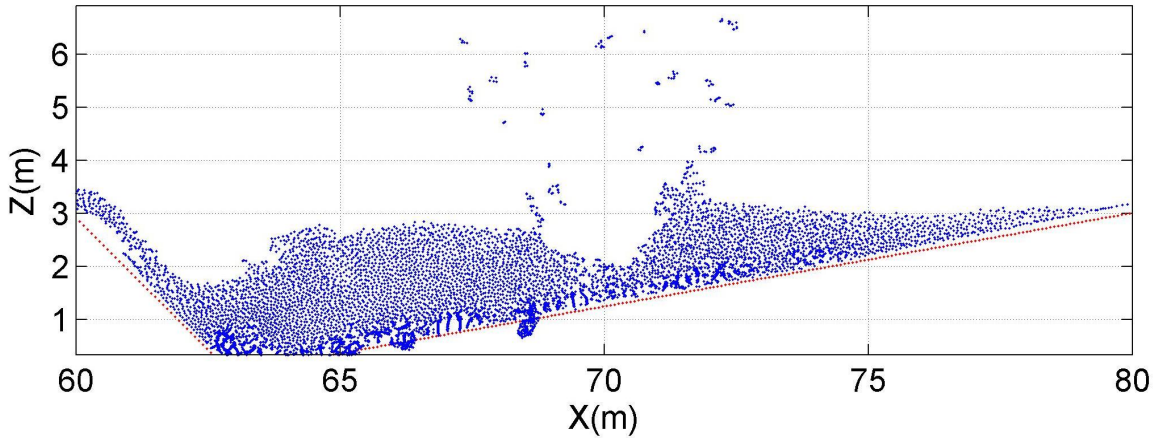

Figure A.11: Full reef at time $t = 10.0s$, illustrating instabilities on the rear slope of the reef

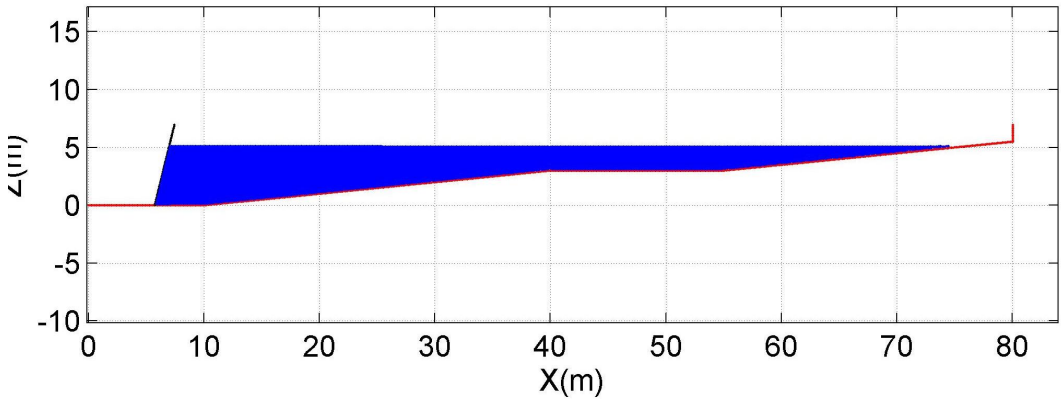

Figure A.12: Flat top reef $t = 0s$

Table A.4: Details of the optimized reef run

Foreshore Slope (-)	1 in 10
Crest Width (m)	20
Depth on Crest (m)	2
Absorption Slope (-)	1 in 10
Wave Height (m)	1
Wave Period (s)	12
Water depth at wavemaker (m)	5
Domain Length (m)	80
Particle Spacing (m)	0.0075
No. of particles	32056
Smoothing Length (m)	0.098
Max. Time Step (s)	6.0×10^{-5}
Time Step (s)	5.8×10^{-5}
Total run length (s)	28.1
Computational Time (Approx. hrs)	17
File Size for dt(kB)	4167

run are attributed to the high number of particles and the long domain.

Up to the breakpoint (Figure A.13) , the model runs well. The plunger is well defined. Vortex parameters can be extracted, although more particles would result in more accurate results. Note the clustering of particles between $X = 58$ and the end at $X = 63$m

However, the clustering of particles (again) on the shallower areas of the slope (Figure A.14) caused problems. This then passes through the boundary that is modelled as impermeable (Figure A.15), and it falls under the action of 'gravity' until it comes to rest at the limits of the model. These limits are defined in the SPHysics code.

The runs with smaller resolution did not yield good results for extraction of vortex parameters. There are too few particles in the plunging jet for the remaining particles in the plunging jet to be influenced by. The particles in the jets were affected too much by the particles in the other parts of the wave, and their motion was erratic at some times. At other times the particles appear to fall under the action of the gravity terms only. The vortex shape could thus not be clearly defined.

Many more runs were conducted on all the domain types, ie, full reef, optimized reef and beach, by varying domain size, particle spacing, number of particles, time step, wave heights and periods.

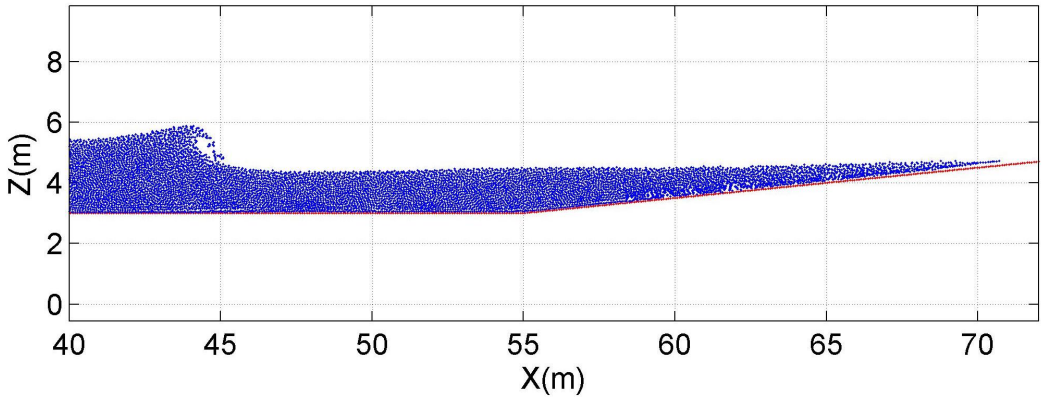

Figure A.13: Snapshot at break point at $t = 6.55s$

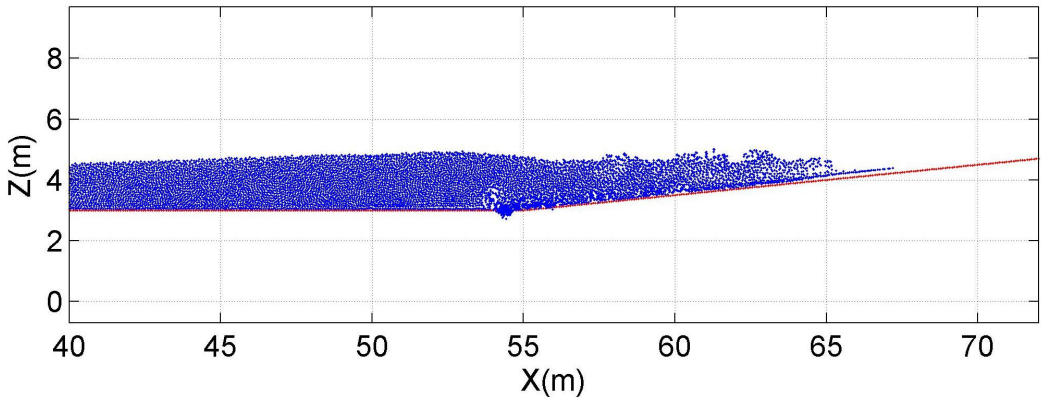

Figure A.14: Snapshot after breaking at $t = 8.55s$

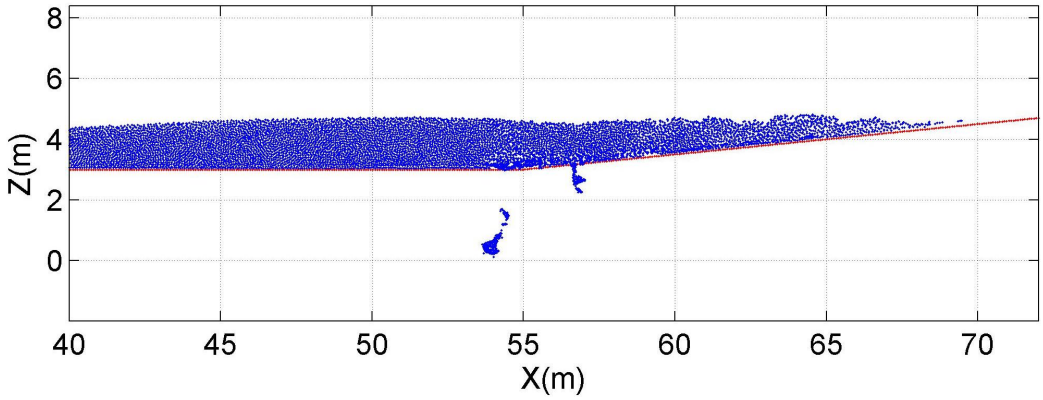

Figure A.15: Snapshot with particles passing through the boundary at $t = 8.90s$

Appendix B

Selected Timeseries Plots

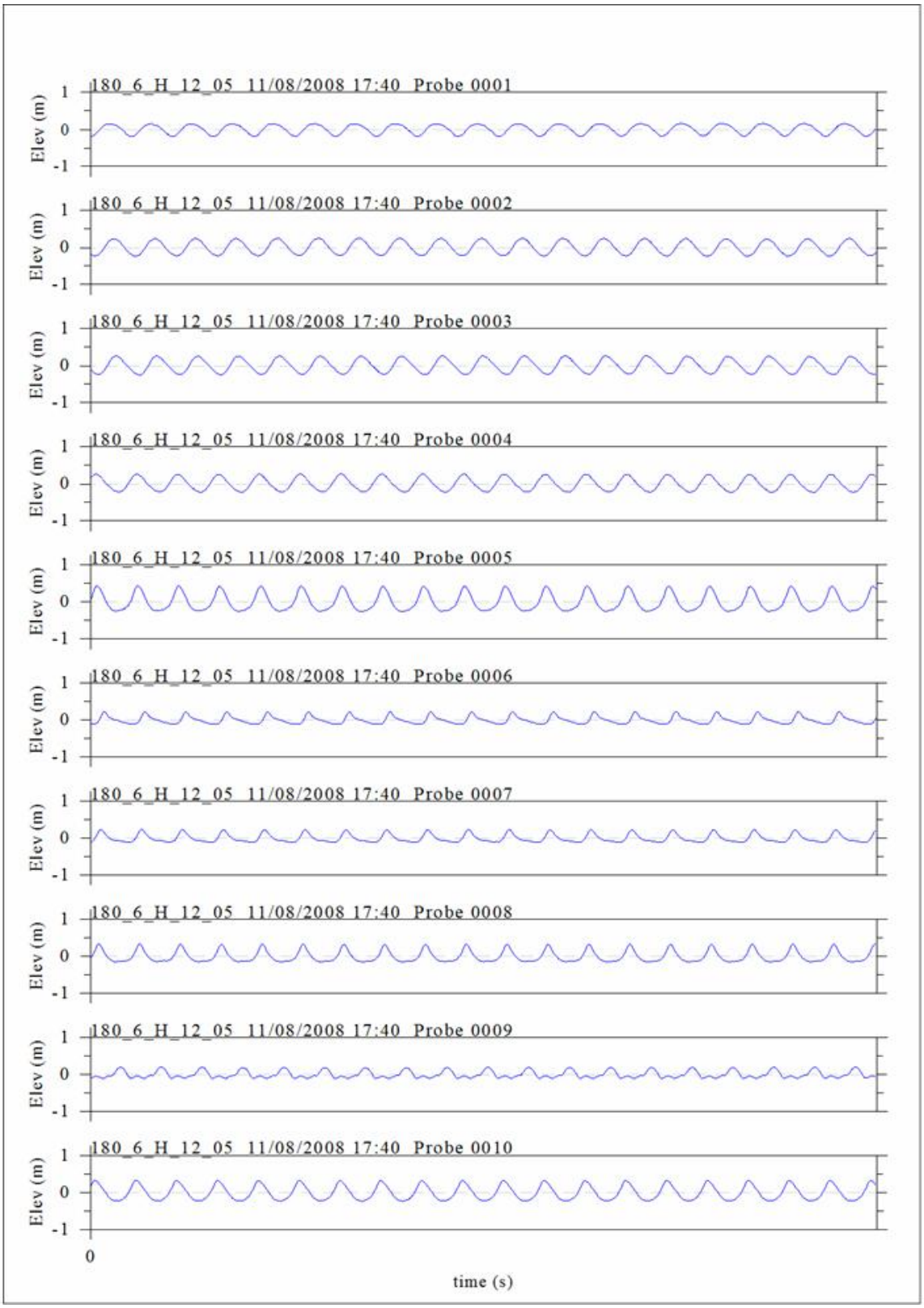

Figure B.1: Timeseries plot for test with target values of 1 in 18 seaward slope, 6m wide crest, high water level of +2.25m above crest level, wave period of 12s, and breaker height of 0.5m (Test reference number 180_6_H_12_05)

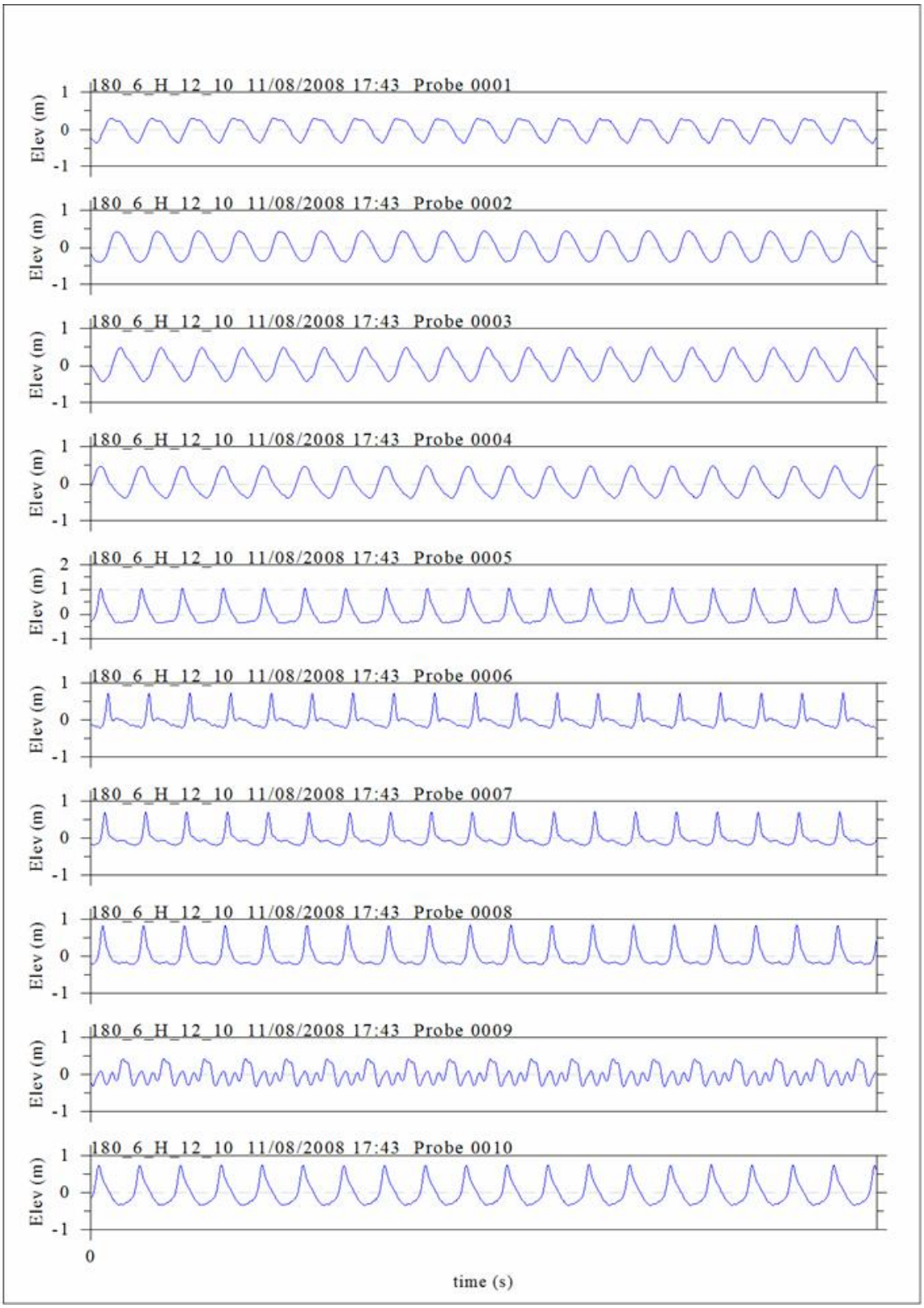

Figure B.2: Timeseries plot for test with target values of 1 in 18 seaward slope, 6m wide crest, high water level of +2.25m above crest level, wave period of 12s, and breaker height of 1.0m (Test reference number 180_6_H_12_10)

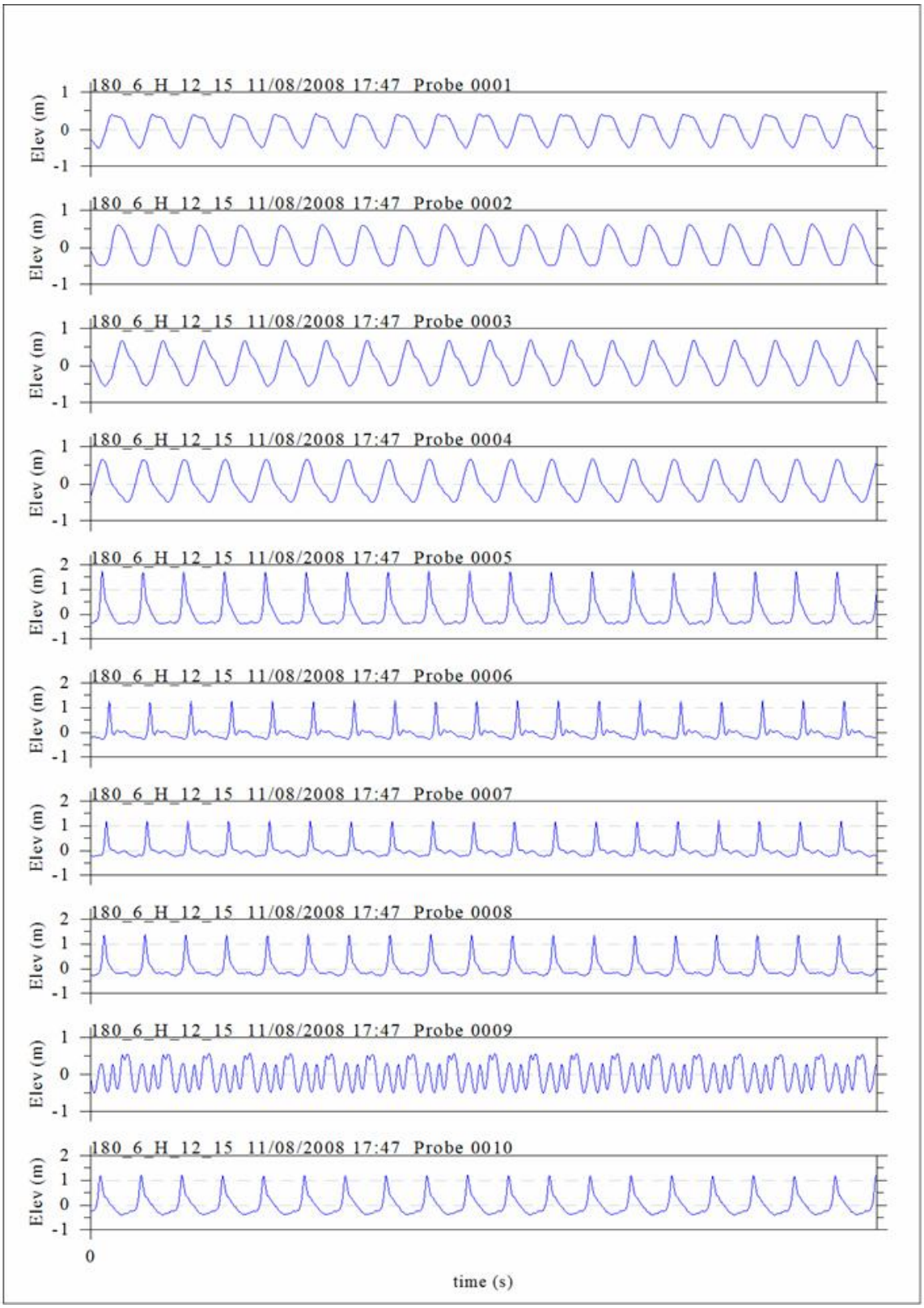

Figure B.3: Timeseries plot for test with target values of 1 in 18 seaward slope, 6m wide crest, high water level of +2.25m above crest level, wave period of 12s, and breaker height of 1.5m (Test reference number 180_6_H_12_15)

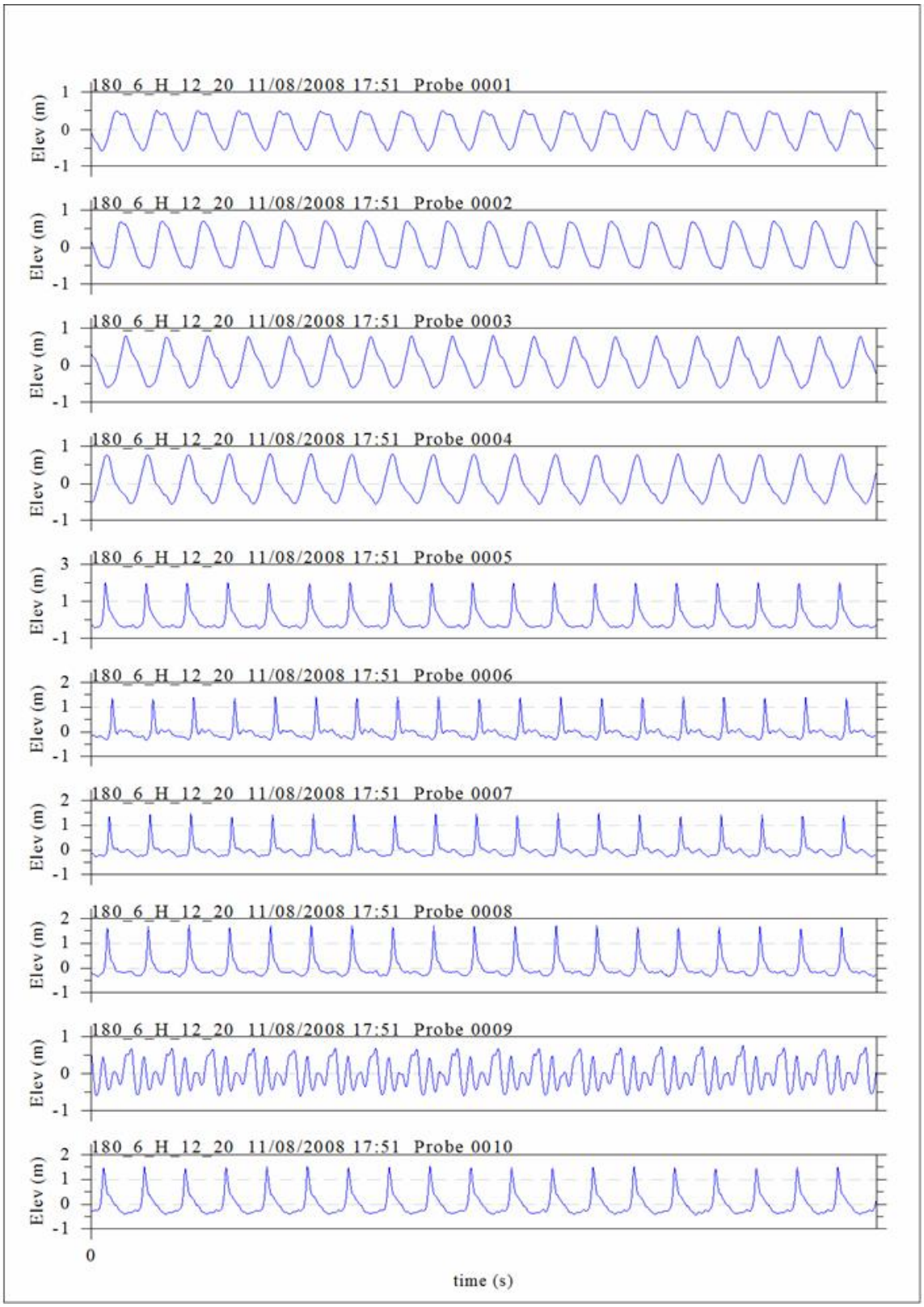

Figure B.4: Timeseries plot for test with target values of 1 in 18 seaward slope, 6m wide crest, high water level of +2.25m above crest level, wave period of 12s, and breaker height of 2.0m (Test reference number 180_6_H_12_20)

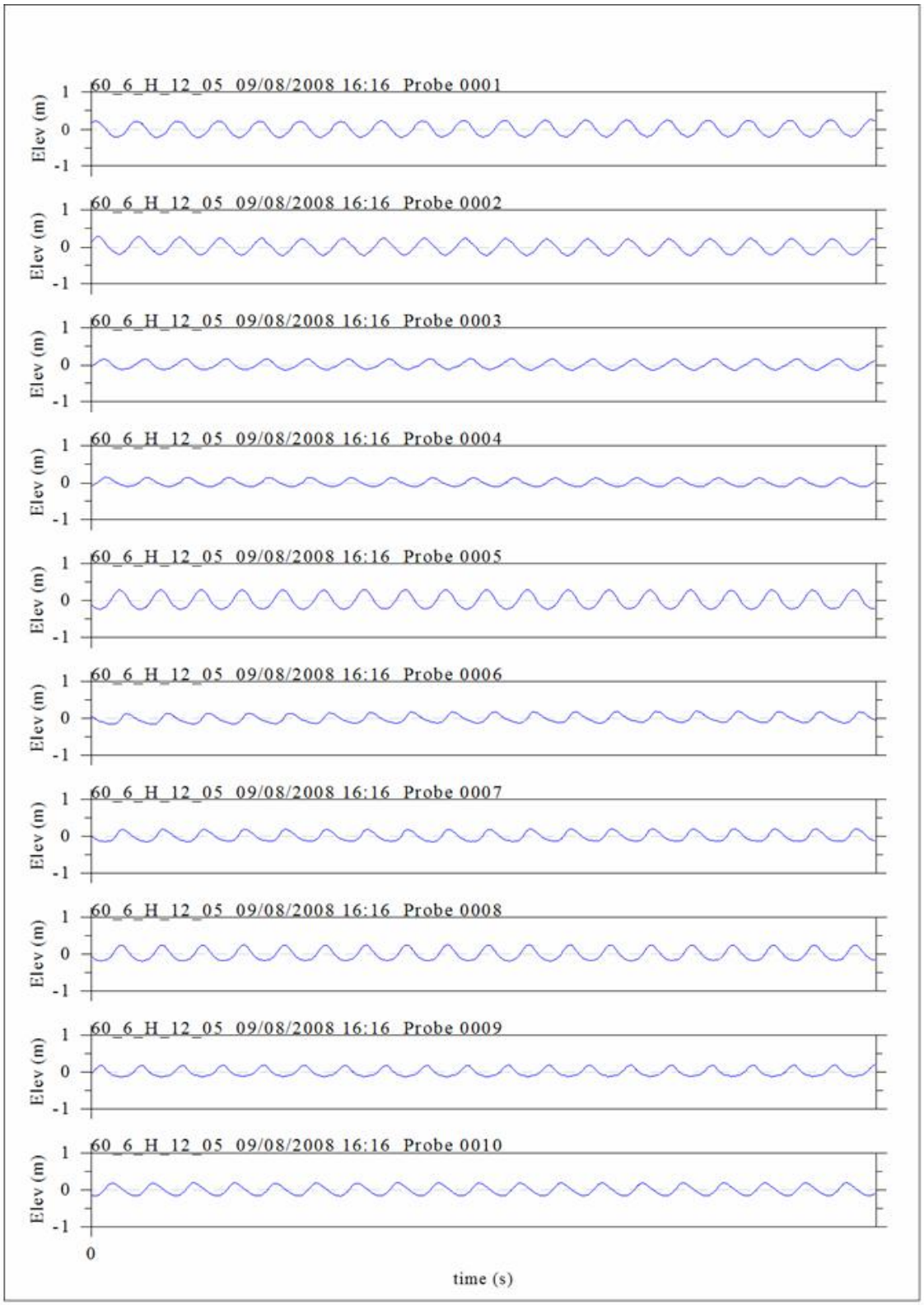

Figure B.5: Timeseries plot for test with target values of 1 in 6 seaward slope, 6m wide crest, high water level of +2.25m above crest level, wave period of 12s, and breaker height of 0.5m (Test reference number 60_6_H_12_05)

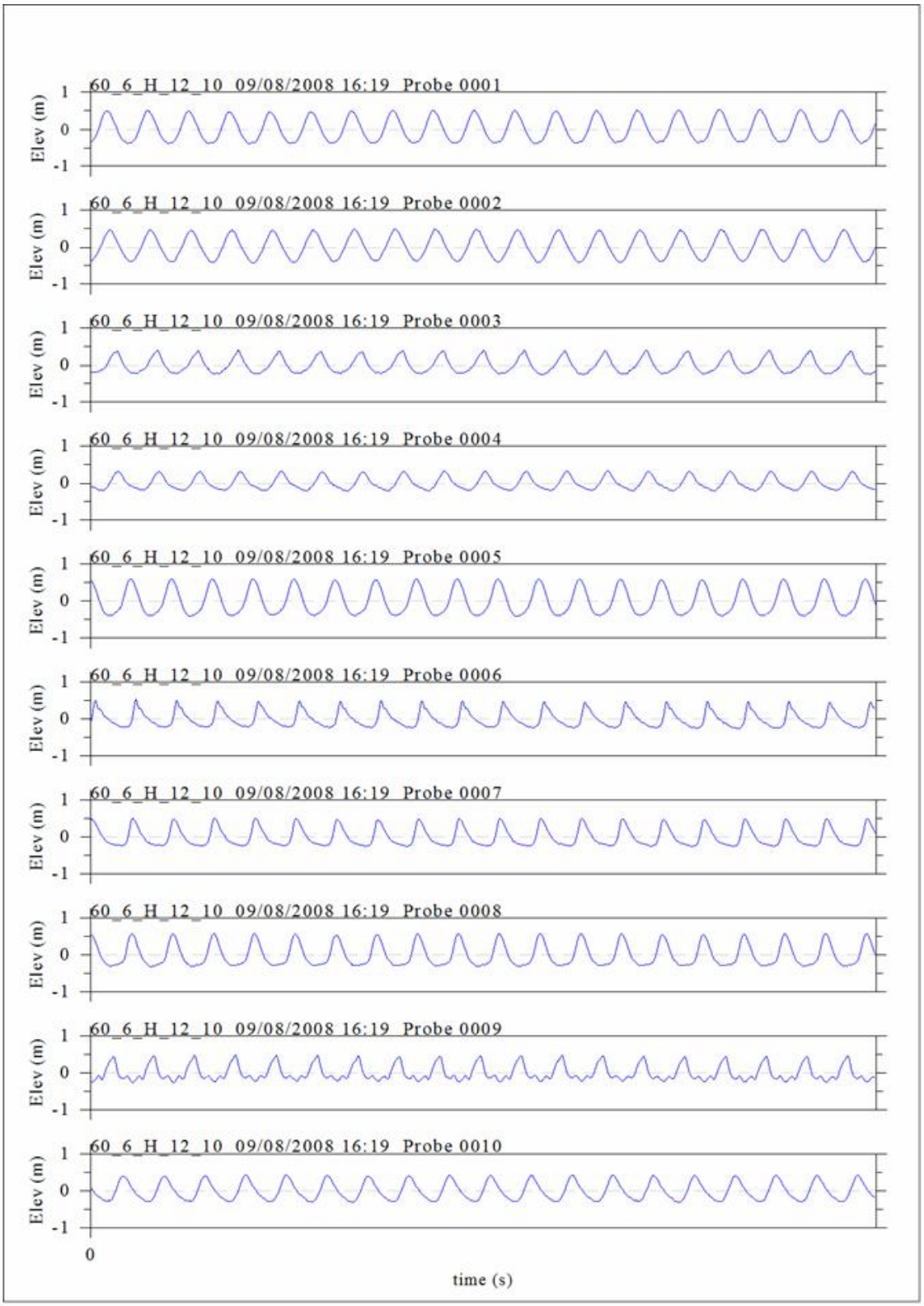

Figure B.6: Timeseries plot for test with target values of 1 in 6 seaward slope, 6m wide crest, high water level of +2.25m above crest level, wave period of 12s, and breaker height of 1.0m (Test reference number 60_6_H_12_10)

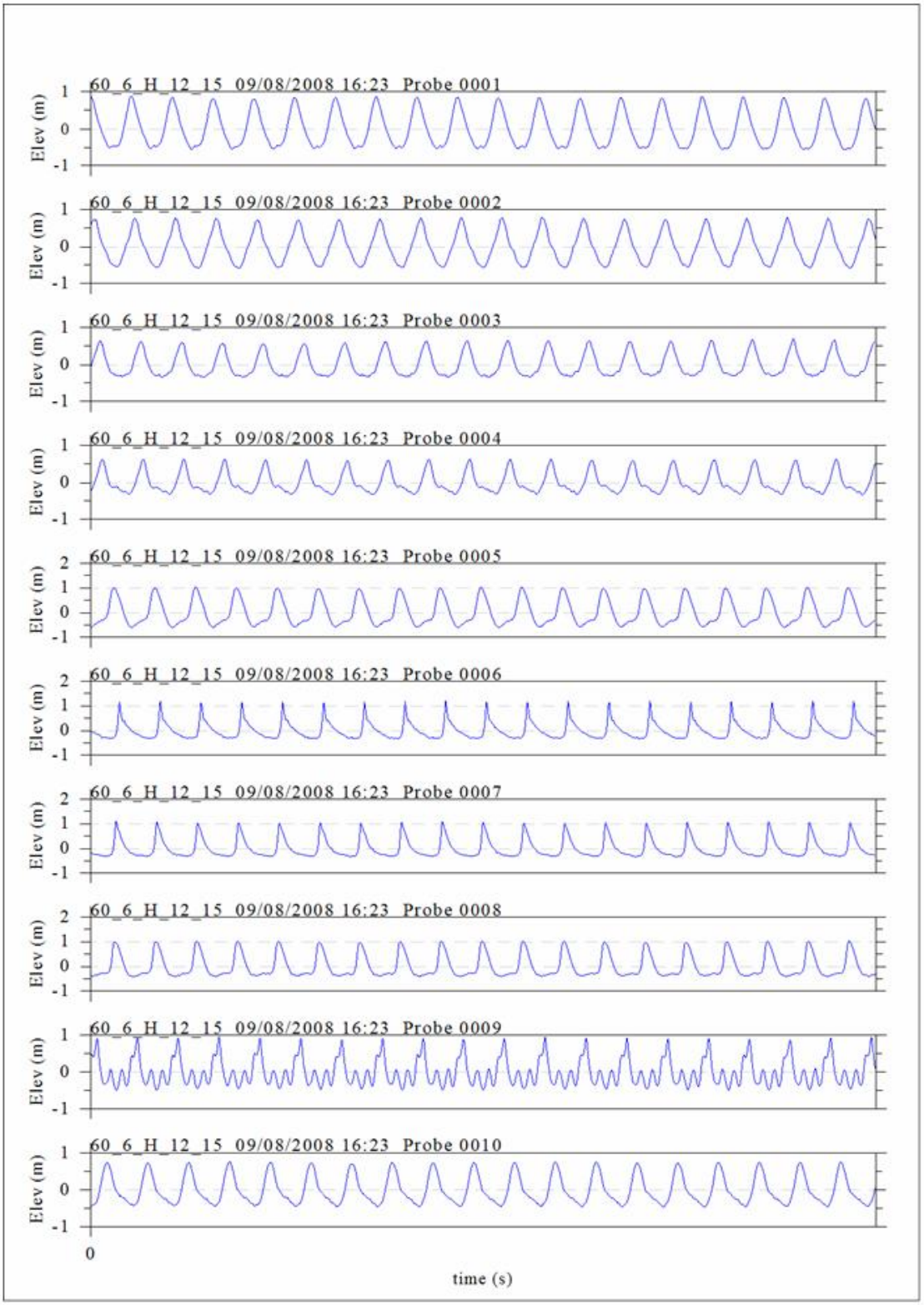

Figure B.7: Timeseries plot for test with target values of 1 in 6 seaward slope, 6m wide crest, high water level of +2.25m above crest level, wave period of 12s, and breaker height of 1.5m (Test reference number 60_6_H_12_15)

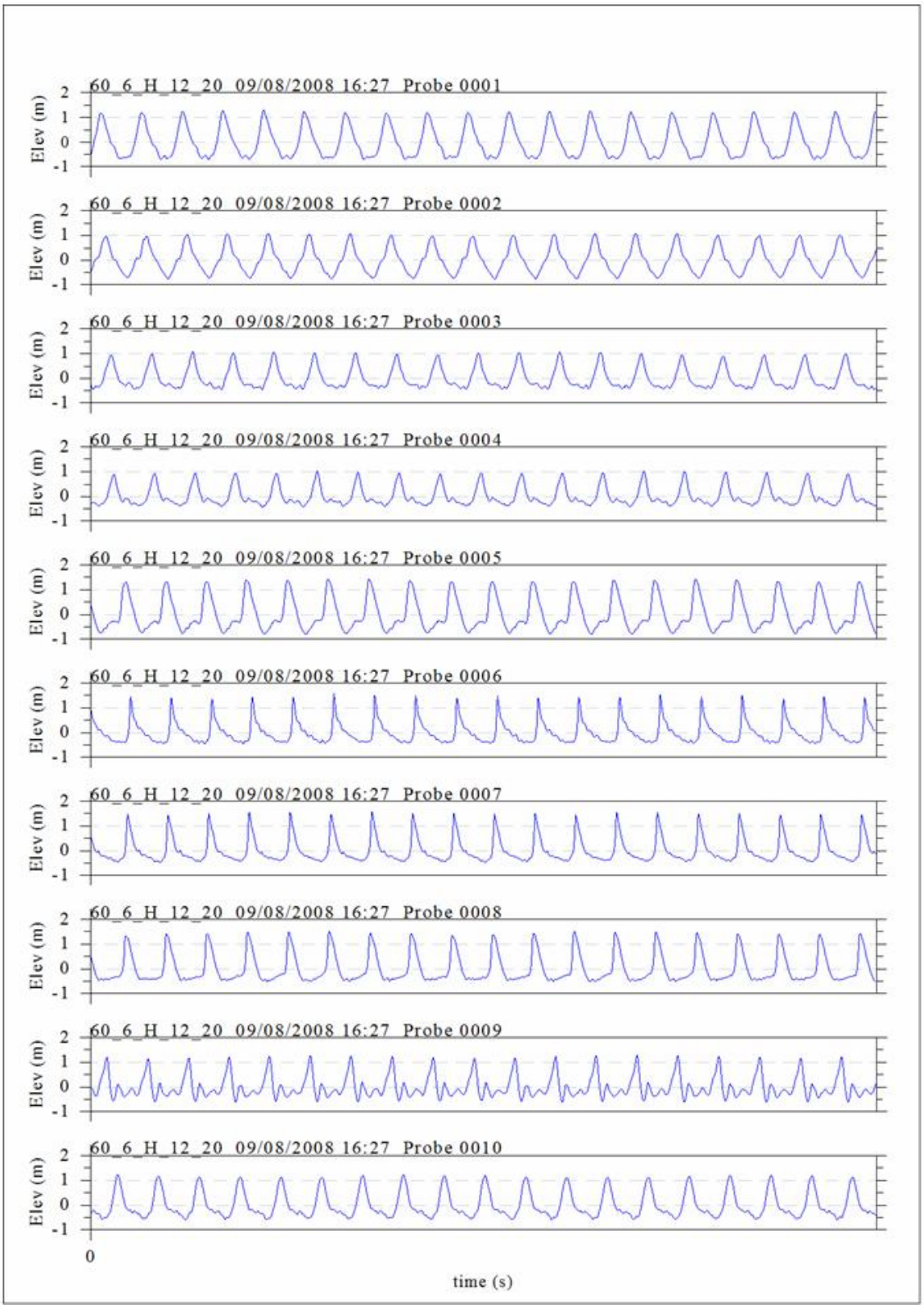

Figure B.8: Timeseries plot for test with target values of 1 in 6 seaward slope, 6m wide crest, high water level of +2.25m above crest level, wave period of 12s, and breaker height of 2.0m (Test reference number 60_6_H_12_20)

Appendix C

Image Analysis

In this Appendix, a typical procedure for extraction of wave breaking parameters and vortex parameters is shown by means of an example. A copy of the MATLAB code is presented.

Methodology

The extracted images from one of the tests are shown below in Figure C.1. The points are selected in MATLAB with an interface that allows for selection of the required points with a cursor. The points shown in the figure are slightly inaccurate, and are shown simply to highlight the method. The description of each point is given Table C.1.

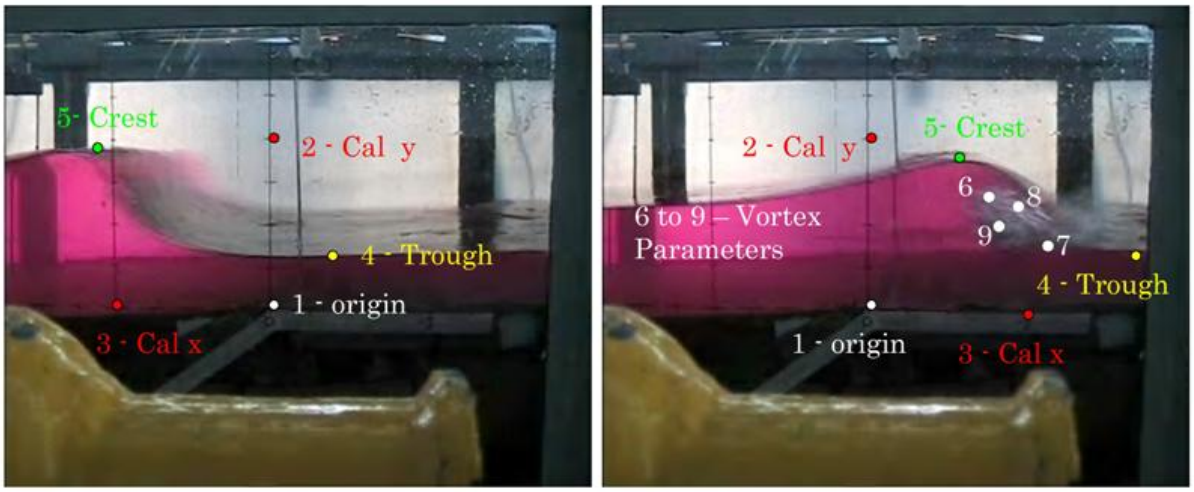

Figure C.1: Image with selected points shown

Table C.1: Selected Points for Image Analysis

Point no.	Incipient Breaking	Vortex Parameters
1	Origin	Origin
2	Calibration point for x plane	Calibration point for x plane
3	Calibration point for y plane	Calibration point for y plane
4	Wave Trough	Wave Trough
5	Wave Crest and breakpoint	Top of closed vortex
6 and 7	-	Define vortex length l_v and vortex angle θ_v
8 and 9	-	Define vortex width w_v

Point 1 defines the origin, whose x and y co-ordinates are entered into the MATLAB program. Points 2 and 3 calculate the calibration factor that enables conversion from pixels to distance. These co-ordinates are also fed into the MATLAB program. Through calibration, points 4 and 5 are used to calculate the breakpoint and the breaker height at incipient breaking, and the height of the vortex when the vortex is fully formed, i.e., the point at which the falling jet first comes onto contact with the wave face. Points 6 through 9, similarly, are used to calculate the vortex parameters.

A correction for the camera not being set to horizontal is applied in the program. This converts all co-ordinates to polar co-ordinates, then rotates them to an axis that is horizontal. The polar co-ordinates are then reconverted into cartesian co-ordinates. Another correction for distortion of the image with increasing distance from the lens is implemented within the

program. This either increases or decreases the angle between the x and y axis in order to return them to being perpendicular to one another.

The model and prototype values are then saved into a text files, and stored into a matrix of all the data gathered from the previous analyses, which is also stored as a text file. The MATLAB program is presented below.

MATLAB code

```
%Matlab program to extract wave breaking and vortex parameters from image
%labelled f1_f2_f3_f4_f5_f6 and save data as f1_f2_f3_f4_f5_f6_refnum.txt
%and to save calculated parameters as a matrix

%Scale conversions to convert file (prototype) parameters to model values
Scale  = 15  %Scale factor  = 1 in 'Scale'
Lsf = Scale
Tsf = sqrt(Scale)

%Load in file name parameters
f1='180' ;           % Foreshore slope 10 in f1 =1/S
f2='15' ;            % Prototype width of reef crest
f3='M' ;             % Prototype water level H = 2.25m above crest
                     % Prototype water level M = 1.50m above crest
                     % Prototype water level L = 0.75m above crest
f4='10';             % Prototype wave period in seconds
f5='20';             % Prototype wave height in seconds
f6='0313810';         % Image extracted from video clip
refnum = '169';      % Reference test number
type='v' ;           % Type of wave breaking; b is incipient breaking, v is
                     % when overturning portion of the plunging wave
                     % impinges the front face

xstart_prot = 12;  % prototype distance along crest where origin starts P1
%- x dir
x_start = xstart_prot/Lsf*1000;   % model distance along crest where origin
 starts P1 - x dir
y_start = 0;         % prototype height from crest where origin starts P1 -
 y dir
dx = 200;            % length of calibration line between point 1 and 2 in
mm- x dir
dy = 200;            % length of calibration line between point 1 and 3 in
mm- y dir

Sx =  str2num(f1)/10; % 1 in slope
S=1/Sx ;              % Slope in decimal

wc =  str2num(f2)/Lsf*1000;  %model crest width in mm

if f3=='H'    %model water depth
WL = 150
elseif f3 == 'M'
```

```
    WL = 100
elseif f3 == 'L'
    WL = 50
else
  WL = str2num(f3)
end;

T_target = str2num(f4)/Tsf ; %Target model wave period
H_target = 1000*str2num(f5)/(10*Lsf); %Target model wave height

testno = str2num(refnum)

file=[ f1 , '_' , f2 , '_' , f3 , '_' , f4 , '_' , f5 , '_' , f6 ];
A = imread ( [ f1 , '_' , f2 , '_' , f3 , '_' , f4 , '_' , f5 , '_' , ...
f6 ] ,'bmp');

J = imadjust(A,[0 1],[0 1]); %Adjusts the shaprness and brightness of the
 original image A if required
imshow (J);                  %shows the adjusted image J
[x,y]=getpts;                %Enables selction of user defined co-ordinate
points from image J

XY = [x y];                  %List of x and y cordinates rel to image
origin
%T List of extracted points = [ 'P1 - Orig' ; 'P2 - Xmax' ; 'P3 - Ymax' ;
 'P4 - BrWT' ; 'P5 - BrWC' ; 'P6 - VTop' ;
  'P7 - VBot' ; 'P8 - Wid1' ; 'P9 - Wid2' ]
T = [ 1 ;2 ;3 ;4 ;5 ;6 ;7 ;8 ;9 ] ;  %List of column refernce numbers
%TXY = [T XY];                %Matrix of referenec numbers and XY co-ords

%convert from picture co-ords to co-ords rel to origin
%xy=[x -y];
for m = 1:9
xo(m) =(x(m)-x(1));
yo(m) =-(y(m)-y(1));
end

%Compensation for misalignment of camera
dtheta =  -atan( (yo(2)-yo(1))/(xo(2)-xo(1)))
for n=1:9;
    if n==1;
    theta(n) = 0;
    else
    theta(n) = abs(atan((yo(n)-yo(1))/(xo(n)-xo(1))));
    end
  if 0 < dtheta
     if xo(1)< xo(n)
        theta(n) = theta(n)
        theta_new(n) = (pi-dtheta)/pi*(theta(n)+ dtheta);
```

```
        r(n) = sqrt(((yo(n)-yo(1))^2 )+((xo(n)-xo(1))^2));
        xr(n) = -r(n) * (cos(theta_new(n)));
        yr(n) = r(n) * sin(theta_new(n));
     elseif xo(n) < xo(1)
        theta(n) = theta(n)
        theta_new(n) = (pi+dtheta)/pi*(theta(n)- dtheta);
        r(n) = sqrt(((yo(n)-yo(1))^2 )+((xo(n)-xo(1))^2));
        xr(n) = r(n) * (cos(theta_new(n)));
        yr(n) = r(n) * sin(theta_new(n));
     else
        theta(n) = theta(n)
        theta_new(n) = (pi+dtheta)/pi*(theta(n)+ dtheta);
        r(n) = sqrt(((yo(n)-yo(1))^2 )+((xo(n)-xo(1))^2));
        xr(n) = r(n) * (cos(theta_new(n)));
        yr(n) = r(n) * sin(theta_new(n));
     end
  else %if dtheta is negative
     if xo(1)< xo(n)
        theta(n) = theta(n)
        theta_new(n) = (pi+dtheta)/pi*(theta(n)+ dtheta);
        r(n) = sqrt(((yo(n)-yo(1))^2 )+((xo(n)-xo(1))^2));
        xr(n) =-r(n) * (cos(theta_new(n)));
        yr(n) = r(n) * sin(theta_new(n));
     elseif xo(n) < xo(1)
        theta(n) = theta(n)
        theta_new(n) = (pi+dtheta)/pi*(theta(n)- dtheta);
        r(n) = sqrt(((yo(n)-yo(1))^2 )+((xo(n)-xo(1))^2));
        xr(n) = r(n) * (cos(theta_new(n)));
        yr(n) = r(n) * sin(theta_new(n));
     else
        theta(n) = theta(n)
        theta_new(n) = (pi+dtheta)/pi*(theta(n)- dtheta);
        r(n) = sqrt(((yo(n)-yo(1))^2 )+((xo(n)-xo(1))^2));
        xr(n) = r(n) * (cos(theta_new(n)));
        yr(n) = r(n) * sin(theta_new(n));
     end
  end
end

%Calibrating from pixels into mm
cal_x=dx/sqrt((yr(2)-yr(1))^2+(xr(2)-xr(1))^2);
cal_y=dy/sqrt((yr(3)-yr(1))^2+(xr(3)-xr(1))^2);

%Converting from pixels to mm
%x-co-ords
for l=1:9;
%xor(l) =xr(l)-xr(1) ;
x_pos(l)=xr(l)*cal_x;
end;
```

```
%Converting from pixels to mm
%y-co-ords
for m=1:9;
%yor(m) =yr(m)-yr(1) ;
y_pos(m)=yr(m)*cal_y;
end

%plot ( xr , yr , '.g' , x_pos, y_pos,'.r');
plot (x , -y , '.b' , xo, yo , '.k' , xr , yr , '.g',x_pos,y_pos , '.r');
axis equal;

XY_POS_pix=[T x_pos' y_pos'];   %positions of co-ord in mm after rotation
of axes relative to user-defined origin
XY_POS_mm_col=[T x_pos'+x_start y_pos'+y_start];  %positions of co-ord in
pixels relative to start of crest

if type=='b'   %calculates breaker parameters xb, Hb, and db
   XY_POS_break_mm = XY_POS_mm_col';
   save ( cat(2,  refnum ,'_', file ,'_', type ,'_', 'XY_pos', '.txt'),
    'XY_POS_break_mm' , '-ascii' );
   xb= XY_POS_mm_col ( 5,2);
   Hb= XY_POS_mm_col ( 5,3) - XY_POS_mm_col ( 4,3);
   if xb > 0;
      db=S*xb + WL;
   elseif 0 >= xb >= -wc ;
      db = WL;
   elseif  -wc >= xb >= -wc-620;   %breaks on back of reef on 1in2 slope;
    620 is horizontal length of the backslope
      db=1/2*abs(xb+wc);
   else db = 300;
   end

elseif type=='v'   %calculates vortex parameters xv, Hv, l, w, and
theta_v
   XY_POS_vortx_mm = XY_POS_mm_col';
   save ( cat(2, refnum ,'_', file ,'_', type ,'_', 'XYpos','.txt'),
     'XY_POS_vortx_mm' , '-ascii' );

   xv = XY_POS_mm_col ( 7,2);
   Hv = XY_POS_mm_col ( 5,3) - XY_POS_mm_col ( 4,3);
   lv = sqrt ((XY_POS_mm_col ( 7,2) - XY_POS_mm_col ( 6,2))^2 +...
    (XY_POS_mm_col ( 7,3) - XY_POS_mm_col ( 6,3))^2);
   wv = sqrt ((XY_POS_mm_col ( 9,2) - XY_POS_mm_col ( 8,2))^2 + ...
    (XY_POS_mm_col ( 9,3) - XY_POS_mm_col ( 8,3))^2) ;
   theta_v =90 - atan(abs((XY_POS_mm_col ( 7,2) - XY_POS_mm_col...
    ( 6,2))/(XY_POS_mm_col ( 7,3) - XY_POS_mm_col ( 6,3))))/pi*180 ;

Colno = [    0    1  2  3     4   5  6  7  8   9 10   11  12 13 ];
```

```
Model = [ testno Sx wc WL T_target H_target xb Hb db lv wv theta_v xv Hv ];
Proto = [ testno Sx Lsf*wc/1000 Lsf*WL/1000 Tsf*T_target Lsf*H_target/1000 ..
Lsf*xb/1000 Lsf*Hb/1000 Lsf*db/1000 Lsf*lv/1000 Lsf*wv/1000 theta_v ..
Lsf*xv/1000 Lsf*Hv/1000 ];
   AA = [ Colno; Model; Proto ];
   save ( cat(2, refnum ,'_', file ,'_','modprot','.txt'), 'AA' ,...
     '-ascii' );

   %Saving and writing all model data up to and incl this test in a matrix
    called All model
   %parameters
   %Allm = [ Colno ]   %Makes an initial temporary matrix for referring to
   Alltempm = [ Allm ] ;
   Allm = [ Alltempm ; Model ] ;
   save ( cat(2,'All Model Parameters','.txt'), 'Allm' , '-ascii' );
   %clear Allm

   %Saving and writing all prototype data up to and incl this test in a
   matrix called
   %All prototpye
   %parameters
   %Allp = [ Colno ]   %Makes an initial temporary matrix for referring to
   Alltempp = [ Allp ] ;
   Allp = [ Alltempp ; Proto ] ;
   save ( cat(2,'All Prototype Parameters','.txt'), 'Allp' , '-ascii' );
   %clear Allp

else
    'error: no "type" specified'
end
```